Analyzing Immunotherapy and Chemotherapy of Tumors through Mathematical Modeling

Summer Student-Faculty Research Project

by
William Chang, Lindsay Crowl, Eric Malm, Katherine Todd-Brown, Lorraine Thomas, Michael Vrable

Lisette de Pillis, Weiqing Gu, Advisors

Abstract

Analyzing Immunotherapy and Chemotherapy of Tumors through Mathematical Modeling

Summer Student-Faculty Research Project

by William Chang, Lindsay Crowl, Eric Malm, Katherine Todd-Brown, Lorraine Thomas, Michael Vrable

Summer 2003

The development of immunotherapy in treating certain forms of cancer has recently become an exciting new focus in cancer research. In some preliminary studies, immunotherapy has been found to be most effective when administered in conjunction with chemotherapy [89]. Precisely how various types of immunotherapy work, and how they should optimally be administered, either alone or in conjunction with chemotherapy, is not yet well understood. We propose to contribute to the emerging body of cancer treatment research by developing and analyzing new mathematical models of the treatment of cancer that include vaccine therapy, activated anticancer-cell transfers, and activation protein injections in combination with chemotherapy. We build on existing models that are already successfully developed. Results of our model simulations have been validated by comparing outcomes to mouse [46] and human [49] data. The mathematical models we develop will enrich the study of cancer treatment and aid in hastening progress toward an increased understanding and more widespread availability of this new type of this new combination approach to cancer therapy.

Table of Contents

List of Figures

List of Tables

Acknowledgments

First and foremost, we would like to thank our advisers, Professor L. de Pillis and Professor W. Gu, who have aided us throughout the research process. In addition, we would like to thank Professor Radnuskya, Dr.J. Orr-Thomas, Dr. Wiseman, and Claire Connelly. In addition we would like to thank Diefenbach, Rosenberg, Jackson, Ferreira for their research and experimental data.

Program: Quantitative Life Sciences

Starting Date of Project: May 2003.

Duration of Project: Ten weeks.

Location of Project: Harvey Mudd College campus.

Part I

Introduction

Chapter 1

Introduction and Background

1.1 Overview

We have developed three distinct tumor-immune models in order to describe and anaylze how specific types of cancer treatment affect both tumor and immune populations in the human body. First we present an ordinary differential equations model to look at overall cell populations, then a spacial model to examine various tumor structures, and finally a geometric model to investigate the macroscopic stages of tumor evolution. The interactions are dealt with on a cellular level as well as on a macroscopic level in order to encompass various degrees of the interaction and form a borader view.

1.2 Background

If current trends continue, one out of three Americans will eventually get cancer. The Cancer Research Institute reports that in 1995, an estimated 1,252,000 cases were diagnosed, with 547,000 deaths in the United States alone. With new techniques for detection and treatment of cancer, the relative survival rate has now risen to 54 per cent. It is vital to explore new treatment techniques, and to advance the state of knowledge in this field as rapidly as possible.

The most common cancer therapy today is chemotherapy. The basic idea behind chemotherapy is to kill cancerous cells faster than healthy cells. This is accomplished by interrupting cellular division at some phase and thus killing more tumor cells then their slower developing normal cells. However some normal cells, for example those that form the stomach lining and immune cells, are also rapidly dividing cells which means that chemotherapy also harms the patient leading to things like a depressed immune system which opens the host to infection [24, 70]. In addition, chemotherapy causes significant side effects in patients, and therefore exploring new forms treatments may prove extremely beneficial.

Therapeutic cancer vaccines and cancer-specific immune cell boosts are currently being studied in the medical community as a promising adjunct therapy for cancer treatment in hopes of combating some of the negative effects of chemotherapy. There are still many unanswered questions as to how the immune system interacts with a tumor, and what components of the immune system play significant roles in responding to immunotherapy.

Mathematical models are tools that help us understand not only the interaction between immune and cancer cells but also the effects of chemotherapy and immunotherapy have on this interaction. This in turn can lead to better treatments, thereby increasing the survival rate and quality of life for those fighting cancer.

What we do know from previous mathematical models of tumor growth is that the immune response is crucial to clinically observed phenomena such as tumor dormancy, oscillations in tumor size, and spontaneous tumor regression. The dormancy and cyclical behavior of certain tumors is directly attributable to the interaction with the immune response [37, 80, 82, 83]. Additionally, it has been shown that chemotherapy treatments cannot lead to a cure in the absence of an immune system response [38].

1.3 Models

1.3.1 Considerations of the Mathematical Cancer Growth Model

Cancer vaccines are a unique form of cancer treatment in that the immune system is trained to distinguish cancerous cells from normal cells. This method shows promising results since the treatment does not deplete non-cancerous cells in the body. A mathematical model of cancer vaccines should exhibit different dynamics from a model of preventative anti-viral vaccines. The behavior of the model should mimic clinically observed phenomena, including tumor-cell tolerance to the immune response before vaccination and antibody levels that remain high for a relatively short time.

The models that we develop should be capable of emulating the following behaviors in the absence of medical interventions:

- Tumor dormancy and creeping through. There is clinical evidence that a tumor mass may disappear, or at least become no longer detectable, and then for reasons not yet fully understood, may reappear, growing to lethal size.

- Mutually detrimental effects of tumor and normal cell populations through competition for space and nutrients.

- Uncontrolled growth of tumor cells, expressed as a global population quality through accelerated growth rates.

- Global stimulatory effect of tumor cells on the immune response.

Additionally, since we ultimately wish to determine improved global therapy treatment protocols, mathematical terms must be developed that represent tumor growth in response to medical interventions:

- System response to chemotherapy (direct cytotoxic effects on tumor, normal, and immune cell populations).

- System response to vaccine therapy (including direct stimulatory effects on the immune system, as well as potential detrimental side effects on tumor and normal cell populations).

- System response to immunotherapy (Increase in the number of activated $CD8^+$ T cells that indirectly affects the tumor population)

In order to capture the behaviors outlined above, our models track not only a population of tumor cells, but also the development of healthy and immune system cell populations. Our models include tumor cell populations, normal cell populations, and one or more immune cell populations, such as natural killer (NK) cells and cytotoxic T-cells. Such multi-population models allow for the simulation of behaviors that can result only from inter-population interactions.

1.4 Analytic Methods

There are many different ways to analyze a model. In this analysis we use:

- Parameter estimation using lab data

- Optimal control

- Bifurcation Analysis

- Matching model predictions with lab data

1.4.1 Parameter Estimation

While a generalized model with scaled parameters is useful in studying the gross behavior patterns of general tumor growth, it is also of interest to study specific tumor types. In particular, we will move from the general to the specific, focusing on particular forms of cancer on which laboratory studies have been carried out. Although system parameters can vary greatly from one individual to another, multiple data sets can be used in order to obtain acceptable parameter ranges. We also plan to perform sensitivity analysis to determine the relative significance of parametric variations. In our most recent works [39] and [40], we have been able to show that the new mathematical terms we developed to describe tumor-immune interactions, along with our parameter fitting techniques, have allowed us to find a general framework in which to predict growth and reaction patterns in both mouse and human data.

1.4.2 Optimal Control Approach to Therapy Design

The goal of chemotherapy is to destroy the tumor cells, while maintaining adequate amounts of healthy tissue. Optimality in treatment might be defined in a variety of ways. Some studies have been done in which the total amount of drug administered is minimized, or the number of tumor cells is minimized, see [114, 116, 117]. The general goal is to keep the patient healthy while killing the tumor.

Within the area of optimal control, there are real challenges, both theoretically and numerically, to discovering truly optimal solutions. While general optimal control problems can be difficult to solve analytically, one can often appeal to numerical methods for obtaining solutions. We have already employed a numerical approach to optimal control to determine a set of potentially optimal courses of treatment in our previous models. A numerical approach has also been used in, for example, [90], [81], [91], [97], [112] and [113], for simpler models without interaction between different cells. In this area, a student researcher can be of particular help, since the testing of various computational optimal control scenarios is a time-consuming, yet highly accessible and fundamentally important task. Despite the challenges of finding an optimal solution, we point out that even

if the optimal control approach simply moves one *closer* to an optimal solution without actually achieving optimality, and that solution is determined to be an improvement to traditional treatment protocols, then progress has been made.

1.4.3 Bifurcation Analysis

Since it is difficult to obtain accurate parameters for immune cell populations in the human body, a bifurcation analysis can be an extremely helpful tool. Although doctors and researchers have completed some successful experiments involving immunotherapy, there is just not enough data available for mathematicians to obtain any tangible parameter precision. Therefore, we are able to observe how a range of parameters affects the local and global behavior of our ODE model.

1.4.4 Model Prediction Matching

Although we do not have exact experimental results, we can test that simulations of our models show reasonable behavior. This is more of a check to see that our models do not produce unrealistic results than it is to find exact results.

Chapter 2

Tumor Growth and the Immune System

2.1 Tumor Formation

A tumor begins to form when a single cell mutates in such a way that leads to uncontrolled growth. Many different factors can cause such mutations, including excess sunlight, carcinogens such as nicotine, and even viruses such as human papilloma virus. While a large number of people are exposed to such factors every day, few develop tumors. One possible reason for this is that mutations are cumulative. Many small, complex mutations may be necessary before a normal cell becomes a cancerous cell [62]. Another reason is that healthy immune systems may kill many of these initial tumor cells before they ever get a chance to divide or spread [24].

According to the accepted theory, a tumor cell can mutate in two important ways: the growth suppression signals telling cells not to divide are turned off or the signals telling cells to begin dividing are left on continuously [62]. Thus, tumor cells are always dividing and depleting large amounts of nutrients necessary for other parts of the body to function. In addition, if a tumor mass grows large enough, it can take over entire organs, or interfere with their ability to function. In this fashion, tumor cells cause illness and eventually death in their host.

Tumors can be either vascular or avascular, that is, attached to a blood vessel or not. Generally a tumor will start out avascular, feeding off nutrients which diffuse from nearby blood vessels. Avascular tumors, with little access to the bloods system, are less likely to metastasize.

In addition to their rapid growth, tumor cells send out a chemical signal encouraging blood vessel growth. This process, called angiogenesis, allows tumors more access to nutrients [62]. The second phase of tumor growth occurs when blood vessels are incorporated into the tumor mass itself. The tumor now has a constant source of nutrients, as well as a way to enter the bloodstream and create more metastases [72].

A vascular tumor has direct access to the body's transportation system, thus the tumor

is more likely to metastasize and spread to other sites in the body. Only a small percentage of tumor cells are mobile; most stay in one place contributing to the overall local tumor size.

2.2 Immune Response

The body is not helpless against cancerous cells. The immune system is able to recognize tumor cells as foreign and destroy them. There are two main types of cells that respond to a tumor's presence and attack. Non-specific immune cells, such as NK cells, travel throughout the body's tissue and attack all foreign substances they find. Specific immune cells, such as CD8$^+$ T-cells, attack only after a complex variety of mechanisms primes them to recognize similar threats [63], [50].

The more white blood cells in the immune system, the more able an individual is able to fight infection. Although there are other factors affecting the strength of the immune system, the most common measure of health is the number of white blood cells, or circulating lymphocytes in the blood stream [68].

2.2.1 NK cells

Natural killer (NK) cells are a type of non-specific white blood cells. Non-specific cells are the body's first line of defense against disease and are always present in healthy individuals. These cells travel through the bloodstream and lymph system to the extracellular fluid, where they find and destroy non-self cells [23].

NK cells can recognize non-self cells in two distinct ways. In the first case they are attracted to foriegn cells that have been covered in chemical signals by other parts of the immune system [44]. In the second case NK cells can destroy body cells. Two types of receptors on the target cell's surface play a role in this destruction. The first are receptors that signal the cell should be destroyed. These receptors are usually overridden by the other type of receptor, which signals that the cell should be preserved. The second signal is destroyed if the cell is invaded or mutates [44]. In particular, this means that cancer cells are unable to stop NK cells, which will recognize them as abnormal and kill them.

2.2.2 CD8$^+$ T-cells

Specific immune cells, such as CD8$^+$ T immune cells, must be primed before they can attack. CD8$^+$ T cells are typically activated inside of lymph nodes, where they are presented with antigens. Because each primed T-cell is specific to a certain antigen, only a small [121, 44]. Those that do recognize an antigen presented to them are considered primed [121]. Some fraction of these cells become memory T-cells, which stay in the lymph nodes and allow the body to respond more quickly if a disease returns. Another large fraction become cytotoxic T-cells [44], multiply, and then leave the lymph node to find the source of the antigens [121].

The homing process that primed CD8$^+$ T-cells use to reach the source of the antigens is very complex and not fully understood. Several signals are used to coordinate their movement. One common path is for the immune cells to travel through the bloodstream. Near the source of infection, the cells lining the blood vessel will have changed in a way that attracts the CD8$^+$ T-cells. The immune cells then push their way out of the bloodstream to the surrounding tissue [121]. There the process is less well understood. One possible mechanism is a chemotactic gradient which the CD8$^+$ T-cells travel up to get to the abnormal cells.

Once they arrive, CD8$^+$ T-cells have at least two ways to kill target cells. They can insert signals causing apoptosis, or planned cell death, into the target. They can also bind to the Fas ligand, on the outside of the target cell and use it to cause apoptosis in the target [44].

Once the threat is gone, the immune system removes the antigens and the non-memory cells primed to handle that particular threat [45]. Because they can only attack the cells they are primed for, CD8$^+$ T-cells that have been primed are obsolete once the threat is gone.

Chapter 3

Immunotherapy and Chemotherapy

3.1 Chemotherapy

At present, chemotherapy is the most well established treatment for fighting cancer. Chemotherapy is the administration of one or more drugs designed to kill tumor cells at a higher rate than normal cells. The drug is typically administered intravenously [26]. Chemotherapy drugs can be divided into two types, cell cycle specific, and cell cycle non-specific. Cell cycle specific drugs can only kill cells in certain phases of the cell cycle, while non-specific drugs can kill cells in any phase of cell division [101].

The distinction between specific and non-specific chemotherapy drugs is important in considering how a tumor population responds to the drug. The response of a population to varying doses of drug is usually found in the context of a dose-response curve, where dose is plotted against the fraction of the cells killed. If the drug is non-specific, its dose response curve is typically linear. A linear dose response curve means that if twice as much drug is given, one would expect twice as many tumor cells to die. Drugs that are specific can usually only kill cells in the process of dividing. However, not all cells of a typical tumor will be dividing at the same time. This means that at some point, all of the cells that can be killed by the drug will be killed, but some will be immune-tolerant and remain [101].

A linear dose-response curve might suggest that the best treatment for cancer is simply to give a patient so much drug that all of the tumor cells die. This unfortunately does not work in practice. There are two major complications to such a plan. First of all, chemotherapy drugs kill cells in the process of division. Although cancer cells divide much more rapidly than most normal cells, fast-growing cells, like those in the bone marrow (where immune cells are produced), hair, and stomach lining are also killed by chemotherapy [70].

Another limitation on the amount of chemotherapeutic drug that can be administered is the side effects. High doses of drug can also damage other tissue in the body [70].

One way around these limitations is to combine several specific drugs that act on cells in different phases. This also helps counteract tumor populations that are immune to one type of drug, and to ensure that no one drug needs to be applied at levels toxic to the body [101].

3.2 Immunotherapy

A relatively new cancer treatment technique currently under intensive investigation is immunotherapy. The basic idea behind immunotherapy that by boosting the immune system in vitro, the body can eradicate cancer on its own. There are many ways in which the immune system can be boosted, including vaccine therapy, IL-2 growth factor injections (in order to increase the production of immune cells), or the direct injection of highly activated specific immune cells, such as $CD8^+$ T cells, into the blood stream.

Early clinical trials and animal experiments in immunotherapy during the 1970s failed and were abandoned because better results with chemotherapy experiments were discovered, and many times the cells injected died once in the body. These first immunotherapy attempts simulated the immune system non-specifically by injecting immune simulators without understanding these cytokines' complex function in the body. The alternative approach, which yields more hopeful results is "passive" immunotherapy. This type of immunotherpay involves the transfer of cells that are antitumor-reactivated in vitro and then injected into a patient [105].

Immunotherapy falls into three main categories: immune response modifiers, monoclonal antibodies, and vaccines.

3.2.1 Vaccine Therapy

Tumor vaccines have recently emerged as an important form of immunotherapy. There are fundamental differences between the use and effects of antiviral vaccines and anticancer vaccines. While many vaccines for infectious diseases are preventative, cancer vaccines are designed to treat the disease after it has begun, and to stop the disease from recurring. There is another significant difference between antiviral vaccines and anti-tumor vaccines. When a patient is given a vaccine for an infectious disease such as measles, antibody levels remain elevated for years. Antibody levels for cancer patients in clinical vaccine trials, on the other hand, remain high for time periods on the order of

only months, or even weeks.

The purpose of cancer vaccines is to alert the body to the existence of the tumor. In contrast to the usual meaning behind a vaccine, this type of treatment is administered to patients who already have cancer. The vaccine increases the body's effectiveness at killing tumor cells, as well stimulating the production and/or activation of more cancer specific immune cells. [46]

3.2.2 IL-2 Growth Factor

Interleukin 2 (IL-2) is a growth factor, naturally secreted in the body primarily by CD4 cells, that causes T cell proliferation [60]. The main idea behind using IL-2 in immunotherapy is to boost the number of active $CD8^+$ T cells beyond the body's natural response to foreign tumor cells. IL-2 has the ability to both activate and induce production of T-cells in culture. It occurs naturally in the body and its production in the body decreases with age in animals studies. The cells generated by IL-2 saturation have the ability to kill tumor cells and not normal cells. This type of therapy is effective in vivo, as shown in clinical trials for both humans and mice in the early 1980s with various immune deficiencies, including cancer related AIDS [105].

3.2.3 Immune Cell Boosts

The idea of boosting immune cells directly is to cultivate a large number of tumor primed $CD8^+$ T cells outside the body, and then inject them into the bloodstream. In order to boost the immune system, primed $CD8^+$ T-cells from a patient are cultured so that they have a chance to multiply, then are re-injected into the patient. This artificial increase in the strength of the immune response may give a patient the assistance needed to eradicate the cancer [105].

Survival capacity of primed $CD8^+$ T cells depends on resistance to death and response to cytokines, such as IL-2. The cells need a certain stimulation strength in order to remain alive and active once in the body [61]. Many clinical trials today use a combination of chemotherapy and immunotherapy in cancer patients, including T cell transfer and high-dose IL-2 therapy after nonmyeloablative lymphodepleting chemotherapy which results in rapid in vivo growth of $CD8^+$ T cells and tumor regression [49].

3.3 Benefits of Modeling Treatment Options

Treatment of cancer advances rapidly and new methods and techniques develop every year. Therefore, simply trying to experimentally determine the best way to implement these new techniques would be both excessively dangerous and expensive. By modeling a new treatment method or combination of methods, mathematical biologists may be able to tell clinicians the best uses for new techniques.

One major question that we hope to shed light on by modeling cancer treatments is how immunotherapy and chemotherapy interact. There is some speculation that the effects are larger than the sum of each being used independently [49]. On the contrary, it is also quite possible that immunotherapy and chemotherapy would target the same cells, and so the effect would be smaller than the sum of the two independently.

Part II

ODE model

Chapter 4

ODE Model Formulation

4.1 Assumptions

The framework for tour ODE model was developed by de Pillis et al.[42], to which we add additional cell interaction terms as well as chemotherapeutic and immunologic elements. For the sake of completeness, we outline the assumptions of the original model [42] here.

- A tumor grows logistically in the absence of an immune response.

- Both NK and CD8$^+$ T-cells are capable of killing tumor cells.

- Both NK and CD8$^+$ T-cells respond to tumor cells by dividing and increasing metabolic activity.

- There are always NK cells in the body, even when no tumor cells are present.

- Tumor-specific CD8$^+$ T-cells are only present in large numbers when tumor cells are present.

- NK and CD8$^+$ T-cells eventually become inactive after some number of encounters with tumor cells.

We add the following assumptions in our model formulation.

- Chemotherapy kills a fraction of the tumor population according to the amount of drug in the system. The fraction killed reaches a saturation point, since only tumor cells in certain stages of development can be killed by chemotherapy [101].

- A fraction of NK and CD8$^+$ T-cells are also killed by chemotherapy, according to a similar concentration vs fractional kill curve [59].

- NK cells regulate the production and elimination of activated CD8$^+$ T-cells.

4.2 Model Equations

Continuing the method developed by de Pillis *et al.* [42], we outline a series of coupled ordinary differential equations describing the kinetics of several populations. Our model tracks four populations (tumor cells and three types of immune cells), as well as two drug concentrations in the bloodstream. These populations are denoted by:

- $T(t)$, tumor cell population at time t

- $N(t)$, total NK cell effectiveness at time t

- $L(t)$, total CD8$^+$ T cell effectiveness at time t

- $C(t)$, number of circulating lymphocytes (or white blood cells) at time t

- $M(t)$, chemotherapy drug concentration in the bloodstream at time t

- $I(t)$, immunotherapy drug concentration in the bloodstream at time t

The equations governing the population kinetics must take into account the growth and death (G), the fractional cell kill (F), per cell recruitment (R), cell inactivation (I) and human intervention(H), in the populations. We attempt to use the simplest expressions for each term that still accurately reflect experimental data and recognize population interactions. Figure 4.1 provides the reader with a schematic of the new model.

$$\frac{dT}{dt} = G(T) - F_N(T, N) - F_L(T, L) - F_{MT}(T, M)$$

$$\frac{dN}{dt} = G(N) + R_N(T, N) - I_N(T, N) - F_{MN}(N, M)$$

$$\frac{dL}{dt} = G(L) + R_L(T, L) - I_L(T, L) + R_L(T, N) + R_L(T, C)$$
$$- I_L(N, L) - F_{ML}(L, M) + F_{IL}(I, L) + H_L$$

$$\frac{dC}{dt} = G(C) - F_{MC}(C, M)$$

$$\frac{dM}{dt} = G(M) + H_M$$

$$\frac{dI}{dt} = G(I) + H_I$$
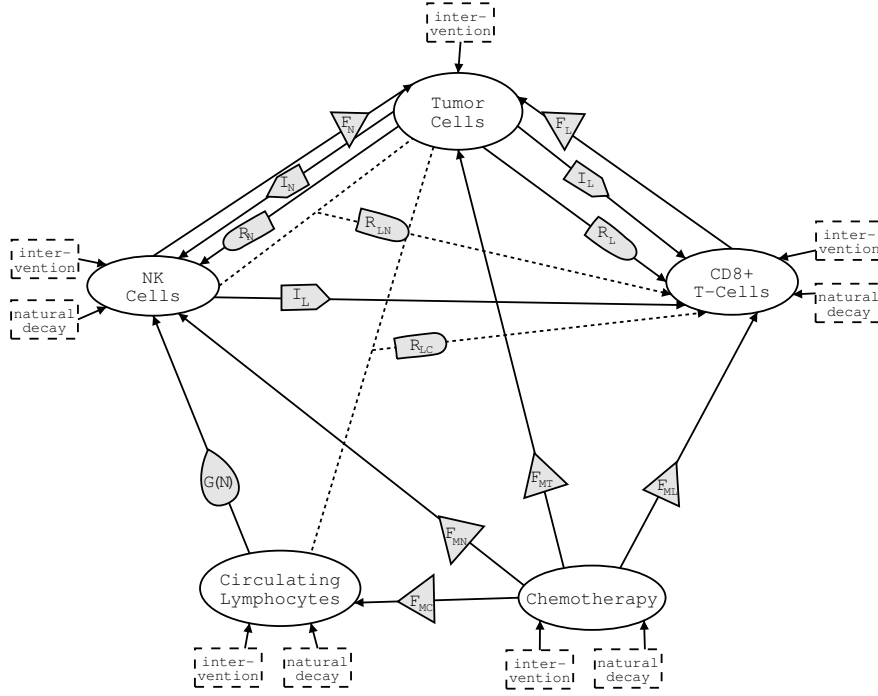
Figure 4.1: A schematic diagram of the tumor-immune model. The arrows represent the direction of influence and the dotted lines signal that the interaction of two populations are influencing the third population. The G interaction term is represented by a teardrop, the F terms are represented by triangles, the R terms are represented by rounded boxes, I terms by pentagons, and H terms by dashed boxes.

4.2.1 Growth and Death Terms

We adapt the growth terms for tumor and CD8$^+$ T-cells from a model developed by de Pillis *et al.* [42]. Tumor growth is assumed to be logistic, based on data gathered from immunodeficient mice [46]. Therefore $G(T) = aT(1 - bT)$. Cell growth for CD8$^+$ T-cells consists only of natural death rates, since no CD8$^+$ T-cells are assumed to be present in the absence of tumor cells. Therefore $G(L) = -iL$.

Rather than assuming a constant NK cell production as in the original model, we tie this growth term to the overall immune health levels via the population of circulating lymphocytes. This allows for the suppression of stem cells during chemotherapy, which lowers circulating lymphocyte counts, to affect the production rate of NK cells. Therefore, $G(N) = eC - fN$, where $e = e_{\text{old}}/C_{\text{equilibrium}}$. We assume that circulating lymphocytes are generated at a constant rate, and that each cell has a natural lifespan. This gives us

the term $G(C) = \alpha - \beta C$. In addition, the chemotherapy drug also has a natural life span, and so we assume that it decays at some constant rate such that $G(M) = -\gamma M$. Similarly, the immunotherapy drug, Interleukin-2 (IL-2), has a natural life span and decays in the same way, $G(I) = -\mu_i I$.

4.2.2 Fractional Cell Kills

We take our fractional cell kill terms for N and L from de Pillis *et al.* [42]. The fractional cell kill terms represent negative interactions between two populations. They can represent competition for space and nutrients as well as regulatory action and direct cell population interaction. The interaction between tumor and NK cells takes the form $F_N(T, N) = -cNT$. Tumor inactivation by CD8$^+$ T-cells, on the other hand, has the form:

$$F_L(T, L) = d\frac{(L/T)^{eL}}{s + (L/T)^{eL}}T.$$

Since this term is used in other parts of the model as the number of tumor cells lysed by CD8$^+$ T cells, we assign the expression to the letter D. This gives us $D = \frac{(L/T)^{eL}T}{s+(L/T)^{eL}}$, and $F_L(T, L) = dD$.

Our model adds a chemotherapy drug kill term to each of the cell populations. Chemotherapeutic drugs are only effective during certain phases of the cell division cycle, so we use a saturation term $1 - e^{-M}$ for the fractional cell kill. Note that at relatively low concentrations of drug, the response is nearly linear, while at higher drug concentration, the response plateaus. This corresponds with the drug response suggested by the literature [59]. We therefore adopt $F_{M\phi} = K_\phi(1 - e^- M)\phi$, for $\phi = T, N, L, C$.

In addition, our model includes an activated CD8$^+$ T boost from the immunotherapy drug, IL-2. This 'drug' is a naturally occurring cytokine in the human body, and it takes on the form of a Michaelis-Menton interaction in the dL/dt term. The presence of IL-2 stimulates the production of CD8$^+$ T cells, and therefore $F_{IL} = \frac{p_i LI}{g_i + I}$. The addition of this term was developed in Kirschner's tumor-immune model [80].

4.2.3 Recruitment

The recruitment of NK cells takes on the same form as the fractional cell kill term for CD8$^+$ T-cells, with eL equal to two, as described by de Pillis *et al.* [42]. This form provides

the best fit for available data [46]. Hence the NK cell recruitment term is

$$R_N(T, N) = g \frac{T^2}{h + T^2} N.$$

It should also be noted that this is a modified Michaelis-Menten term, commonly used in tumor models to govern cell-cell interaction[83], [42], [80]. This type of term has been questioned in the past by Lefever *et al.* [85] as an oversimplification of the steady state assumption without necessary conditions. Although this type of term has been contested, this modified term does fit available our data and agrees with NK-tumor conjugation frequency studies, [57]. As such, we continue to use it in our model, noting the stady state assumption may not apply for extreme conditions.

CD8$^+$ T-cells are activated by a number of things, including the population of tumor cells that have been lysed by other CD8$^+$ T-cells. The CD8$^+$ T cell recruitment term follows a similar format of the NK cell recruitment, however the tumor population is replaced with the lysed tumor population from the tumor-CD8$^+$ T cell interaction, D.[1] Thus our new recruitment term is of the form:

$$R_L(T, L) = g \frac{D^2}{k + D^2}.$$

CD8$^+$ T-cells can also be recruited by the debris from tumor cells lysed by NK cells. This recruitment term is dependant on some fraction of the number of cells killed. From this, we procure the term $R_L(N, T) = r_1 NT$. The immune system is also stimulated by the tumor cells to produce more CD8$^+$ T-cells. This is also assumed to be a direct cell-cell interaction term, and is written $R_L(C, T) = r_2 CT$.

4.2.4 Inactivation Terms

Inactivation occurs when an NK or CD8$^+$ T cell has interacted with tumor cells several times and eventually fails to be effective at destroying more foriegn cells. We use the inactivation terms developed by de Pillis *et al.* [42]. These parameters do not directly match the fractional cell kill terms, since they represent a slightly different biological concept. The parameters in front of the inactivation terms represent mean inactivation rates. This

---

[1]In adopting the equations developed by de Pillis *et al.* we move d out of the expression for D. Therefore our parameter k differs from the value used for dePillis's model by a factor of $1/d^2$ for the $R_L(N, L)$ term.

gives us terms of the form $I_N = -pNT$ and $I_L = -qLT$.

The third inactivation term, $I_{CL} = -uNL^2$, describes the NK cell regulation of CD8$^+$ T-cells, which occurs when there are very high levels of activated CD8$^+$ T cells without responsiveness to cytokines present in the system [61]. The exact interaction is still not well understood, but there is experimental data, showing that CD8$^+$ T cells proliferate in the absense of NK cells. This term includes a squared L since the data reveals that CD8$^+$ T cell level has a larger effect on CD8$^+$ T cell inactivation than the amount of NK cells. This term comes into play when immunotherapy increases the amount of CD8$^+$ T cells in the body, and experimental data document that these cells rapidly become inactivated even with a tumor present [105]. The cytokine IL-2 aids in their resistance to this inactivation.

4.3 Drug Intervention Terms

The TIL drug intervention term, $H_L = v_L(t).$, for the CD8$^+$ T cell population represents immunotherapy where the immune cell levels are directly boosted. Similarly, the drug intervention terms in the dM/dt and dI/dt equations reflect the amount of chemotherapy and immunotherapy drug given over time. Therefore, they are given the form $H_M = v_M(t)$ and $H_I = v_I(t)$.

4.3.1 Equations

The full equations, once all of the terms have been substituted in, are listed below. The expression for D is one that appears in several locations, and so is listed seperately below and referenced in the differential equations.

$$\frac{dT}{dt} = aT(1 - bT) - cNT - dD - K_T(1 - e^{-M})T \tag{4.1}$$

$$\frac{dN}{dt} = eC - fN + g\frac{T^2}{h + T^2}N - pNT - K_N(1 - e^{-M})N \tag{4.2}$$

$$\frac{dL}{dt} = -mL + j\frac{D^2}{k/d^2 + D^2}L - qLT + (r_1N + r_2C)T - uNL^2 - K_L(1 - e^{-M})L + \frac{p_iLI}{g_i + I} + v_L(t) \tag{4.3}$$

$$\frac{dC}{dt} = \alpha - \beta C - K_C(1 - e^{-M})C \tag{4.4}$$

$$\frac{dM}{dt} = -\gamma M + v_M(t) \tag{4.5}$$

$$\frac{dI}{dt} = -\mu_i I + v_I(t) \tag{4.6}$$

$$D = \frac{(L/T)^{eL}}{s + (L/T)^{eL}}T \tag{4.7}$$

Chapter 5

Parameter Derivation

To facilitate simulations of our proposed model, it is necessary to obtain accurate parameters for our equations. Unfortunately there is no plethora of tumor-immune interaction data available to choose from. Therefore we make use of both murine experimental data [46] and human clinical trials [49] as well as previous model parameters that have been fitted to experimental curves [42, 83]. We then run simulations with both sets of parameters in order to evaluate the behavior of our model[1].

5.1 Chemotherapy Parameters

We estimate the values of the kill parameters, K_T, K_N, K_L, and K_C, based on the log-kill hypothesis. We then assume the drug strength to be one log-kill, as described in [102]. K_N, K_L, and K_C are assumed to be smaller than K_T, but similar in magnitude, since immune cells are one of the most rapidly dividing normal cell populations in the body.

We calculate the drug decay rate, γ, from the drug half-life and the relation $\gamma = \frac{\ln 2}{t_{1/2}}$. We estimated the drug half-life $t_{1/2}$ to be 18+ hours, based on the chemotherapeutic drug doxorubicin [24].

5.2 New IL-2 Drug Parameters

In addition to the original model that includes a chemotherapy differential equation, we introduce a immunotherapy drug into our system of differential equations. The cytokine Interleukin 2 (IL-2) simulates CD8$^+$ T cell proliferation. It has been administered in clinical trials on its own, in combination with chemotherapy, as well as after a TIL (tumor infiltrating lymphocyte) injection, in which a large number of highly activated CD8$^+$ T cells are added to the system at a certain point in time [105], [36], [67] [88]. In order to

---

[1]See Appendix A for a full listing all of the parameters with their units and descriptions.

incorporate this type of immunotherapy into our model, we create a new variable for IL-2 concentration over time, and adjust the CD8$^+$T cell population variable accordingly.

Our three new parameters, p_i, g_i, μ_i, come from Kirschner's model with minor alterations to adapt to the fact that we are only concerned with the amount of IL-2 that is not naturally produced by the immune system. Since the presence of IL-2 in the body stimulates the production of CD8$^+$ T cells, we include a Michaelis-Menton term for the CD8$^+$ T cell growth rate induced by IL-2. The drug equation for IL-2 is identical in form to our chemotherapy term, and its half-life, μ_i is taken from Kirschner's model as well [80].

5.3 Additional Regulation Parameters

The values of r_2 and u are based on reasonable simulation outcomes of our model. The conditions we set on u is that the term uNL^2 must be smaller in magnitude, for most tumor burdens, than the negative terms that involved the tumor population in our equation for dL/dt. Our reason for this is primarily qualitative since NK cells only eliminate CD8$^+$ T cells in excess or in the absence of a tumor burden.

5.4 Mouse Parameters

The mouse parameters shown in Table 5.1 primarily originate from curve fits by de Pillis *et al.* [42]. The experimental data for these curve fits came from a set of murine experiments that investigated the absence of immune response to tumor cells by using the innovative idea of ligand transduction, an idea that uses the immune system to fight cancer more efficient. Cells that are primed with specific antigens so that the immune system can easily recognize them as a foreign threat are ligand transduced. This process works in a similar way to a vaccine in that dead primed tumor cells are first injected into the patient so that the immune system will react and kill the foreign material. Since these cells were primed, the immune cells are now aware of any similar threat that presents itself with the same kind of priming [46].

In our model, we obtain the values of a, b, c, d, eL, f, g, h, j, m, p, q, r_1 and s from curve fits of the ligand transduced data [42]. de Pillis *et al.* fit most of the data by plotting the immune cell to tumor ratio against the percent of cells lysed. Our value of k is equal to the value of k_{old}/d^2 since in our model the parameter d exists outside of the expression for D (see de Pillis *et al.* [42]).

In order to calculate α and β, values not included in de Pillis's model, we first calculate several intermediate values. The first of these is the number of milliliters of blood in the average mouse. This information was obtained from [1]. We assume that the mice weigh 30 g and therefore contained approximately 1.755 mL of blood. Based on the white blood cell count, 6×10^8, of the mice, 50 to 70 percent of the WBC count are made up of circulating lymphocytes [68]. We obtain an equilibrium amount of circulating lymphocytes in the absence of tumor or treatment that is approximately equal to 1.01×10^7. We assume the lifespan of human white blood cells listed in [10] is approximately equal to their lifespan in mice, and take the reciprocal of this to find the decay rate, β. We then use the equilibrium solution of the differential equation for C in the absence of treatment, $1.01 \times 10^7 = C_{\text{equilibrium}} = \alpha/\beta$, to calculate α. We then use the equilibrium number of circulating lymphocytes to convert the parameter e [42] to our new model, according to $e_{\text{old}}/C_{\text{equilibrium}} = e$. We calculate e so that $e \times C_{\text{equilibrium}}$ equals 1.3×10^4, the value of e given in [42].

In order to implement our vaccine therapy model, we examined the parameters for murine experiments involving non-ligand transduced tumor cells. The altered parameters are c, d, eL, g, j, and s [42]. Their values are shown in Table 5.2. These values correlate to a mouse in the absence of vaccine treatment. By comparing these values to the original, we get a sense for how a vaccine would affect the system for humans. When we examine the changes that vaccine therapy makes upon these mouse parameter, we are looking for resonable parameters values in the human model and not exact changes.

5.5   Human parameters

The values shown in Table 5.3 and Table 5.4 are sets of human parameters that originate from the curve fits created by dePillis *et al.* [42], human patients from clinical trials [49], as well as from an additional and similar tumor model [83]. We separate these parameters into two tables, since only a subset of them are patient specific according to previous investigations.

We obtain the values of $b, c, d, eL, f, g, h, j, m, p, r_1$, and s from data collected from patient 9 in a clinical trial for combination therapy [42], [49]. We use the value of a from curve fits by dePillis *et al.* and the murine experiments since this parameter is strictly for tumor growth and is independent of the human or mouse immune cells. We take the values of additional parameters f and h from Kuzenetsov's tumor-immune model.

$$a = 0.43078 \qquad b = 2.1686 \times 10^{-8} \qquad c = 7.131 \times 10^{-10} \qquad d = 8.165$$
$$e = 1.29 \times 10^{-3} \qquad eL = 0.6566 \qquad f = 0.0412 \qquad g = 0.498$$
$$h = 2.019 \times 10^{7} \qquad j = 0.996 \qquad k = 3.028 \times 10^{5} \qquad m = 0.02$$
$$p = 1 \times 10^{-7} \qquad q = 3.422 \times 10^{-10} \qquad r_1 = 1.1 \times 10^{-7} \qquad r_2 = 3 \times 10^{-11}$$
$$s = 0.6183 \qquad u = 1.8 \times 10^{-8} \qquad K_T = 0.9 \qquad K_N = 0.6$$
$$K_L = 0.6 \qquad K_C = 0.6 \qquad \alpha = 1.21 \times 10^{5} \qquad \beta = 0.012$$
$$\gamma = 0.9$$

Table 5.1: Model parameters for mice challenged and re-challenged with ligand transduced tumor cells, [42], [46].

$$c = 6.41 \times 10^{11} \qquad d = 0.7967 \qquad eL = 0.8673$$
$$g = 0.1245 \qquad j = 0.1245 \qquad s = 1.1042$$

Table 5.2: Parameters adjusted from Table 5.1 for mice challenged and re-challenged with non-ligand transduced tumor cells, representing a less effective immune response, [42], [46].

$$
\begin{array}{lll}
a = 0.43078 & b = 1 \times 10^{-9} & c = 6.41 \times 10^{-11} \\
e = 2.08 \times 10^{-7} & f = 0.0412 & g = 0.01245 \\
h = 2.019 \times 10^{7} & j = 0.0249 & k = 3.66 \times 10^{7} \\
r_1 = 1.1 \times 10^{-7} & K_T = 0.9 & K_N = 0.6 \\
K_L = 0.6 & K_C = 0.6 & u = 3 \times 10^{-10} \\
\alpha = 7.5 \times 10^{8} & \beta = 0.012 & \gamma = 0.9 \\
p_i = 0.1245 & g_i = 2 \times 10^{7}, & \mu_i = 10
\end{array}
$$

Table 5.3: Model parameters shared by Patient 9 and Patient 10 [42, 49, 80].

The value of q that we use in our model is similar in magnitude to that of dePillis *et al.*, however we adjust it accordingly after the addition of the new r_1, r_2, and u terms in the dL/dt equation.

In order to calculate α and β for the human population, we estimate the amount of blood in the average human to be 5 liters [30]. Based on a typical white blood cell count for humans of 4.2×10^{10}, and the percentage made up of circulating lymphocytes of about 25 to 70 percent of white blood cells [68]. Therefore we obtain an equilibrium number of circulating lymphocytes of 6.25×10^{10}.

Once we find the lifespan of circulating lymphocytes [10], we take the reciprocal to find β. We then use the equilibrium solution of the differential equation for C in the absence of treatment, $6.5 \times 10^{10} = C_{equilibrium} = \alpha/\beta$, to calculate α. We then use the equilibrium number of circulating lymphocytes to convert the parameter e from [42] to our new model, according to $e_{old}/C_{equilibrium} = e$.

5.6 Further Parameter Investigation

We use these sets of parameters to produce simulations for our model and determine its qualitative behavior in the next three chapters. Chosing a variety of parameter sets allows us to test our model with several sets of experimental data and take a closer look at patient specific behavior.

	Patient 9		Patient 10	
$d = 2.3389$	$eL = 2.0922$	$d = 1.8792$	$eL = 1.8144$
$k = 3.66 \times 10^7$	$m = 0.2044$	$k = 5.66 \times 10^7$	$m = 9.1238$
$p = 3.422 \times 10^{-6}$	$q = 1.422 \times 10^{-6}$	$p = 3.593 \times 10^{-6}$	$q = 1.593 \times 10^{-6}$
$r_2 = 2 \times 10^{-11}$	$s = 0.0839$	$r_2 = 6.81 \times 10^{-10}$	$s = 0.512$

Table 5.4: Model parameters that differ between Patient 9 and Patient 10 [42, 49, 80].

Chapter 6

Model Behavior: Mouse Parameter Experiments

6.1 Mouse Data Sample

We test the accuracy of our model with the results from a set of murine experiments
presented in Diefenbach's work [46]. This data has been tested in simulations for dePillis's
model [42]; we test it again here with our adapted model and observe its behavior. We
examine cases where the immune system cannot fight a growing tumor on its own and
cases where neither chemotherapy or immunotherapy alone can kill the tumor. We also
discover a case where both types of treatment are necessary to cause a large tumor to die.
For the following experiments, we use the mouse parameters provided in Table 5.1.

6.2 Immune System's Tumor Response

In the first set of experiments for the mouse model, we examine a case where the tu-
mor grows too large for the immune system alone to handle, and so it reaches carrying
capacity and we assume the mouse dies under this extreme tumor burden. The initial
conditions for this situation are a tumor burden of 10^6 cells, a circulating lymphocyte
population of 1.1×10^7, a natural killer cell population of 5×10^4, and a population of
100 CD8$^+$ T cells (see Figure 6.1).

6.3 Chemotherapy or Immunotherapy

We next test our model's behavior for a tumor of size 3×10^7, with all initial immune
cell populations consistent with the first experiment, in order to analyze our treatment's
effectiveness on tumor population decline. We observe how the immune system reacts
to the tumor with the addition of pulsed doses of chemotherapy treatment, as well as
with an injection of TIL (tumor infiltrating lymphocytes), an immunotherapeutic injection
of a large number of highly activated CD8$^+$ T cells. For this particular tumor burden,
the tumor survives despite both methods of intervention (see Figure 6.2 and Figure 6.3).
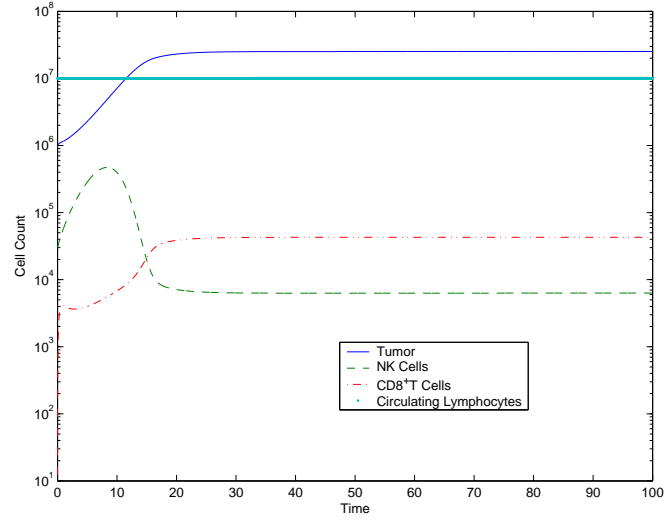
Figure 6.1: Immune system without intervention where the tumor reaches carrying capacity and the mouse 'dies'. Parameters for this simulation are provided in table 5.1.
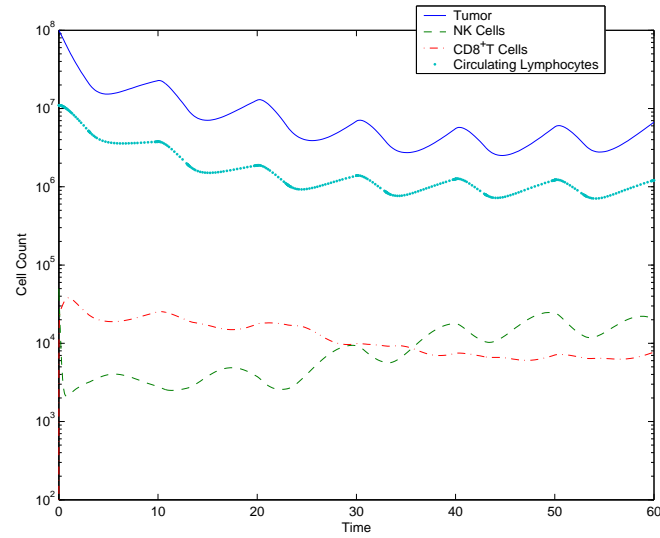
Figure 6.2: The immune system response to high tumor burden with chemotherapy administered for three consecutive days in a ten day cycle. Parameters for this simulation are provided in Table 5.1.
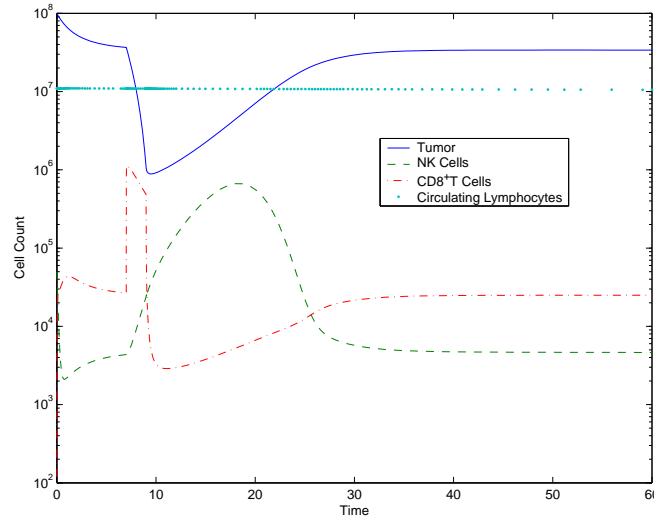
Figure 6.3: Immune system response to high tumor burden with the administration of immunotherapy on days 7 through 10. Parameters for this simulation are provided in Table 5.1.

There are cases for which chemotherapy and immunotherapy will work to kill a tumor (not shown here) that the immune system could not kill alone, but this range of initial conditions is relatively small in comparison to the progress of combination treatment. This result is consistent with experimental investigations [89].

6.4 Combination Therapy

Figure 6.4 displays a combination treatment experiment. Specifically, we administer a pulsed amount of chemotherapy every 10 days for 3 days in a row, coupled with an injection of a 10^8 dose of CD8$^+$ T cells given in between a cycle of chemotherapy treatment on day nine through ten. The simulation shown in Figure 6.4 has initial conditions of 1×10^8 tumor cells, 5×10^4 natural killer cells, 100 CD8$^+$ T cells, and 1.1×10^7 circulating lymphocytes. According to our model, combination therapy works much more effectively at killing a tumor than either type of treatment alone. However, the drop in tumor population for this case is extremely drastic. This may be caused by the extremely high, and perhaps unrealistic level of CD8$^+$ T cells in the body at that time. The drop may also be caused by our Michaelis-Menton terms that assume a steady state. With such a sudden high number of CD8$^+$ T cells in the body, this steady state may not be an appropriate
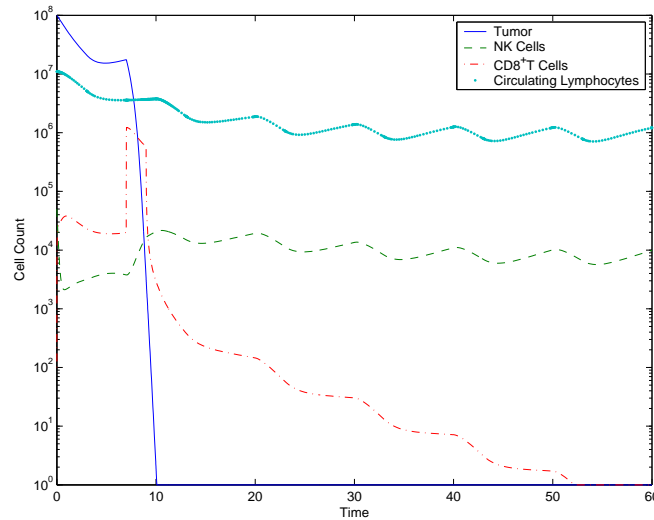
Figure 6.4: A depleted immune system population when tumor appears. The small population size of NK cells means that the population growth of CD8$^+$ T cells is not regulated as much, leading to more effective control of the tumor with combination therapy.

term.

Since neither can be used to the extreme without chemotherapy harming the body or too many CD8$^+$ T cells being administered so quickly that they are automatically killed by NK cells before they have a chance to attack tumor cells. Therefore, it makes sense that combination therapy allows for faster tumor elimination as well as an easier return to a normal level of circulating lymphocytes in the blood stream. The circulating lymphocyte level shows that the health of the mouse has not suffered to a great extent during treatment.

Chapter 7

Model Behavior: Human Data

7.1 Tumor Experiments in the Human Body

We test the behavior and accuracy of our model with experimental results of two patients in Rosenberg's study on metastatic melanoma [49]. We modified our additional parameters, r_2 and u, to fit these results.

First we examine the model with the set of parameters provided in Table 5.4, which is taken from results of Rosenberg's clinical trials. We discover a case where a healthy immune system can control a tumor that a weak immune system cannot, a case where chemotherapy or immunotherapy can kill a tumor burden, and a case where combination therapy is essential to the survival of the patient. We then compare these results for patient 9 to the behavior of our model with patient 10 parameters in order to investigate patient-specific parameter sensitivity.

7.2 Immune System's Tumor Response

In the first set of human experiments, we examine a tumor of 10^6 cells. For this tumor burden, immune system strength is very important in determining whether or not the body alone can kill a tumor. In this situation, a healthy immune system with 1×10^5 natural killer cells, 1×10^2 CD8$^+$ T cells, and 6×10^{10} circulating lymphocytes (see Figure 7.1) has the ability to kill the tumor burden. However, when the immune system is weak enough, a tumor of the same size grows to a dangerous level if left untreated (see Figure 7.2).

7.3 Chemotherapy Treatment

For cases in which the tumor would grow to a dangerous level if left untreated (i.e. the depleted immune system example shown in Figure 7.2), we model pulsed chemotherapy administration into the body after the tumor is large enough to be detected. We carefully
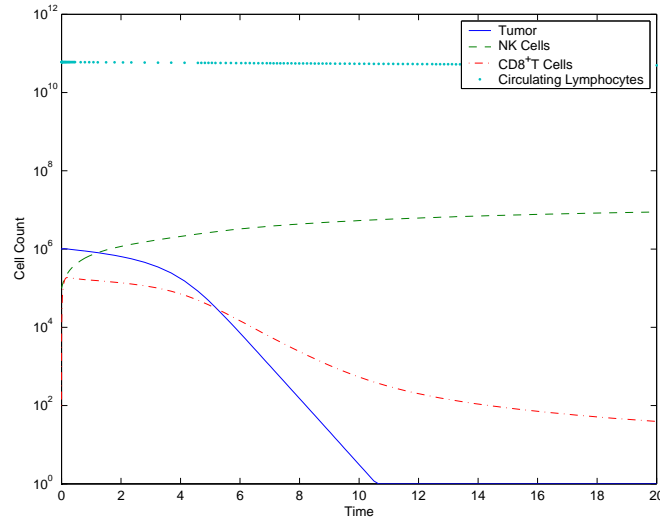
Figure 7.1: A healthy immune system effectively kills a small tumor. Initial Conditions: 1×10^6 Tumor cells, 1×10^5 NK cells, 100 CD8$^+$ T cells, 6×10^{10} circulating lymphocytes. Parameters for this simulation are documented in Table 5.4.
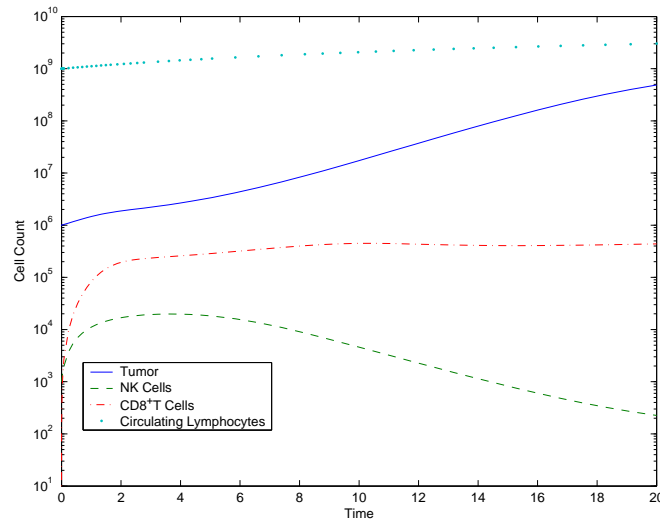
Figure 7.2: A depleted immune system fails to kill a small tumor when left untreated. Initial Conditions: 1×10^6 Tumor cells, 1×10^3 NK cells, 10 CD8$^+$ T cells, 6×10^9 circulating lymphocytes. Parameters for this simulation are documented in Table 5.4.
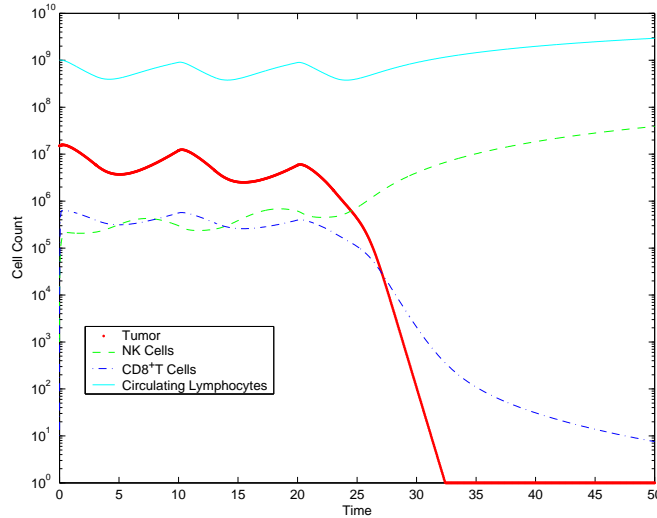
Figure 7.3: A case where three doses of chemotherapy is enough to kill off a tumor. Initial Conditions: 2×10^7 tumor cells, 1×10^3 NK cells, 10 CD8$^+$ T cells, 6×10^9 circulating lymphocytes. Parameters for this simulation are documented in Table 5.4.

examine the tumor's response to pulsed chemotherapy by incrementing pulses and determine that for a tumor burden of 2×10^7 cells, three pulses of chemotherapy are necessary to kill the tumor, and does so within 35 days of treatment commencement (see Figure 7.3). The amount of chemotherapy necessary to cure the cancer is significant, since a treatment with one less pulse of chemotherapy (see Figure 7.5) will allow the tumor to regrow.

7.4 Combination Therapy

While we did find cases in our model for which chemotherapy alone kills a tumor, there are situations in which chemotherapy is not strong enough to kill the tumor without causing serious damage to the immune system. We measure the patient's immunological health by the number of their circulating lymphocytes in the body and do not allow the circulating lymphocytes to drop below a level where risk of infection is not too high. For our case that limit was on the order of 10^8 cells, similar to cutoff levels of chemotherapy for white blood cell counts monitored during chemotherapy treatment [49].

For the case in Figure 7.7, chemotherapy alone is not enough to effectively fight a tumor burden of 10^9 cells, a tumor which would weigh about a gram. This is about
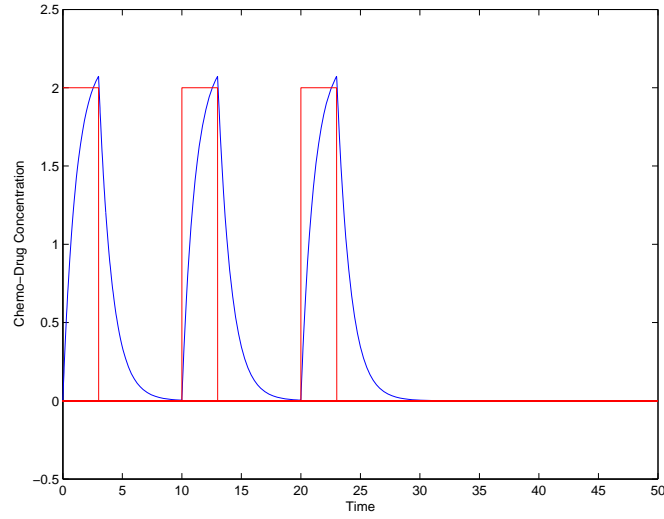
Figure 7.4: The drug administration for Figure 7.3. Chemotherapy is administered for three consecutive days in a ten day cycle.
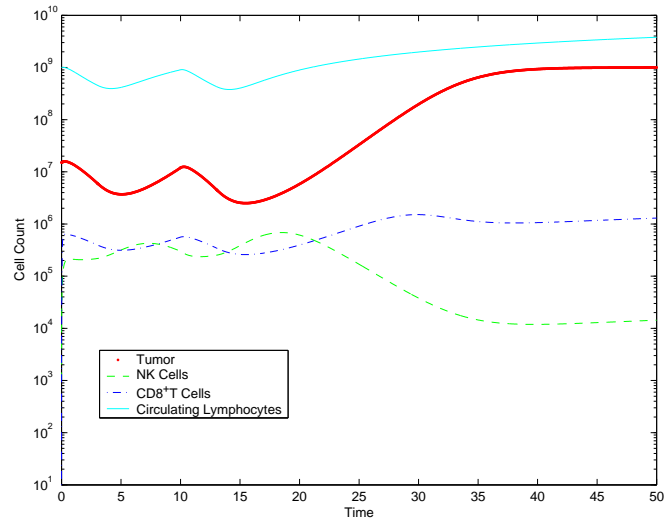
Figure 7.5: A case where a dosage of two intervals of chemotherapy is given and the tumor shows regrowth. Initial Conditions: 2×10^7 Tumor cells, 1×10^3 NK cells, 10 CD8$^+$ T cells, 6×10^9 circulating lymphocytes. Parameters for this simulation are documented in Table 5.4.
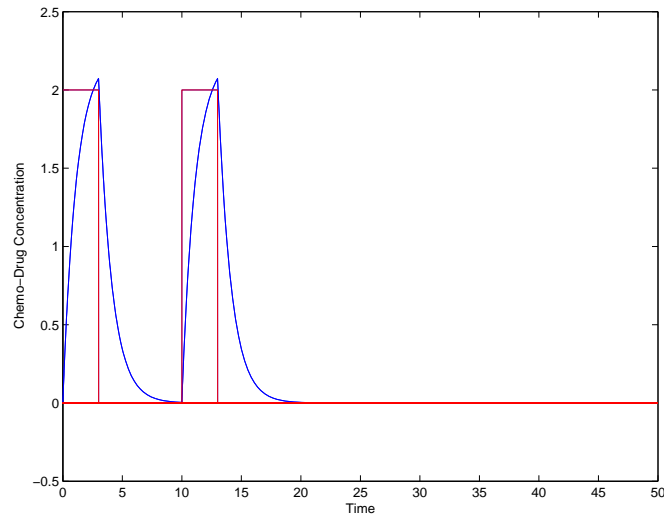
Figure 7.6: The drug administration for figure 7.5. Chemotherapy is administered for three consecutive days in a ten day cycle.
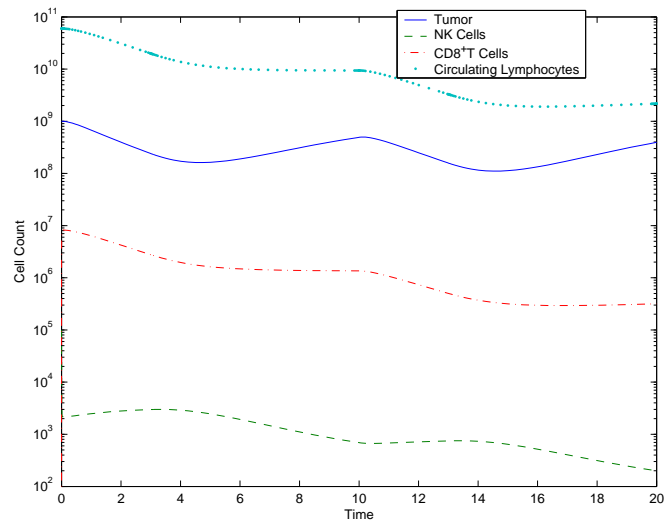
Figure 7.7: A 10^9 cell tumor is not killed by the body with only the aid of chemotherapy. Parameters for this simulation are documented in Table 5.4. See the lower plot of Figure 7.9 for chemotherapy administration.
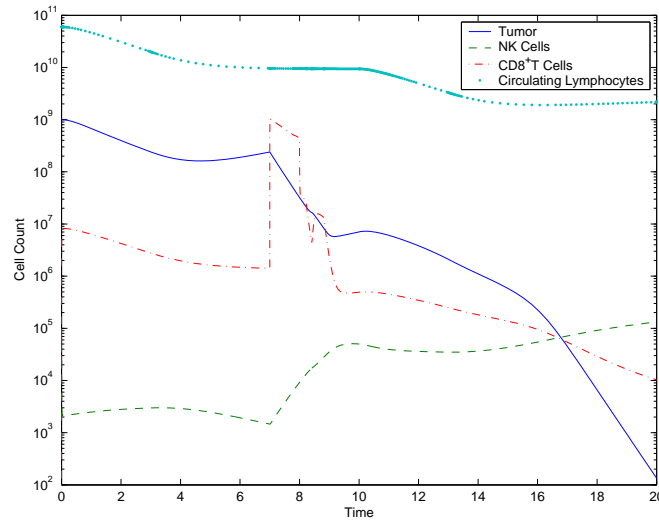
Figure 7.8: Combination therapy is effective in eliminating a tumor burden of 10^9 cells. Parameters for this simulation are documented in Table 5.4. See Figure 7.9 for chemo and immuno therapies administered.

the size that many types of cancer get detected [24]. Since our chemotherapy treatment alone does not work, we add immunotherapy in combination with a modest dosage of chemotherapy (see exact doses in Figure 7.9) and investigate tumor elimination, as is shown in Figure 7.8. In this case, a tumor of size 10^9 is eliminated by the immune system with the help of chemotherapy, followed by an injection of TILs, followed by a series of doses of IL-2. When IL-2 doses were not administered to the patient, the tumor was not effectively killed (figure not shown).

The simulation in Figure 7.8 is consistent to Rosenberg's experiments [49] for patient 9, for whom the treatment shown was in fact effective at attacking a metastatic melanoma. When we create a treatment simulation equivalent to this patient's actual treatment during the clinical trial that was effective at eliminating his cancer, for tumor burdens in a reasonable range for his true tumor size, the outcome was the same. In addition to this experiment, we examined combination therapy for an even larger tumor of size 10^{10}, to ensure that our experiments provide reasonable results and cannot cure extremely large tumor burdens without surgery. In Figure 7.10, the tumor does in fact survive after immunotherapy treatment ends and our simulations seem reasonable.

Figure 7.9: The drug concentration for chemotherapy and immunotherapy. The simulations for these drug concentrations are found in Figures 7.8 and 7.10.
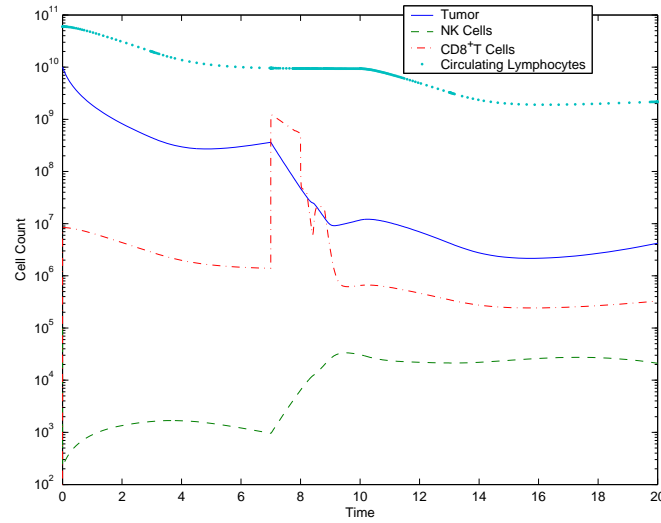
Figure 7.10: Combination therapy is ineffective for a tumor burden of size 10^{10}. Parameters for this simulation are documented in Table 5.4. The treatments administered for this simulation are provided in Figure 7.9.

7.5 Immunotherapy

In addition to pure chemotherapy treatments, we examined pure immunotherapy treatments. One of the major advantages in mathematical modeling, is that while we can model chemotherapy and combination therapy for which clinical trials have been performed, we can also use our model to simulate immunotherapy alone. Immunotherapy alone has never been clinically tested on humans yet because of the risk, but a computer simulation is perfectly safe. Since we can compare chemotherapy and combination therapy to actual results, we can calibrate our parameters. For this reason, we can have some confidence in our immunotherapy simulations alone, even though there are no clinical trials to directly compare them to.

In this section we examine experiments with only immunotherapy treatment, specifically a TIL injection followed by short doses of IL-2, similar to the treatment that was given to patients 9 and 10 in Rosenberg's experiments [49] following a seven day dose of chemotherapy.

In Figure 7.11, we investigate a 10^6 cell tumor for a case where the immune system cannot handle on its own, but as we have seen in prior trials, doses of chemotherapy are effective for treating patient 9. Figure 7.11 shows what immunotherapy alone would do for this tumor, and this amount of TILs and IL-2 administered here are equivalent to those shown in the lower half of Figure 7.9. The main advantage of this treatment is that the immune system is not being depleted as it is with chemotherapy treatment.

However, it must be mentioned that the range of immunotherapy effectiveness is limited to a small range of tumor sizes. Figure 7.12 shows that immunotherapy alone is not effective at treating the tumor burden of size 10^9 that could be cured by combination therapy as shown in Figure 7.8.

7.6 Comparison with Patient 10

In order to look at how much these treatment simulations vary from patient to patient, we change patient specific parameters from Rosenberg's study, and run similar experimental simulations with the parameters for patient 10 [49]. These parameters are presented in Table 5.4.

First we repeat the experiment simulated in Figure 7.1 for a tumor burden of size 10^6 that the immune system in a healthy state can kill on its own in patient 9. The same
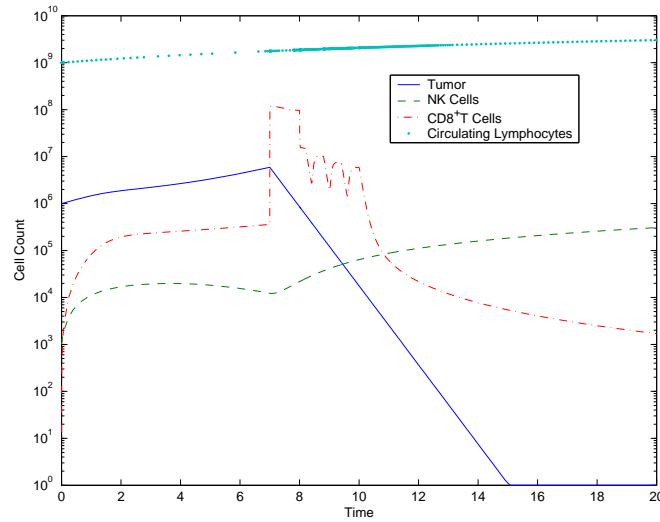
Figure 7.11: Immunotherapy is able to kill a tumor burden of size 10^6 cells. Parameters for this simulation are provided in Table 5.4. 10^9 TILs are administered from day 7 through 8. IL-2 is administered in 6 pulses from day 8 to day 10.
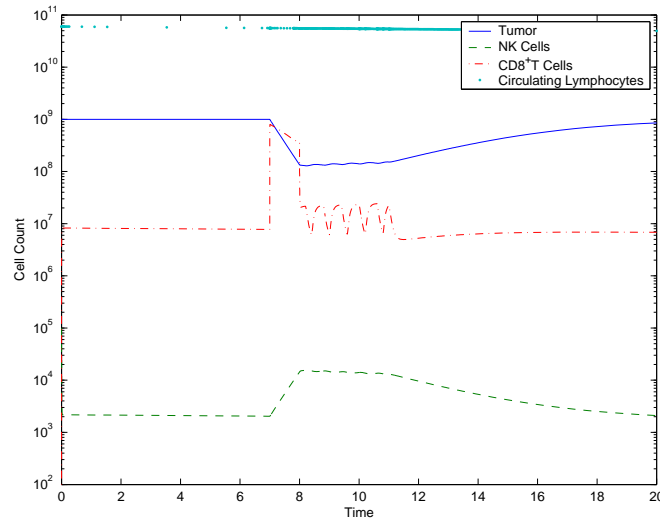
Figure 7.12: Immunotherapy is unable to kill a tumor burden of size 10^9 cells. Parameters for this simulation are provided in Table 5.4. 10^9 TILs are administered from day 7 through 8. IL-2 is administered in 6 pulses from day 8 to day 11.
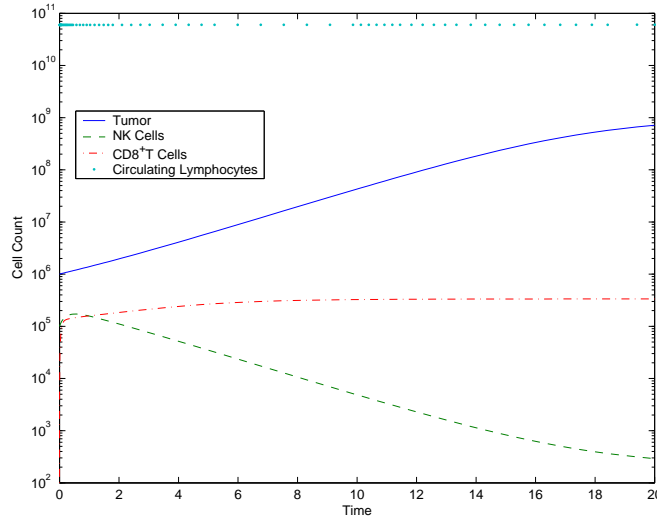
Figure 7.13: Patient 10 cannot kill a 10^6 cell tumor with a healthy immune system of 10^5 NK cells, 100 CD8$^+$ T cells, and 6×10^{10} circulating lymphocytes. Parameters for this simulation are provided in Table 5.4.

healthy immune system conditions that killed the tumor in patient 9 are ineffective at treating the same size tumor in patient 10 (see Figure 7.13). Patient 10's immune system is able to handle a tumor of size 10^5 under the same immune cell count, as we show in Figure 7.14. Unfortunately, the immune system's tumor handling capacity appears very patient specific, which should be unsurprising since the combination therapy administered to 13 patients in Rosenberg's study [49], was only effective at treating two patients.

In addition to the differing results of the immune system alone, we examine the initial conditions where chemotherapy was effective at treating a tumor of size 10^6 with a weak immune system for patient 9. This same simulation with patient 10's parameters yields a different result. Again, the tumor is not killed in this situation, shown in Figure 7.15. We also perform simulations of immunotherapy and combination therapy on patient 10 for a tumor of size 10^6 for the weak immune system. As shown in Figure 7.16, immunotherapy is ineffective at killing this tumor burden. In fact, patient 10 needs combination therapy with pulsed chemotherapy for 100 days before the tumor is eliminated (see Figure 7.17).

In this case it is a good idea to administer more immunotherapy treatment, involving additional doses of IL-2. This expansion in treatment is effective at speeding tumor death. For example, if we allow for three additional days of IL-2 doses of immunotherapy,
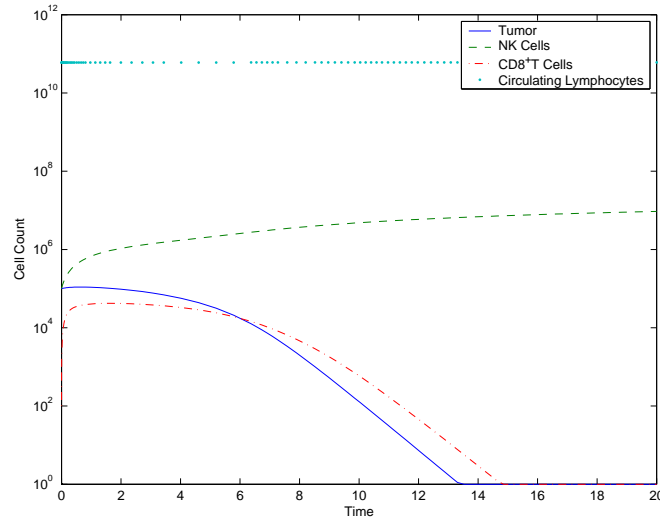
Figure 7.14: Patient 10 kills a 10^5 cell tumor with a healthy immune system of 10^5 NK cells, 100 CD8$^+$ T cells, and 6×10^{10} circulating lymphocytes.
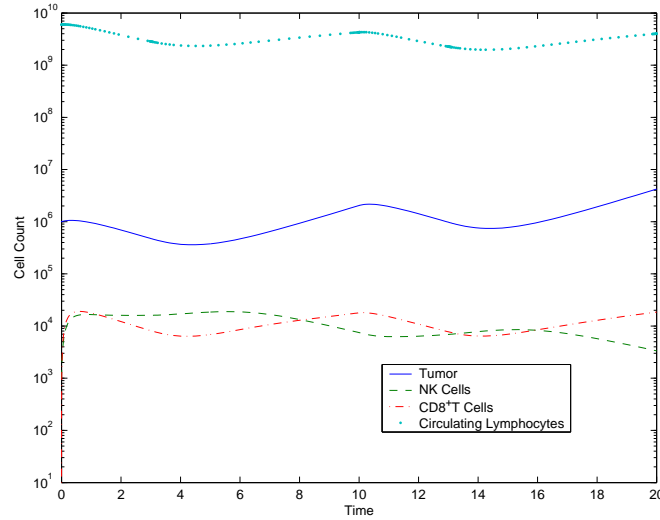
Figure 7.15: Pulsed chemotherapy fails to kill the 10^6 cell tumor in patient 10, even with a healthy immune system of 10^5 NK cells, 100 CD8$^+$ T cells, and 6×10^{10} circulating lymphocytes. The parameters for this simulation are provided in Table 5.4.
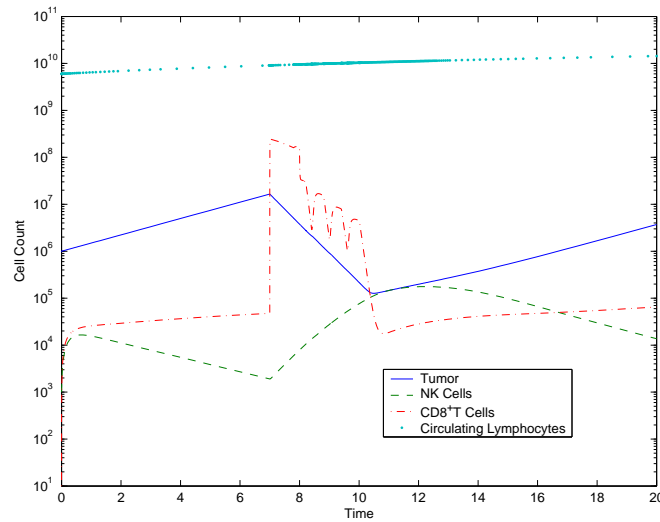
Figure 7.16: TIL and IL-2 immunotherapy fails to kill the 10^6 cell tumor in patient 10, even with a healthy immune system of 10^5 NK cells, 100 CD8$^+$ T cells, and 6×10^{10} circulating lymphocytes. 3×10^8 TIL cells are injected on day 7 through 8. IL-2 is pulsed 4 times between day 8 and day 10. The parameters for this simulation are provided in Table 5.4.
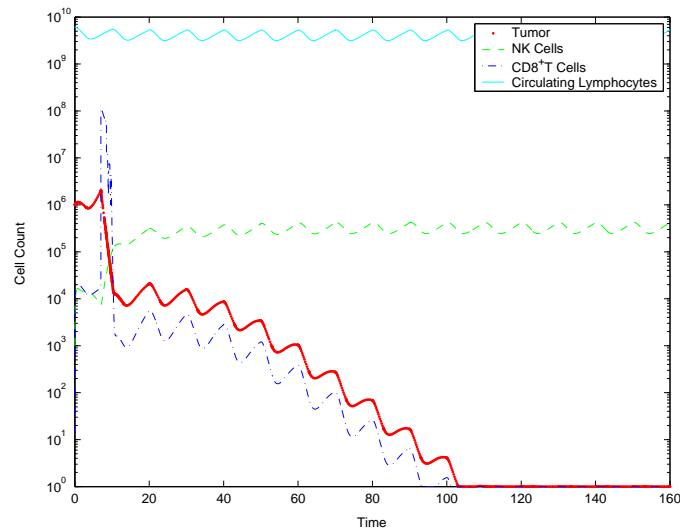
Figure 7.17: Combination therapy kills the 10^6 cell tumor in patient 10. The initial conditions for the immune system are 10^5 NK cells, 100 CD8$^+$ T cells, and 6×10^{10} circulating lymphocytes. Chemotherapy is pulsed 3/10 days as in Figure 7.15 and immunotherapy is administered as in Figure 7.16. The parameters for this simulation are provided in Table 5.4.
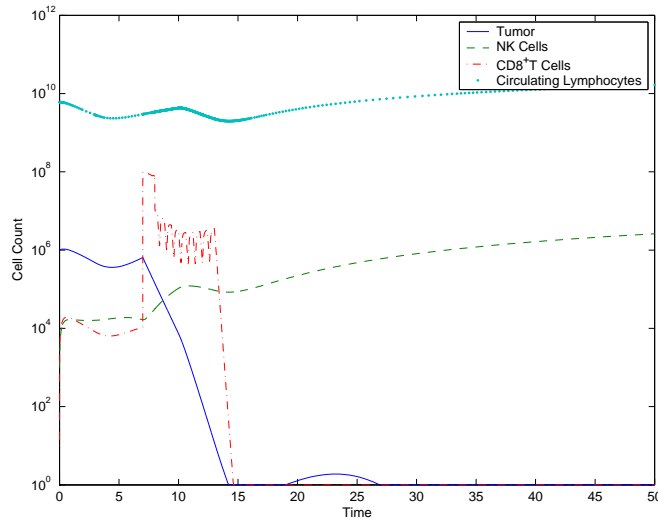
Figure 7.18: Combination therapy kills the 10^6 cell tumor in patient 10 quicker than in Figure 7.17. The initial conditions for the immune system are 10^5 NK cells, 100 CD8$^+$ T cells, and 6×10^{10} circulating lymphocytes. Chemotherapy is pulsed 3/10 days for 15 days. Immunotherapy is administered for longer: 10^8 TILs from day 7 through 8, and then pulses of IL-2 from day 8 through 13.5. The parameters for this simulation are provided in Table 5.4.

with drug treatment shown in Figure 7.19, the tumor will die in less than thirty days (see Figure 7.18).

Since the tumor almost dies within 15 days, we ended the pulsed chemotherapy cycle at that point. However, we do see a relapse in tumor growth once we end chemotherapy. The tumor appears to arise out of nowhere after chemotherapy treatment ends in Figure 7.18, however the immune system is now strong enough to keep it in control.
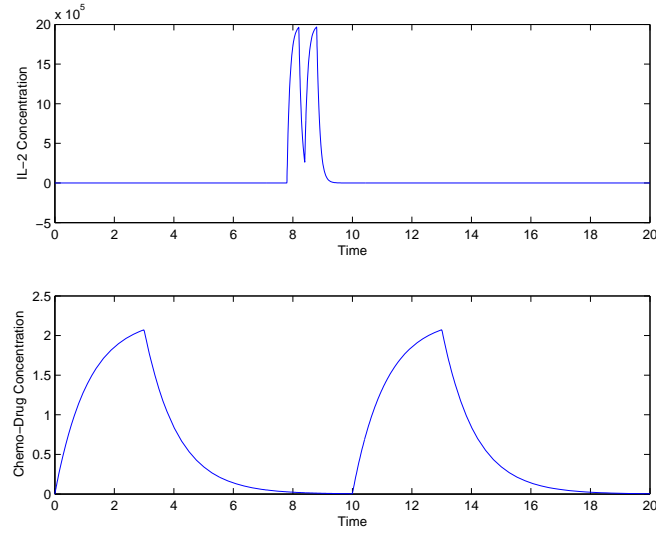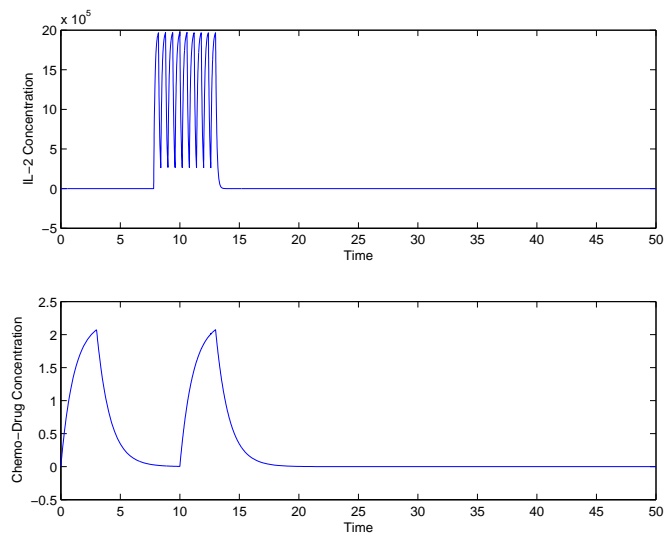
Figure 7.19: Drugs concentration for immunotherapy and chemotherapy. The simulations for these drug concentrations are found in Figure 7.17 and 7.18.

Chapter 8

Model Behavior: Vaccine Therapy

8.1 Vaccine Therapy and a Change of Parameters

In order to simulate vaccine therapy for human patients, we change the values of five parameters at the time of vaccination. These parameter changes are documented by the experimental data found in Diefenbach's results on mouse vaccine trials [46] and the experimental curves produced by these data are fitted to dePillis's model [38]. The parameters that change according to these results are c, the fractional tumor cell kill by natural killer cells, g, the maximum NK-cell recruitment rate by tumor cells, j, the maximum CD8$^+$ T cell recruitment rate, s, the steepness coefficient of the tumor-CD8$^+$ competition term, d, the saturation level of fractional tumor cell kill by CD8$^+$ T cells, and eL, the exponent of fractional tumor cell kill by CD8$^+$ T cells.

We use the original patient 9 parameter set and simulate a possible vaccine therapy treatment by altering parameters in the same direction as they change in Diefebach's murine model [46], [42]. We increase the values of c, g, j, and d and decrease the value of s. We leave eL constant because does not have a simple direct or indirect correlation to vaccine therapy according the changes that a vaccine made on the mouse parameters.

$$
\begin{array}{lll}
c = 7.131e - 9 & g = 0.5 & j = 1 \\
s = .0019 & d = 15 &
\end{array}
$$

Table 8.1: Approximate human vaccine parameters adapted from Table 5.2.
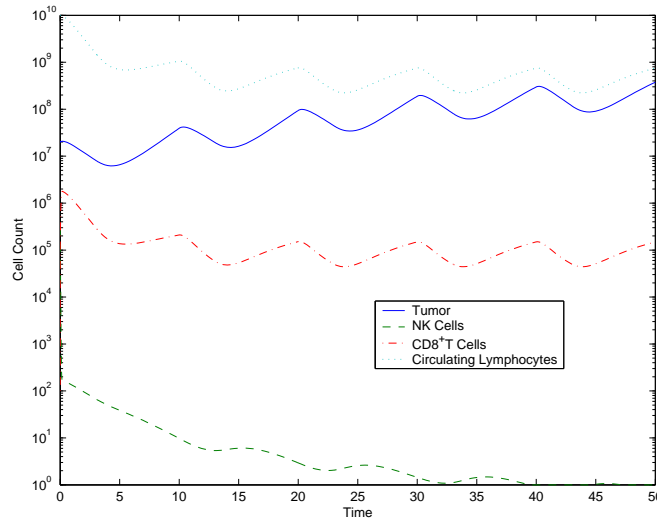
Figure 8.1: Chemotherapy alone cannot kill a 2×10^7 tumor burden with an immune system of 3×10^5 NK cells, 100 CD8$^+$ T cells, and 10^{10} circulating lymphocytes. Chemotherapy is administered for 3 consecutive days in a 10 day cycle. The parameters for this simulation are provided in Table 5.4.

8.2 Vaccine and Chemotherapy Combination Experiments

We first present a theoretical case in which a patient has a detectable tumor of size 2×10^7 and a reasonably healthy immune system of 3×10^5 NK cells, 10^2 CD8$^+$ T cells, and 10^{10} circulating lymphocytes. For this particular case, the patient's body is not strong enough to handle a tumor of this size on its own. As shown in Figure 8.1, the body cannot handle this tumor burden when treated with pulsed chemotherapy for 50 days. In addition, when given a vaccine that changes the original set of parameters after 10 days of tumor growth after the initial conditions also fails to kill the tumor burden (see Figure 8.2). Only the combination of both treatments can kill a tumor of this magnitude (see Figure 8.3).

8.3 Vaccine Therapy Time Dependence

Of course there are also cases for which vaccine therapy alone determines whether or not a tumor dies. However, this is more time dependent since vaccine therapy strength cannot be controlled as we have defined it. We model vaccine therapy as a set change in parameters, and not as a drug population. Therefore the amount of vaccine cannot be
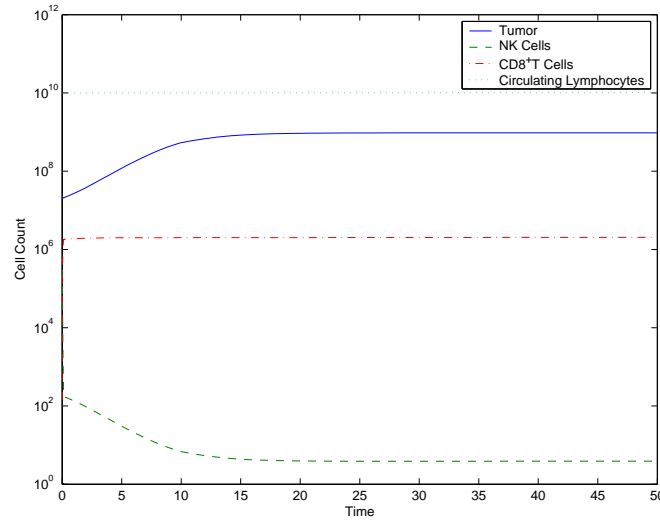
Figure 8.2: Vaccine therapy alone cannot kill the tumor burden shown in Figure 8.1. The parameters for this simulation are provided in Table 5.4, with modified parameters listed in Table 8.1.
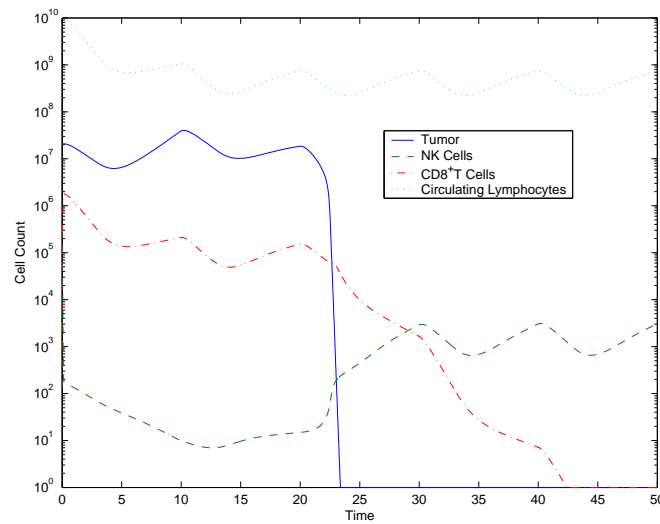
Figure 8.3: Combination Therapy is effective at treating the tumor burden. The parameters for this simulation are provided in Table 5.4, with modified parameters listed in Table 8.1.
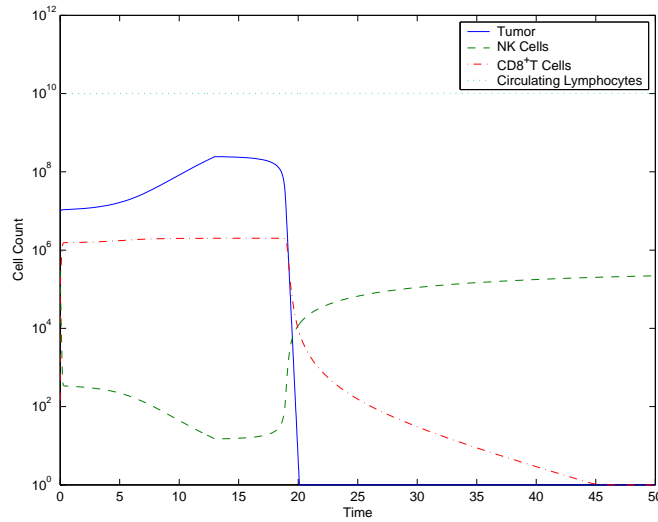
Figure 8.4: Vaccine administered after 13 days. The parameters for this simulation are provided in Table 5.4, with modified parameters listed in Table 8.1.

altered. For the case where a tumor is half the size as in the previous experiments (10^7 cells) and the same immune system initial conditions, vaccine therapy works effectively at tumor elimination if it is administered to the patient no more than 13 days after it is hypothetically detected at 10^7 tumor cells. We show how the timing of vaccine therapy affects the final outcome in Figures 8.4 and 8.5.
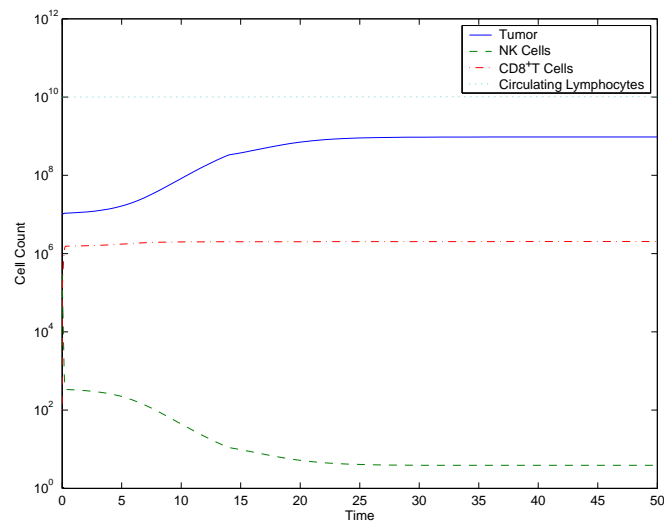
Figure 8.5: Vaccine administer after 14 days. The parameters for this simulation are provided in Table 5.4, with modified parameters listed in Table 8.1.

Chapter 9

Non Dimensionalization

In order to examine the qualitative behavior of our system and uncover the dominating parameters, we simplify the relationship between variables by a non-dimensionalization. The purpose behind this process is to determine which parameter variations will have the greatest effect on our system, as well as to decrease the total number of parameters that can be altered.

We rescale all variables so that all cell populations are approximately equal to unity at their equilibrium values. We let $\tilde{T}$ denote the non-dimensionalized version of T, and then chose an order of magnitude cell population scale, T_0. Similarly, we scale the values for N, L, C, and t as below.

$$T = T_0\tilde{T}, \qquad N = N_0\tilde{N}, \qquad L = L_0\tilde{L}, \qquad C = C_0\tilde{C}, \qquad t = t_0\tilde{t}.$$

We also non-dimensionalize the auxiliary variables by setting

$$\tilde{D} = \frac{D}{T_0} = \frac{(\tilde{L}/\tilde{T})^{eL}}{\frac{s}{(L_0/T_0)^{eL}} + (\tilde{L}/\tilde{T})^{eL}}\tilde{T},$$

$$\tilde{F}_\phi = F_\phi t_0 = K_\phi t_0(1 - e^{-M}) = \tilde{K}_\phi(1 - e^{-M}).$$

We treat the two drug concentrations, M and I, as non-dimensionalized variables. Next we note that this non-dimensionalization transforms Equations (4.1)–(4.4) into the follow-

ing:

$$\frac{d\tilde{T}}{d\tilde{t}} = at_0\tilde{T}(1 - bT_0\tilde{T}) - cN_0t_0\tilde{N}\tilde{T} - dt_0\tilde{D} - \tilde{T}\tilde{F}_T,$$

$$\frac{d\tilde{N}}{d\tilde{t}} = \frac{et_0C_0\tilde{C}}{N_0} - ft_0\tilde{N} + \frac{gt_0\tilde{T}^2\tilde{N}}{\frac{h}{T_0^2} + \tilde{T}^2} - pt_0T_0\tilde{N}\tilde{T} - \tilde{N}\tilde{F}_N,$$

$$\frac{d\tilde{L}}{d\tilde{t}} = -mt_0\tilde{L} + jt_0\frac{\tilde{D}^2}{k/T_0^2 + \tilde{D}^2}\tilde{L} - qt_0T_0\tilde{L}\tilde{T} + \frac{rt_0T_0}{L_0}(N_0\tilde{N} + C_0\tilde{C})\tilde{T}$$

$$+ \frac{t_0p_i}{L_0}\frac{I}{g_i + I}L - ut_0L_0(N_0\tilde{N} + C_0\tilde{C})\tilde{L}^2 - \tilde{L}\tilde{F}_L,$$

$$\frac{d\tilde{C}}{d\tilde{t}} = \frac{t_0\alpha}{C_0} - \beta t_0\tilde{C} - \tilde{C}\tilde{F}_C.$$

We then simplify this new system by choosing T_0 and other new constants as follows:

$$t_0 = \frac{1}{a}, \qquad T_0 = L_0 = \frac{1}{b}, \qquad N_0 = \frac{e\alpha}{f\beta}, \qquad C_0 = \frac{\alpha}{\beta}.$$

This yields a final non-dimensionalized system of equations, similar to the original system in structure:

$$\frac{d\tilde{T}}{d\tilde{t}} = \tilde{T}(1 - \tilde{T}) - \chi\tilde{N}\tilde{T} - \delta\tilde{D} - \tilde{T}\tilde{F}_T$$

$$\frac{d\tilde{N}}{d\tilde{t}} = \varepsilon(\tilde{C} - \tilde{N}) + \tau\frac{\tilde{T}^2}{\eta + \tilde{T}^2}\tilde{N} - \pi\tilde{N}\tilde{T} - \tilde{N}\tilde{F}_N$$

$$\frac{d\tilde{L}}{d\tilde{t}} = -\mu\tilde{L} + \theta\frac{\tilde{D}^2}{\kappa + \tilde{D}^2}\tilde{L} - \xi\tilde{L}\tilde{T} + (\rho_1\tilde{N} + \rho_2\tilde{C})\tilde{T} + \pi_i\frac{I}{g_i + I}\tilde{L} - \zeta\tilde{N}\tilde{L}^2 - \tilde{L}\tilde{F}_L$$

$$\frac{d\tilde{C}}{d\tilde{t}} = \lambda(1 - \tilde{C}) - \tilde{C}\tilde{F}_C$$

$$\frac{dM}{d\tilde{t}} = v\tilde{M}(\tilde{t}) - \bar{\gamma}M$$

$$\frac{dI}{d\tilde{t}} = \tilde{v}_i(\tilde{t}) - \bar{\mu}_i I$$

$$\tilde{D} = \frac{(\tilde{L}/\tilde{T})^{eL}}{s + (\tilde{L}/\tilde{T})^{eL}}\tilde{T}$$

with new non-dimensionalized constants

$$\chi = \frac{ce\alpha}{af\beta} \qquad \delta = \frac{d}{a} \qquad \varepsilon = \frac{f}{a} \qquad \tau = \frac{g}{a}$$

$$\eta = hb^2 \qquad \pi = \frac{p}{ab} \qquad \mu = \frac{m}{a} \qquad \theta = \frac{j}{a}$$

$$\kappa = kb^2 \qquad \xi = \frac{q}{ab} \qquad \rho_1 = \frac{r_1 e\alpha}{af\beta} \qquad \rho_2 = \frac{r_2\alpha}{a\beta}$$

$$\zeta = \frac{ue\alpha}{abf\beta} \qquad \lambda = \frac{\beta}{a} \qquad \pi_I = \frac{p_i}{a} \qquad \bar{\gamma} = \frac{\gamma}{a}$$

$$\bar{\mu}_i = \frac{\mu_i}{a}.$$

This new non-dimensionalized version of our model is useful for further qualitative analysis. Specifically we utilize it to determine equilibria, perform a bifurcation analysis, and investigate optimal control experiments in the next two chapters.

Chapter 10

Equilibria Analysis

10.1 Model Simplification

In order to examine the behavior of these cell populations according to our model, we first examine the simplified system without drug present in the patient by setting $M = 0$. Our system simplifies to

$$\frac{dT}{dt} = aT(1 - bT) - cNT - dD \tag{10.1}$$

$$\frac{dN}{dt} = eC - fN + g\left(\frac{T^2}{h + T^2}\right)N - pNT \tag{10.2}$$

$$\frac{dL}{dt} = -mL + j\frac{D^2}{k + D^2}L - qLT + r_1NT + r_2CT - uNL^2 \tag{10.3}$$

$$\frac{dC}{dt} = \alpha - \beta C \tag{10.4}$$

$$\frac{dM}{dt} = 0. \tag{10.5}$$

The purpose of this investigation is to discover how close to a tumor free state a patient needs to be in order to be considered cured without the threat of relapse. We search for a stable basin of attraction for a tumor free state as well as for additional equilibria that may exist as a state of tumor dormancy.

For the analysis of cell population dynamics, we reduce the system down to three equations by allowing the number of circulating lymphocytes in the body remain to constant at its equilibrium, $C = \frac{\alpha}{\beta}$. Since the differential equation for circulating lymphocytes is independent of the other cell populations, this is its only stable state. Even without drug intervention, there should be a stable basin of attraction around a tumor free equilibrium. The immune system has the ability to fight small tumor burdens on its own, as we see in simulations with the mouse and human parameters.

By setting the derivatives in each of these equations to zero and examining the inter-

sections of the null-surfaces, we can locate stable points for tumor, NK cell, and CD8$^+$ T cell equilibria. On each of these surfaces, the respective cell population is constant since the surface is determined by setting $d\phi/dt = 0$ for all cell populations. Therefore at intersections between all three surfaces, there exist equilibria since then all cell populations will remain constant according to our equations. The equations for the three null-surfaces in our model are described below in terms of N as functions of T and L.

$$\frac{dT}{dt} = 0: \qquad T = 0 \text{ or } N = \frac{a - abT - dD}{c}$$

$$\frac{dN}{dt} = 0: \qquad N = \frac{e\frac{\alpha}{\beta}(h + T^2)}{fh + phT + (f - g)T^2 + pT^3}$$

$$\frac{dL}{dt} = 0: \qquad N = \frac{j\frac{D^2}{k+D^2}L - mL - qLT + r_2\frac{\alpha}{\beta}T}{uL^2 - r_1T}$$

10.2 Tumor Free Equilibrium

If we let the change in tumor population be set to zero by forcing $T = 0$, we see that there exists a tumor free equilibrium with surviving NK and circulating lymphocyte populations but no CD8$^+$ T cells. When $T = 0$,

$$D = \frac{\frac{L}{T}^{e_L}}{s + \frac{L}{T}^{e_L}}T = \frac{TL^{eL}}{sT^{eL} + L^{eL}} = \frac{0 \times L^{eL}}{L^{eL}} = 0 \tag{10.6}$$

$$\frac{dT}{dt} = 0 \tag{10.7}$$

$$\frac{dN}{dt} = eC - fN \tag{10.8}$$

$$\frac{dL}{dt} = -mL - uNL^2 = L(-m - uNL) \tag{10.9}$$

$$\frac{dC}{dt} = \alpha - \beta C \tag{10.10}$$

$$\frac{dM}{dt} = 0 \tag{10.11}$$

and therefore, since $(-m - uNL) < 0$, this tumor free equilibrium exists when

$$T = 0, \qquad N = \frac{e\alpha}{f\beta}, \qquad L = 0, \qquad C = \frac{\alpha}{\beta}.$$

The coexisting equilibria may be too complex to solve analytically and involve solving the roots of polynomials on the order of four or five. Therefore we must use find them numerically.

10.3 Null-surfaces

The intersections between all three null-surfaces indicate where equilibria exist. Figure 10.1 shows the intersection between the non-zero tumor null-surface and NK cell null-surface while Figure 10.2 shows the intersection between the CD8$^+$ T and NK cell null-surfaces. These null-surfaces are taken from the non-dimensionalized model for simplicity, however the dimensionalized surfaces are quite similar in structure. These two sets of intersecting surfaces produce two lines whose intersection provides incite to the system's equilibria.

10.3.1 Tumor Null Surface

The tumor null-surface, shown in Figure 10.1, has the shape similar to a parabola when viewed looking down onto the tumor vs. CD8$^+$ T plane. On the inside of this parabola, where the CD8$^+$ T cell population is small, $dT/dt > 0$. This makes physical sense since the tumor population can grow more easily if there are not many activated CD8$^+$ T cells available nearby to regulate and kill off replicating tumor cells. Since the surface represents a state for which $dT/dt = 0$, it also represents a change in sign between the volumes it separates. On the outside of the parabolic nullcline, where the CD8$^+$ T cell population is high, $dT/dt < 0$. This indicates that there are enough CD8$^+$ T cells to control the tumor burden and the CD8$^+$ T cells are effectively eradicating the tumor.

If chemotherapy or immunotherapy can move a trajectory from the inside to the outside of the tumor null-surface, the body may be able to eradicate the tumor, as long as its trajectory does not fall back into the inside of the parabolic null-surface, allowing tumor regrowth.

10.3.2 NK Null-surface

The NK null-surface, shown in black in both Figure 10.1 and Figure 10.2, is independent of the CD8$^+$ T cell population, and is simply a cubic function of the tumor population. For most cases, $dN/dt < 0$, unless the tumor population is extremely small. For high NK
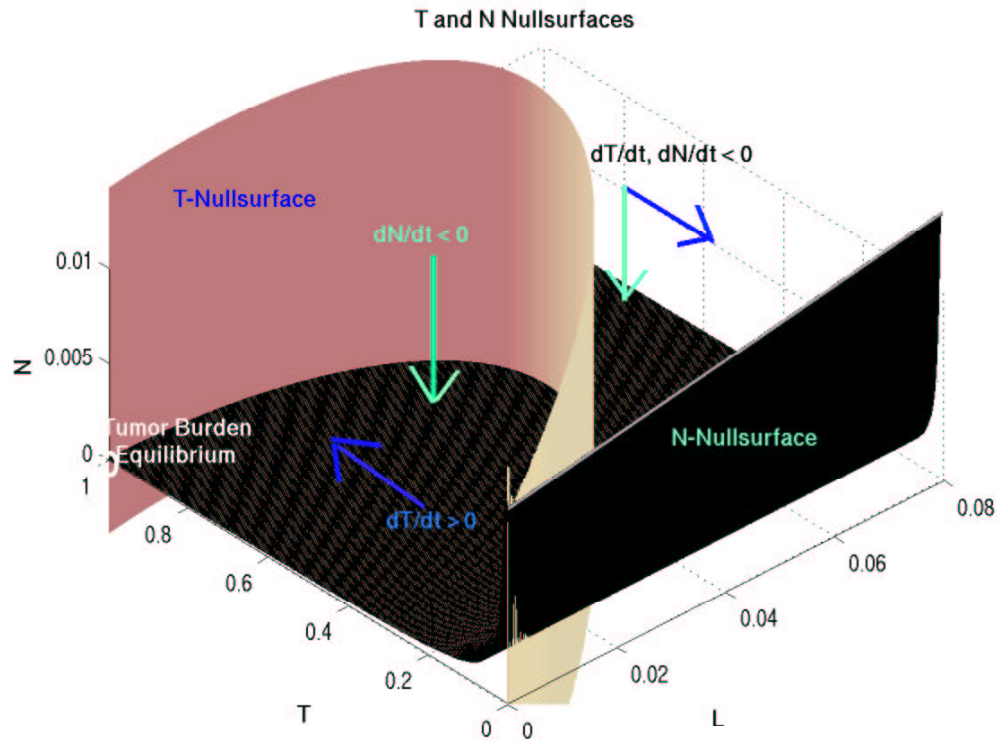
Figure 10.1: Plot of the tumor and NK cell null-surfaces. These surfaces split the volume into four sections within the positive region. For low CD8$^+$ T cell and high NK cell populations, the tumor grows and the NK cells decrease. For high immune cell populations (NK and CD8$^+$T), both tumor cells and NK cells are depleted. If both immune populations are low, both the tumor and the NK cells grow. For high CD8$^+$ T and low NK cell populations, the NK cell populations multiplies and the tumor population is depleted. The parameters used to create this plot are taken from non-dimensionalized patient 9 data. The intersection between these two surfaces is the line for which $dN/dt = dT/dt = 0$.
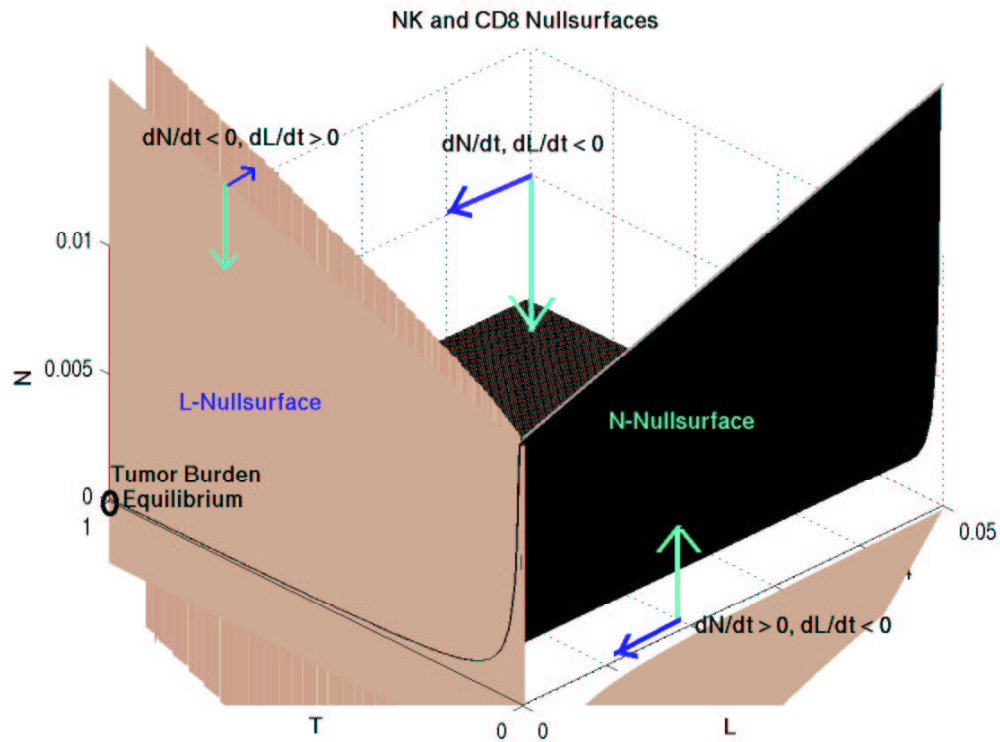
Figure 10.2: Plot of the NK and CD8$^+$ T cell null-surfaces. These surfaces split the volume into four sections within the positive region. If the immune populations (both NK and CD8$^+$T) are high (low), both immune populations decrease (increase). The parameters used to create this plot are taken from non-dimensionalized patient 9 data. The intersection between these two surfaces is the line for which $dN/dt = dL/dt = 0$.
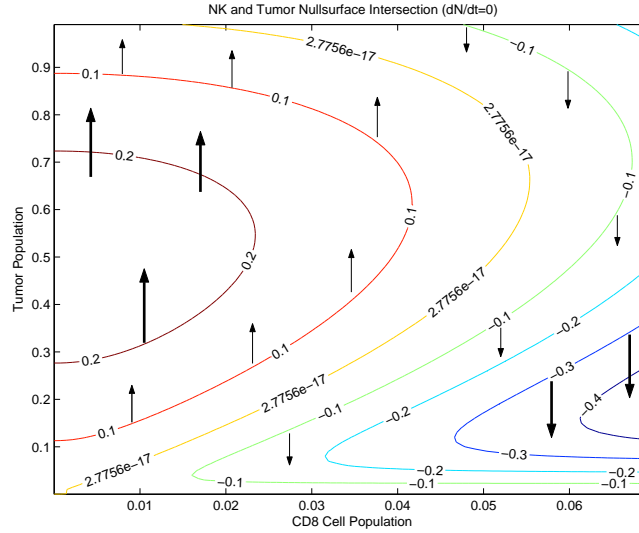
Figure 10.3: This is a contour plot of dT/dt on the NK cell null-surface. The line indicated by $2.77 \times 10^{-17} \approx 0$ represents the intersection between the tumor null-surface and the NK cell null-surface. The parameters here are taken from non-dimensionalized patient 9 data.

cell populations, $dN/dt < 0$, and for low NK cell populations, $dN/dt > 0$. Therefore, since this null-surface is approximately planar, perpendicular to the NK cell axis, and its trajectories move toward the planar surface from both top and bottom, there is a natural NK population being approached over time for which $dN/dt = 0$.

10.3.3   CD8$^+$ T Cell Null-surface

The CD8$^+$ T null-surface, shown in Figure 10.2, exists very close to the T-CD8$^+$ plane at $N \approx 0$ and near the N-T plane at $L \approx 0$. This plane varies from patient to patient, especially near the $L \approx 0$ area. For large values of CD8$^+$ T and NK cells, $dL/dt < 0$, unless the tumor population is large enough. This makes physical sense since a large tumor population should cause a CD8$^+$ T cell activation, while a large number of immune cells would cause the activation to slow or move in reverse.

10.3.4   Contour Plot Equilibria Finder

Figure 10.3 is a contour plot that shows the intersection between the NK and tumor cell null-surfaces, which exists along the line labeled 2.77×10^{-17}, which is approximately
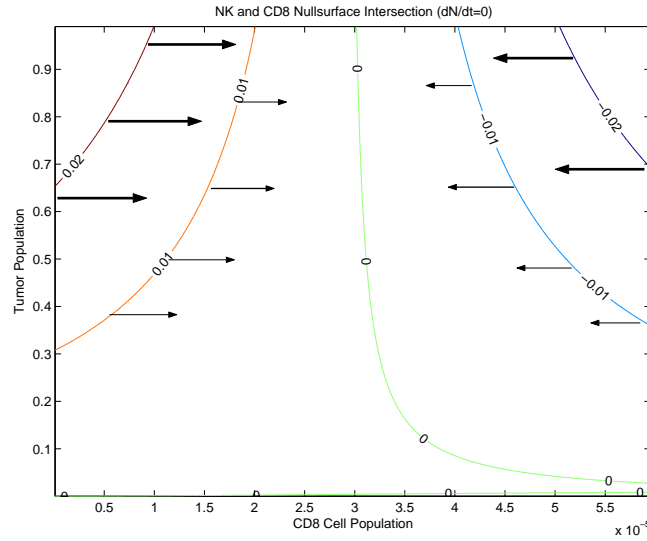
Figure 10.4: This is a contour plot of dL/dt on the NK null-surface. The line indicated by zeros represents the intersection between the CD8$^+$ T cell null-surface and the NK null-surface. The parameters here are taken from non-dimensionalized patient 9 data.

zero. The lines represent the value of dT/dt when dN/dt is set to zero. Similarly, Figure 10.4 shows the intersection between the NK and the CD8$^+$ T cell null-surfaces, which exists along the line labeled zero. These two lines from Figures 10.3 and 10.4 appear to intersect near the carrying capacity of the tumor population as well as near the origin. Figure 10.5 shows the high tumor intersection of these two lines, and this equilibrium exists at approximately $(T, N, L) = (1, 1 \times 10^{-4}, 3 \times 10^{-5})$. Figure 10.6 shows the low tumor intersection of there two lines, and this equilibrium exists at approximately $(T, N, L) = (5.5 \times 10^{-4}, .152, 8 \times 10^{-5})$. There are a total of three equilibria in our system.

10.4 Stability Analysis

In order to analyze the nature of a fixed point, we linearize the governing equations and examine a neighborhood about the point. From this simplified system we determine the eigenvalues of the resulting Jacobian. Finding stable points in a nonlinear system is very important in determining the global behavior of the system and general paths of its trajectories.
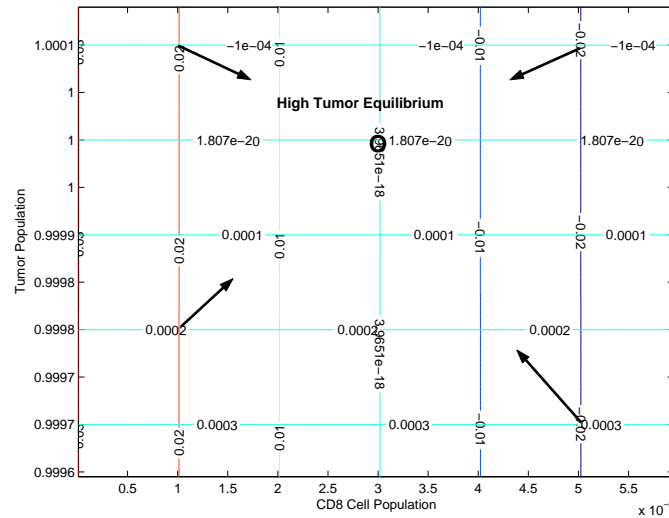
Figure 10.5: This is the intersection of both contour plots from Figures 10.3 and 10.4, focused on a high tumor region. It appears from this contour plot that this point is stable since all trajectories on the $dN/dt = 0$ surface within the region move toward this equilibrium. The parameters for this plot are taken from non-dimensionalized patient 9 data.
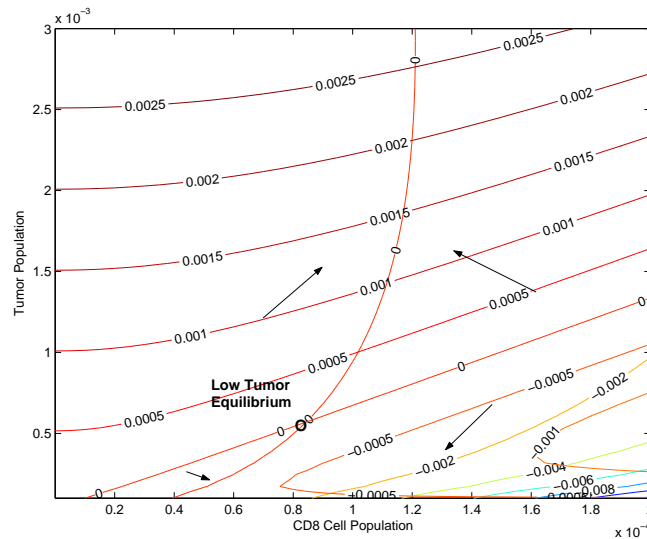
Figure 10.6: This is the intersection of both contour plots from Figures 10.3 and 10.4 focused on a high NK cell region. It appears from this plot that this equilibrium is a saddle point. The tumor nullcline in this region appears to separate the basins of attraction between high and low tumor outcomes.

10.5 Tumor Free Equilibrium

In order to determine the Jacobian matrix for this system of equations about the fixed point, $(T, N, L) = (0, \frac{e\alpha}{f\beta}, 0)$ (the non-dimensionalized version simplifies to $(0, 1, 0)$), we need to define D to be zero when T both and L are zero, since it is undefined at that point. Then we take the limits of the partial differential equations for all terms containing D. Since the term D contains the fraction L/T, we define

$$D = 0 \text{ and therefore } \frac{D^2}{k + D^2} = 0 \text{ when } L = T = 0$$

in order to make it continuous. We then analyzed the partial differential equations for $\dot{T}$ and $\dot{L}$ separately.

$$\frac{\partial}{\partial T}\left(\frac{D^2}{k + D^2}\right)\bigg|_{(0,0)} = \lim_{T \to 0} \frac{D^2}{k + D^2}\bigg|_{(T,0)} = 0$$

$$= \frac{0 \times L^{2e_L}}{k(0 + L^{e_L})^2 + 0 \times L^{2e_L}} = 0$$

$$\frac{\partial}{\partial L}\left(\frac{D^2}{k + D^2}\right)\bigg|_{(0,0)} = \lim_{L \to 0} \frac{D^2}{k + D^2}$$

By linearizing the system about the tumor free equilibrium, we find that

$$\begin{bmatrix} \dot{T} \\ \dot{N} \\ \dot{L} \end{bmatrix} = \begin{bmatrix} a - \frac{ce\alpha}{f\beta} & 0 & 0 \\ -pN & -f & 0 \\ rN & 0 & -m \end{bmatrix} \begin{bmatrix} T \\ N \\ L \end{bmatrix}$$

This linearization produces two purely negative eigenvalues, $-f$ and $-m$, since these parameters can only represent positive constants. Therefore this point is stable under the condition that the third eigenvalue is also negative, in other words that $af\beta < ce\alpha$. Unfortunately for our parameter set, this inequality is not true and the tumor free equilibrium is an unstable saddle point. This inequality indicates that the necessary criteria for stable tumor free equilibria is that the tumor growth, a, is low, the death rate of NK cells, f, is lower, the fractional tumor cell kill by NK cells, c, is larger, and the production of NK cells, $e\frac{\alpha}{\beta}$, is larger.

Parameter Value	Stability Threshold	Ability to Change
$a = 0.43078$	$a < 4 \times 10^{-5}$	Patient Specific
$c = 6.41 \times 10^{-11}$	$c > 7 \times 10^{-7}$	Vaccine: $c = 7 \times 10^{-9}$
$e = 1.24 \times 10^{-6}$	$e > 4 \times 10^{-3}$	Health Related
$f = .0412$	$f < 4 \times 10^{-4}$	Patient Specific
$\alpha = 7.5 \times 10^{8}$	$\alpha > 7.5 \times 10^{12}$	Health Related
$\beta = 0.012$	$\beta < 1.2 \times 10^{-6}$	Patient Specific

Table 10.1: Parameters that affect the stability of the tumor free equilibrium. Consistent with eigenvalue $a - \frac{ec\alpha}{f\beta}$. The values are taken from Table 5.4, and the vaccine parameter change is taken from curve fits of data collected in Diefenbach's study, [42], [46].

10.5.1 Transcritical Bifurcation Analysis

Transcritical bifurcations occur when an equilibrium changes stability. These bifurcation points are critical for our model since we would prefer to have a cancer patient with a stable tumor free equilibrium.

The signs of the Jacobian's eigenvalues determine whether an equilibrium is stable or unstable. For the tumor free equilibrium, there exists a simple inequality that judges the point's stability. If we can determine parameter adjustments that will change the stability of the system's equilibrium, the system will settle in a tumor free state if it lies within a neighborhood of this point. Table 10.1 provides the parameter adjustments that will make this point stable. Unfortunately these parameter variations are as large as four orders of magnitude, and therefore it may be more realistic to alter several parameters to a smaller degree to achieve stability.

10.5.2 Ability to Adjust Parameters

Parameters are patient specific and vaccine treatment can change the value of a subset of parameters in our model. The only parameter important for the stability of the tumor free equilibrium that appears to be altered by vaccine therapy is c [46]. Figure 10.7 shows how a two parameter variation can create a stable tumor free equilibrium; when c is varied with vaccine therapy and e is increased by an improved immune system that may cause an increase in NK cell production naturally. Another parameter that may be altered by an improved immune system, by means of a healthier lifestyle, is α. A two parameter
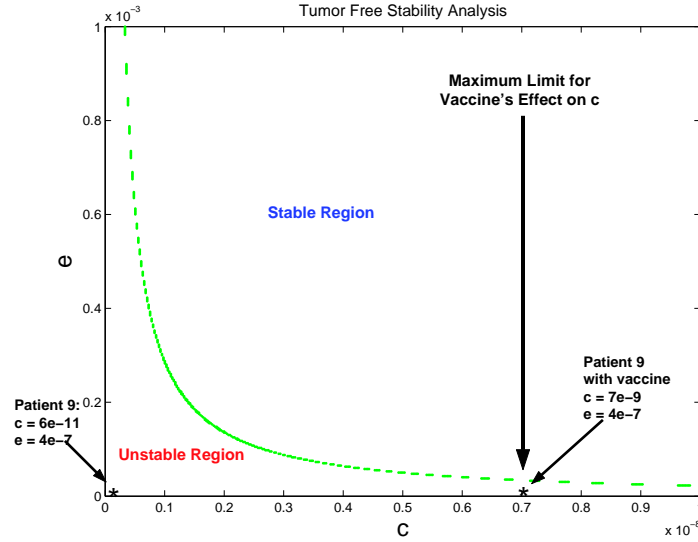
Figure 10.7: The value of c is altered with a cancer vaccination. The parameter e is adjustable with improved health style. The original parameter set for this alteration is shown in Table 5.4.

variation of e and α after vaccination is shown in Figure 10.8.

10.6 The High Tumor Equilibrium

Now that we have pinpointed the high tumor equilibrium at $(T, N, L) = (1, 10^{-4}, 3 \times 10^{-5})$, we continue with to analyze its stability as well. We linearize the system about this fixed point and find the eigenvalues of its Jacobian using Matlab's built in eigenvalue solver. For the non-dimensionalized parameter set of patient 9 data, this equilibrium is stable.

The general Jacobian matrix for the unsimplified (dimensionalized) version of our model is

$$J = \begin{bmatrix} a - 2abT - cN - d\frac{dD}{dT} & -cT & -d\frac{dD}{dL} \\ \frac{2ghTN}{(h+T^2)^2} - pN & -f + \frac{gT^2}{h+T^2} - pT & 0 \\ \frac{2jkLD\frac{dD}{dT}}{(k+D^2)^2} - qL + r_1N + \frac{r_2\alpha}{\beta} & r_1T - uL^2 & \frac{-m+jD^2}{k+D^2} + \frac{jkLD\frac{dD}{dL}}{(k+D^2)^2 - qT - 2uNL} \end{bmatrix}$$
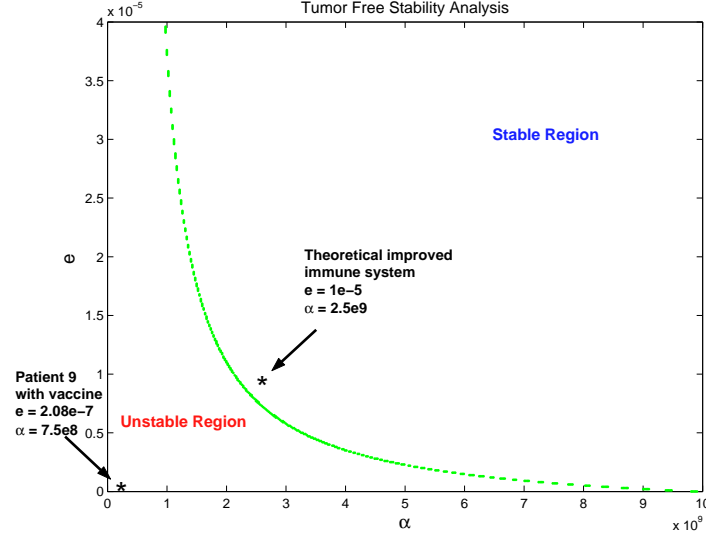
Figure 10.8: The parameters α and e may be adjustable by health improvement. These calculations are based on the parameters provided in Table 5.4 and the vaccine value of $c = 7 \times 10^{-9}$.

where

$$\frac{dD}{dT} = \frac{(1 - eL)sL^{eL}T^{eL} + L^{2eL}}{(sT^{eL} + L^{eL})^2}, \qquad \frac{dD}{dL} = \frac{eLsL^{eL-1}T^{eL+1}}{(sT^{eL} + L^{eL})^2}.$$

Next we look at the non-dimensionalized case where $T \approx 1, T \gg N, T \gg L$, and $L^{eL} \gg s$. This allows us to approximate

$$sT^{eL} + L^{eL} \approx sT^{eL} \approx s$$

which further simplifies to

$$\frac{dD}{dT} \approx \frac{(1 - eL)L^{eL} + sL^{2eL}}{s} < 0$$
$$\frac{dD}{dL} \approx \frac{(eL)L^{eL-1}}{s} > 0$$
$$D = \frac{L^{eL}}{sT^{eL} + L^{eL}} \approx \frac{L^{eL}}{s} < 1$$

In order to take a closer look for parameters that may change the stability of this stationary

point, we non-dimensionalize the Jacobian as well. Non-dimensionalizing the system also allows us to see which parameters dominate each element of the Jacobian by their magnitude. The parameters π, ξ, and ζ are two degrees of magnitude higher than the rest.

$$J = \begin{bmatrix} -1 - \chi N - \delta\frac{dD}{dT} & -\chi & -\delta\frac{dD}{dL} \\ N(2\tau\eta - \pi) & -\epsilon + \tau - \pi & 0 \\ \frac{2\theta\kappa LD\frac{dD}{dT}}{(\kappa+D^2)^2} - \xi L + \rho_1 N + \frac{\rho_2\alpha}{\beta} & \rho_1 - \zeta L^2 & \frac{-\mu+\theta D^2}{\kappa+D^2} + \frac{\theta\kappa LD\frac{dD}{dL}}{(\kappa+D^2)^2 - \xi T - 2\zeta NL} \end{bmatrix}$$

10.6.1 Saddle-node Bifurcation

Further analysis leads to the conclusion that this high tumor burden is a stable equilibrium for most realistic parameter sets. We implement the Routh test [14] to investigate the stability controlling parameters. According to the Routh test, the values on the diagonal are the most important to stability determination. These values are all negative for our parameter set, and in order to change this we would have to increase χ, a parameter related to the kill rate of tumor cells by NK cells, to be on the order of $1/N$ or decrease π (a parameter related to NK cell inactivation by tumor cells) to be smaller than τ (a parameter related to NK cell activation by tumor cells). The equation for the third diagonal element requires a bit more complex analysis, and we leave it to say that this value will become positive when the values of ξ (a parameter related to CD8$^+$ T cell inactivation by tumor cells) and ζ (a parameter related to CD8$^+$ T cell inactivation by NK cells) are sufficiently small.

In order to force this high tumor equilibrium into an unstable point, we must drastically decrease, for instance, the values of π and ξ, down to values smaller than 5, as well as increasing χ up to 12. These parameter alterations ultimately cause the equilibrium to disappear instead of changing its stability since the systems N and T nullclines no longer intersect as in Figure 10.9. This is called a saddle-node bifurcation. Unfortunately these parameter alterations are unrealistic and this high tumor point will always be stable for our purposes. Therefore we must examine other options for cancer treatment.
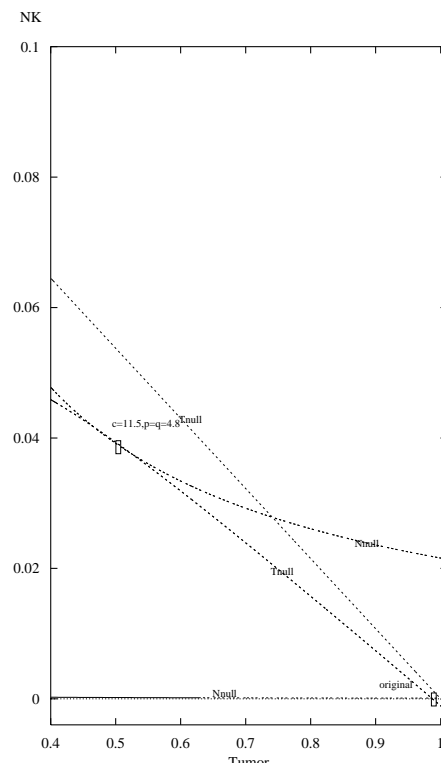
Figure 10.9: The nullclines for N and T at $dL/dt = 0$ on a tumor vs NK cell graph. The parameter changes push the N-nullcline up from the tumor axis, and lower the decline angle of the T-nullcline.

10.7 Low Tumor Equilibrium

In addition to the tumor free and the high tumor equilibria, there also exists a low tumor equilibrium that we can locate using the contour nullcline intersection method. This fixed point exists at approximately $(\tilde{T}, \tilde{N}, \tilde{L}) = (5.5 \times 10^{-4}, .152, 8 \times 10^{-5})$, and is shown in Figure 10.6. Although this point is located near the tumor free equilibrium, its is a valuable point to consider. We find that this stationary point is a saddle point after linearizing it and using Matlab's built in eigenvalue solver.

10.8 Basins of Attraction

In order to further investigate the global behavior of our nonlinear system, we analyze its trajectories across a range of initial conditions. It is useful to determine basins of attraction for stable points, however in order to do this there must exist more than one stable equilibrium. The zero tumor stationary point appears to act as a stable point in our model, since it is a saddle point whose trajectories move from nonzero tumor and $CD8^+$ T cell populations to near zero tumor, and then continue to negative infinity. However our model realistically prevents this and the trajectories eventually reach this zero tumor point along the $T = 0$ path as if the saddle point were stable.

By examining the basins of attraction, we may be able to use immunotherapy or chemotherapy to push initial conditions from reaching the high tumor equilibrium safely back into the tumor free basin without harming an individual with excess drug until the tumor has been completely destroyed. The basins of attraction for these stable states are displayed in Figure 10.10.

The addition of chemotherapy as well as immunotherapy in the form of a combination of $CD8^+$ T cell injection and IL-2 therapy change the shape and size of the basins. The high tumor region shrinks in both therapy cases, as in Figures 10.11 and 10.12. These figures show that the high tumor basin shrinks in size more drastically at high tumor levels.

10.9 Cancer Treatment Options

Since we are unable to change the stability of the high tumor equilibrium, it will always have a basin of attraction. The best we can do in this case is to shrink the size of its basin of
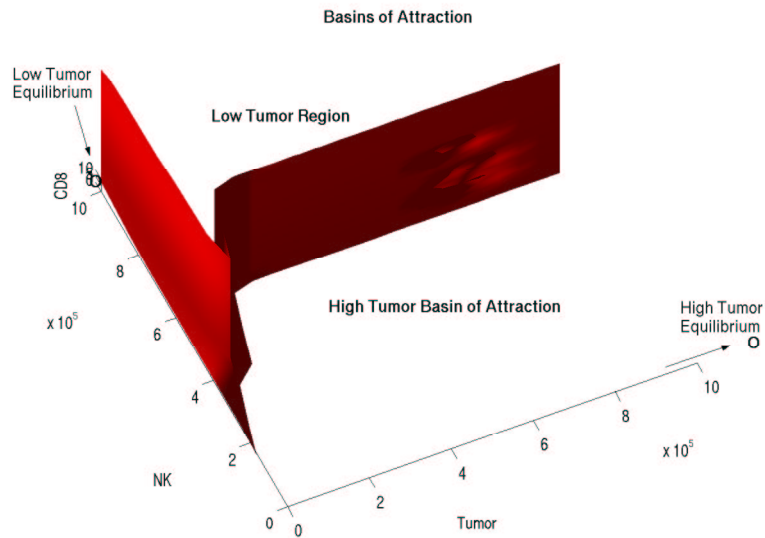
Figure 10.10: The surface shown separates basin of attraction between two competing equilibria. The parameters used for this graph are taken from from Table 5.4.
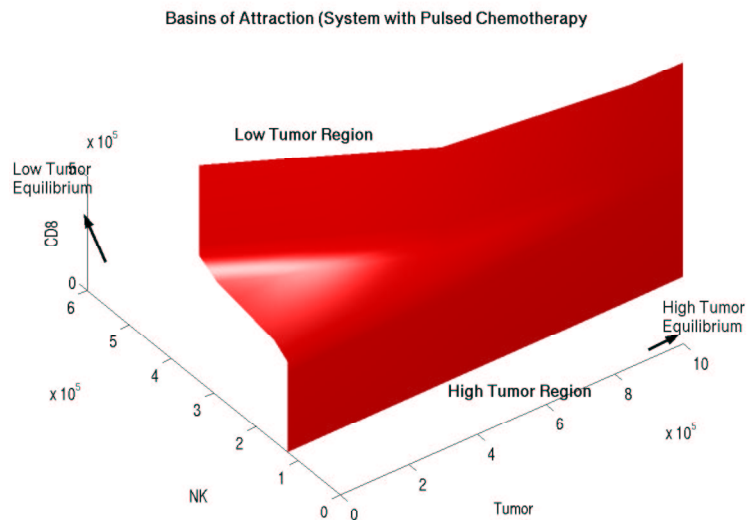
Figure 10.11: The surface in this graph separates the basin of attraction between two competing equilibria when pulsed chemotherapy is introduced. The amount administered was of magnitude 1, pulsed over a 10 period where drug was given for 3 day intervals. The parameters used for this graph are taken from Table 5.4.
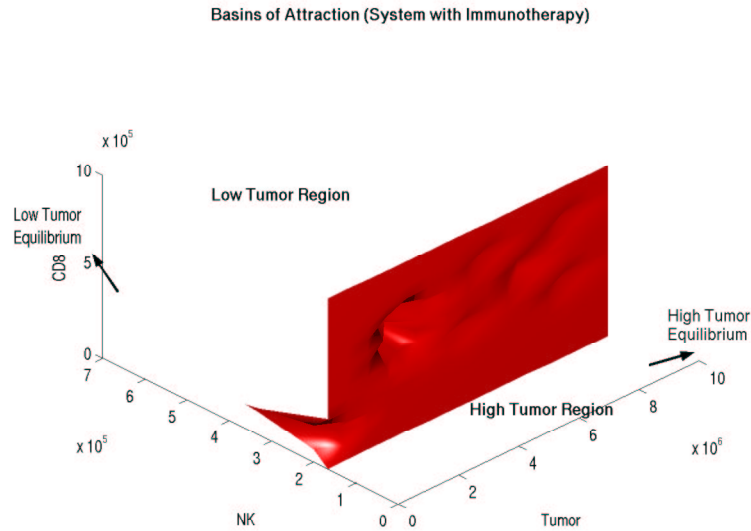
Figure 10.12: The surface shown separates basin of attraction between two competing equilibria when immunotherapy is introduced. 3×10^{10} CD8$^+$ T cells are administered for day during the simulation. Afterwords IL-2 drug is administered for two days, pulsed over a .6 day period where 5×10^6 IL-2 was given in .4 day intervals. The parameters used for this graph are taken from Table 5.4.

attraction. This is possible by changing the parameters so that the tumor free equilibrium is stable and by giving the patient chemotherapy or immunotherapy treatment.

Chapter 11

Optimal Control

We apply techniques from optimal control theory to discover how chemotherapy and immunotherapy can best be combined for the effective treatment of cancer. For this analysis, we use the non-dimensionalized set of model equations, including both chemotherapy and immunotherapy terms. We chose to use the non-dimensionalized version of our system since this investigation is more qualitative than quantitative.

The optimal control problems are solved numerically, with the aid of DIRCOL[122], a Fortran library for solving optimal control problems by a direct collocation method.

We do not expect to be able to get quantitative results that can be immediately used for treatment, but we do hope to learn something about how, qualitatively, chemotherapy and immunotherapy may best be combined. We compare the computed optimal treatment regimens to more traditional treatments as well, to see how much the treatments may be improved by optimal control theory.

11.1 Objectives and Constraints

We define constraint functions that limit possible solutions to be physically reasonable and to keep the patient healthy. The primary constraints are

$$0 \leq v_M(t) \leq 1, \qquad\qquad 0 \leq v_I(t) \leq 1,$$

limiting the maximum dose of medicine (of either variety) administered at any given time. In addition,

$$\int_0^{t_f} v_M(t)dt = V_M,$$
$$\int_0^{t_f} v_I(t)dt = V_I$$

which require that a certain total quantity of medicine be administered. Limiting this prevents too much chemotherapy or immunotherapy from being given. Comparisons with non-optimal schedules is easier, since other schedules with the same total quantity of medication but different timing can be compared. The specific total quantities used, V_M and V_I for chemo- and immuno-therapy, are chosen later.

Additionally, we may require that

$$v(t) = v_I(t) = 0 \text{ for } t > t_{\text{cutoff}},$$

so that treatment stops at some time t_{cutoff}. This allows the simulated patient to be monitored to see the behavior of the tumor, specifically whether the tumor dies or reemerges.

The objective function is used to rank potential cancer treatments. We search for the drug administration functions, subject to the above constraints, that minimize the value of

$$J = T(t_f) + \frac{1}{t_f} \int_0^{t_f} T(t)dt.$$

We wish to minimize the final tumor burden of the patient, but would also like to prevent the tumor from growing too large during treatment, and so we also add the average tumor size into the objective function.

11.2 Optimal Control Experiments

We perform a series of experiments with optimal control. For these simulations we start with parameters from mouse experiments (not ligand-transduced) [46], with the addition of immunotherapy parameters. In order to obtain interesting and helpful results, the regulatory effect of NK cells on CD8$^+$ T cells, ζ, are also suppressed. The non-dimensionalized parameters used are given in Table 11.1. The optimal control simulations are plotted up until $t_f = 8$ (about 19 days). The non-dimensionalized time that we use in the experiments is t/a, a cell division related term.

Immunotherapy is simulated entirely by the injection of IL-2, and not by direct boosts to any of the immune cell populations.

With initial conditions of $(T, N, L, C) = (10^{-4}, 1, 10^{-3}, 1)$ and no treatment, the tumor grows and will kill the subject—by time 20 (about 45 days). At this time, the tumor has reached its carrying capacity, and the immune system is not capable of a response. This is

$$\delta = 1.8494 \qquad \varepsilon = 0.09564 \qquad \zeta = 10^4$$
$$\eta = 9.495 \times 10^{-9} \qquad \theta = 0.28901 \qquad \kappa = 1.4959 \times 10^{-8}$$
$$\lambda = 0.027856 \qquad \mu = 0.046427 \qquad \xi = 0.036631$$
$$\pi = 10.7045 \qquad \rho_1 = 0.080618 \qquad \rho_2 = 1.5917 \times 10^{-5}$$
$$\tau = 0.28901 \qquad \chi = 4.6978 \times 10^{-5} \qquad \bar{\gamma} = 2.0892$$
$$eL = 0.8673 \qquad s = 1.1042 \qquad kT = 2.0892$$
$$kN = 1.3928 \qquad kL = 1.3928 \qquad kC = 1.3928$$
$$\pi_I = 2321.4 \qquad gI = 2.0 \qquad \bar{\mu}_I = 23.214$$

Table 11.1: Model parameters used in the optimal control simulations.

shown in Figure 11.1.

11.2.1 Chemotherapy

We first study the effect of chemotherapy alone on the treatment of a tumor. Figure 11.2 shows these results.

The total quantity of chemotherapy given is two time units at the maximum dose ($V_M = 2$). No immunotherapy is administered. Compared to no treatment at all, the subject is in better health, but the given dose of chemotherapy is not sufficient to kill the tumor; the tumor grows back after treatment ends. Given more time (and assuming no more treatment), this subject will look very much like the one in Figure 11.1.

The treatment schedule, subject to the constraints, is shown in the lower half of Figure 11.2. With the limited total supply of chemotherapy available, the optimal treatment consists of the largest initial pulse of chemotherapy possible, to kill the tumor while it is still small. Unfortunately, this is not quite enough.

11.2.2 Immunotherapy

We also look at the use of immunotherapy for cancer treatment. Figure 11.3 illustrates the results when immunotherapy is administered without chemotherapy.

As with chemotherapy, we constrain the total quantity of immunotherapy drugs to be equal to the equivalent of two time units at the maximum dose ($V_I = 2$). With these
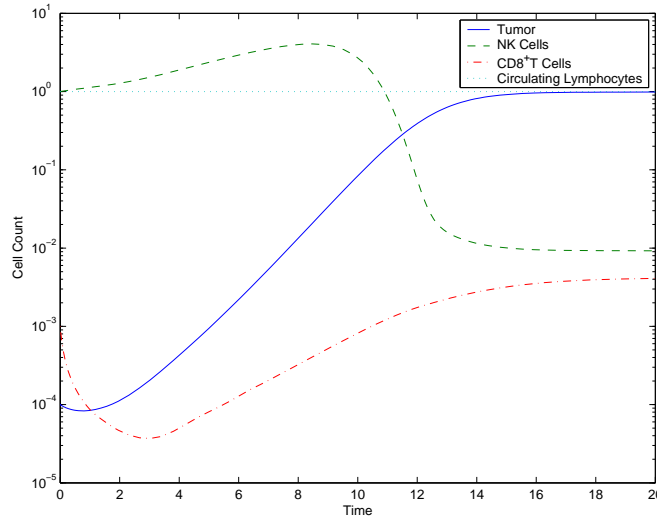
Figure 11.1: Tumor growth when no treatment is administered.

parameters, immunotherapy is sufficient to kill the tumor.

The effect of the immunotherapy is that $CD8^+$ T cell populations are boosted during the early parts of the time interval. The $CD8^+$ T cell population actually increases at the beginning of the simulation, unlike in the two earlier cases, where $CD8^+$ T cell populations decrease. This larger population of $CD8^+$ T cells is capable of killing the tumor.

Notably unlike the chemotherapy case, in this case it is not advantageous to administer all of the immunotherapy at the beginning of the treatment period. Instead, it is better to administer a lower dose of immunotherapy over a longer time period, with the dose gradually tapering off. Compared to giving the entire immunotherapy dose at the beginning of the treatment period, this method gives an approximately 5% decrease in the objective function.

11.2.3 Combination Therapy

We can do even better by combining both chemotherapy and immunotherapy. An optimal treatment schedule when both chemotherapy and immunotherapy are allowed ($V_M = V_I = 2$) is shown in Figure 11.4.

The combination of chemotherapy and immunotherapy is similar to simply administering both treatments at once, though not completely. Chemotherapy is still adminis-
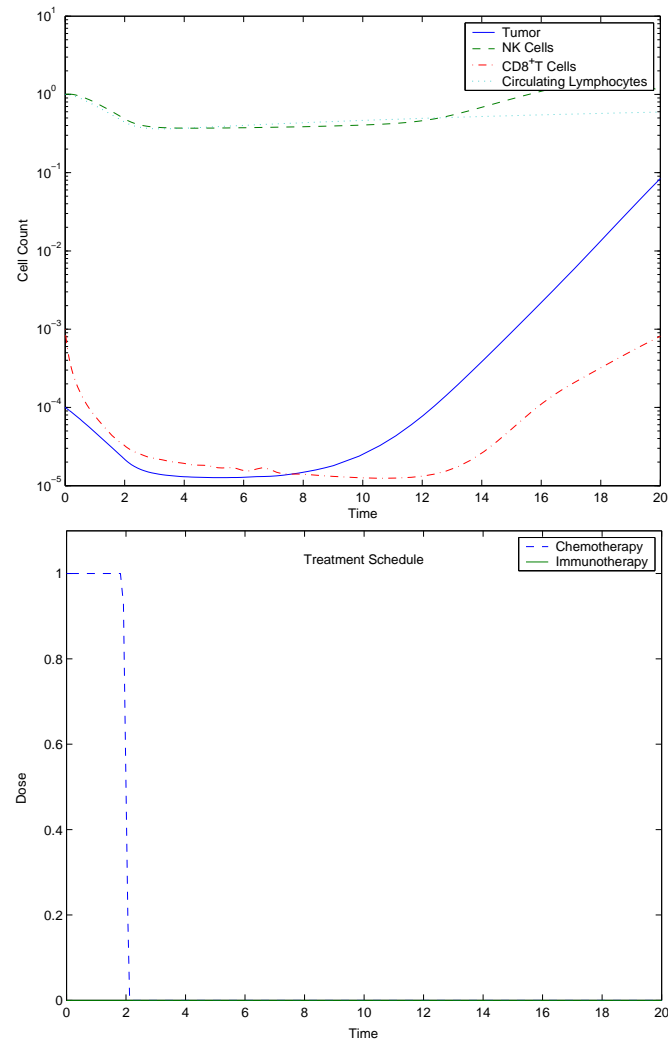
Figure 11.2: Tumor growth with optimal application of chemotherapy (top). Also shown is the schedule for chemotherapy administration (bottom).
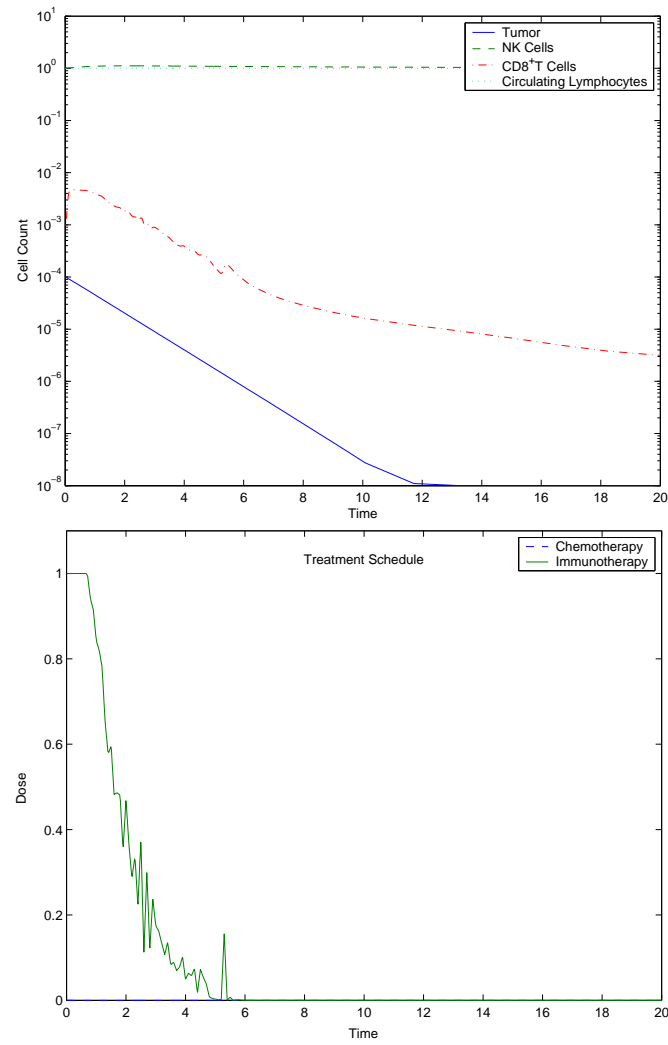
Figure 11.3: Tumor growth with the optimal use of immunotherapy. The lower figure shows the actual rate at IL-2 is injected.
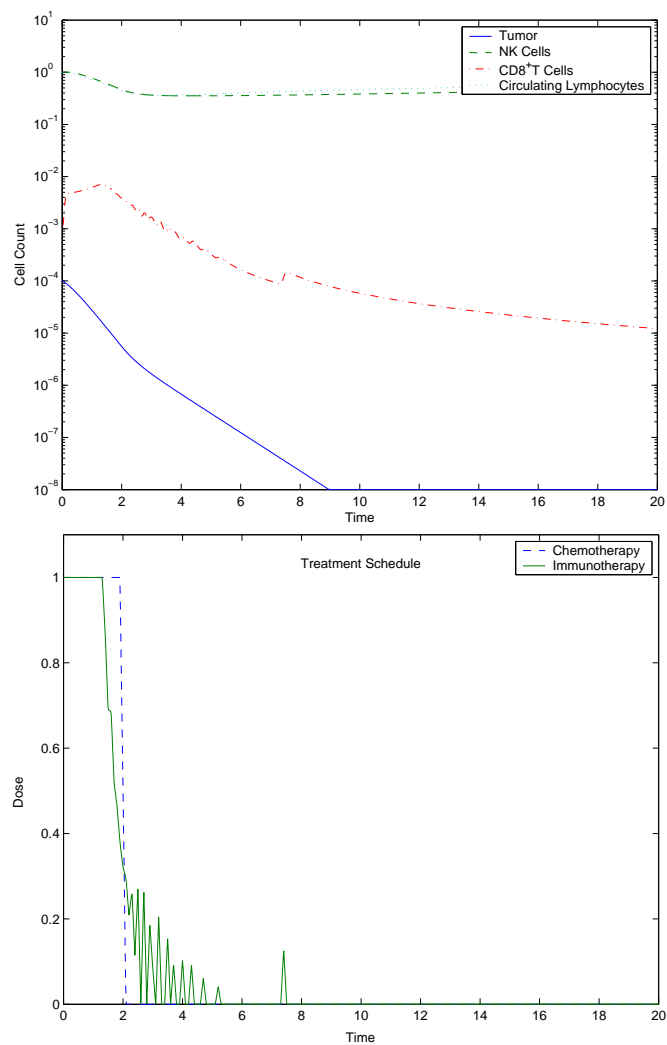
Figure 11.4: Combination chemotherapy and immunotherapy.

tered in a large dose at the beginning of the simulation. Immunotherapy is again given in an amount that decreases over time, though it is more concentrated at the start of the treatment period than it is with the pure immunotherapy treatment.

Both pure immunotherapy and combined therapy are able to kill the tumor, but the combination therapy is approximately 40% more effective (as measured by the objective function).

11.2.4 Optimal Control Summary

The optimal control experiments here demonstrate how chemotherapy and immunotherapy might be combined for more effective treatment. In the situation where chemotherapy alone cannot kill the tumor, there is little that can be done to optimize the treatment, at least with these conditions. Immunotherapy, which can in this case kill the tumor, does have a more optimal solution than a simple pulse of IL-2 injections. And in combination, the two are more effective at curing a subject of cancer quickly.

11.3 Other Directions

11.3.1 Alternative Objective Functions

There are several variations on the optimal control problem other than that listed above. Other possible objective functions were considered. In addition to the individual objective functions listed below, combinations are possible.

- **Minimize final tumor burden:**
$$J = T(t_f)$$

- **Minimize average tumor burden only:**
$$J = \frac{1}{t_f} \int_0^{t_f} T(t)dt$$

- **Minimize chemotherapy and immunotherapy:**
$$J = \int_0^{t_f} v(t)dt \qquad \text{or} \qquad J = \int_0^{t_f} v_I(t)dt$$

- **Maximize immune system health:**

$$J = -C(t_f) \qquad \text{or} \qquad J = -\int_0^{t_f} C(t)dt$$

When combining objective functions, there is freedom in how to do so. The simplest is to let the combined objective be the weighted sum of the individual objective functions. Another method that we attempt is to sum the logarithms of the values (with a lower-cutoff) so that even objectives which differed by orders of magnitude could be combined reasonably.

11.3.2 *Alternative Constraints*

Some of the constraints imposed on the problem are necessary to ensure physically reasonable solutions, such as $v_M(t) \geq 0$. Others were imposed to prevent solutions that would kill the subject, or to limit the solution space to make the problem easier to solve.

Many constraints were tested. Among them:

- **Maintain immune system health:** The level of circulating lymphocytes must be kept above some threshold for the entire simulation.

$$C(t) \geq C_{\min}$$

- **Restrict timing of chemotherapy and immunotherapy:** During certain times in the simulation, treatment cannot be administered. This can be used to monitor the patient after treatment ceases.

$$v(t) = v_I(t) = 0 \text{ if } t \text{ is in some disallowed range}$$

- **No concurrent chemotherapy and immunotherapy:** A patient can receive chemotherapy or immunotherapy, but not both at the same time.

$$v(t)v_I(t) = 0$$

11.4 Limitations and Future Work

While the results so far are encouraging, there are areas that could definitely be improved.

11.4.1 Mathematical Analysis of Solution Forms

There has been no attempt to determine, analytically, the form that optimal solutions must take. In previous models, it was found analytically that the optimal solutions should either have the full dose of chemotherapy or no chemotherapy administered at any instant (so-called bang-bang solutions). Numerical simulations indicate that in this model this is not true. To verify this, an analytical solution for the optimal control problem should be sought.

11.4.2 Numerical Convergence and Parameters

Solving optimal control problems in DIRCOL can be tricky at times, as DIRCOL will often terminate without finding a solution. Using reasonable initial guesses can help with numerical convergence. Convergence is also affected by the parameter values chosen.

Some parameter sets are easier to use in DIRCOL than others. Mouse parameters work reasonably well; parameters derived from human data (the patient 9 parameters, in particular) are much less likely to yield a solution in DIRCOL. This might be due to the fact that the system of equations can sometimes be stiff, depending upon the parameters, and DIRCOL cannot handle the stiff system very well.

Searching for new and better parameter sets, or at the least determining which parameter adjustments have a large effect on the numerical convergence to a solution, would be useful as future work.

11.4.3 Short Time Spans

These optimal control runs were only made up to a final times $t_f = 8$. Ideally, it should be possible to run optimal control simulations up through a time of at least $t_f = 30$ or even $t_f = 50$. Unfortunately, with our problem formulation, it becomes increasingly difficult to actually find a solution in DIRCOL the longer the simulation length. Depending upon the parameters chosen, convergence to a solution becomes difficult for after t_f exceeds 15–20.

Longer simulations are useful for several reasons. First, they would allow for a more representative picture of what happens to a subject over a long time span—whether the tumor is eventually killed, or comes back later, or something else. Longer simulations also give the opportunity for more interesting therapies, such as pulsed treatments, where chemotherapy is turned on and off over long periods of time.

Balancing this, however, is the fact that under most parameter sets, the tumor is either killed reasonably early in the treatment, or grows to a size where it cannot be controlled by any combination of immune system and medical treatment. Due to this, the ability to run longer simulations is not as important as it could have been.

11.4.4 Additional Experimentation

More experimentation with optimal treatment would be beneficial. In particular, looking at wider ranges of initial conditions, and possibly different parameter values, would help to better understand how chemotherapy and immunotherapy should be used.

Finding a parameter set where both chemotherapy and immunotherapy alone are insufficient to kill the tumor, but the combination is sufficient, would be a good starting point. Comparisons with more traditional treatment, such as pulsed chemotherapy, or chemotherapy followed by immune therapy, can be made to see how, with other initial conditions and parameters, those compare to optimal solutions.

Part III

Probability model

Chapter 12

Probability Model Formulation and Implementation

We can learn a number of things by looking at the systemic populations of immune and cancer cells however we need a different approach if we are going to investigate tumor morphology and the effects of chemotheropy and the immune system. To investigate this we chose to base our work on a model diveloped by Ferreira discribed in *"Reaction-diffusion model for the growth of avascular tumor"* [53] and extend this work to include simulations of chemotherapy and the immune system.

In this chapter we will discuss the formulation and subsaquent Matlab implimentation of this model, both reviewing the basic elements developed by Ferreira and discussing our chemotheropy and immune extentions.

12.1   The Grid

In this model we consider a two-dimensional cellar biological system with two basic elements: chemical and cellular. This two dimentional cellular grid is of size (L+1)x(L+1) units which are some width Δ. Further consider that the behavior of the chemicals are modeled using a PDE diffusion equation with appropriate boundary conditions and the cells are modeled using a cellular automita.

12.2   Chemical Diffusion

Because chemicals diffuse much faster then the cellular time steps we are looking at we can solve them at steady state

We begin with a basic diffusion equation

$$\frac{\partial N}{\partial t} = D\nabla^2 N$$

To which we add a consumption term from the cells

$$\frac{\partial N}{\partial t} = D\nabla^2 N - KN$$

Where K is dependent on the type and number of cells occupying a given node on the cellular grid. Thus K may be expressed as:

$$K = \gamma N \sigma_n + \lambda_N \gamma N \sigma_c$$

where γ is the consumption proportion of normal cells, σ_n the number of normal cells on a grid node, λ_N the ratio of cancer:normal cell chemical consumption and σ_c is the number of cancer cells. This leads us to the the following equation:

$$\frac{\partial N(\vec{x}, t)}{\partial t} = D\nabla^2 N(\vec{x}, t) - \gamma N(\vec{x}, t)\sigma_n(\vec{x}, t) - \lambda_N \gamma N(\vec{x}, t)\sigma_c(\vec{x}, t) \tag{12.1}$$

Our model simulates the diffusion of three chemicals. Nutrients key to division (N), nutrient key to survival (M), and chemotherapy (C). Resulting in the following system of independent equations:

$$\frac{\partial N(\vec{x}, t)}{\partial t} = D\nabla^2 N(\vec{x}, t) - \gamma_N N(\vec{x}, t)\sigma_n(\vec{x}, t) - \lambda_N \gamma_N N(\vec{x}, t)\sigma_c(\vec{x}, t) \tag{12.2}$$

$$\frac{\partial M(\vec{x}, t)}{\partial t} = D\nabla^2 M(\vec{x}, t) - \gamma_M M(\vec{x}, t)\sigma_n(\vec{x}, t) - \lambda_M \gamma_M M(\vec{x}, t)\sigma_c(\vec{x}, t) \tag{12.3}$$

$$\frac{\partial C(\vec{x}, t)}{\partial t} = D\nabla^2 C(\vec{x}, t) - \gamma_C C(\vec{x}, t)\sigma_n(\vec{x}, t) - \lambda_C \gamma_C C(\vec{x}, t)\sigma_c(\vec{x}, t) \tag{12.4}$$

For the sake of simplicity the following boundary conditions were applied.

$$N(0, y, t) = K_0 \tag{12.5}$$

$$N(x, 0, t) = N(x, L\Delta, t) \tag{12.6}$$

$$\frac{\partial N(L\Delta, y, t)}{\partial t} = 0 \tag{12.7}$$

Biologically this translates into a blood vessel at the top (Equation 12.5) providing a constant source of nutrient, a periodic boundary condition along the side (Equation 12.6) and a constant amount of chemical leaving the system at the bottom (Equation 12.7).

12.2.1 Non-dementionalize

Following Ferreira's paper [53] we then non-dementionalize the PDE with the following dementionless varaibles

$$t' = \frac{Dt}{\Delta^2}, \qquad \vec{x}' = \frac{\vec{s}}{\Delta}, \qquad N' = \frac{N}{K_0}, \qquad M' = \frac{M}{K_0}, \qquad \alpha' = \Delta\sqrt{\frac{\gamma}{D}} \qquad (12.8)$$

we now modify the chemical difusion equations to be demetionless, leaving the primes for simplisity and alowing $\Delta = 1$.

$$PDE : \frac{\partial N(\vec{x}, t)}{\partial t} = \nabla^2 N(\vec{x}, t) - \alpha^2 N \sigma_n - \lambda_n \alpha^2 N \sigma_c \qquad (12.9)$$

$$BC : N(0, y, t) = 1 \qquad (12.10)$$

$$N(x, 0, t) = N(x, L, t) \qquad (12.11)$$

$$\frac{\partial N(L, y, t)}{\partial t} = 0 \qquad (12.12)$$

12.3 Cellular Behavior

cancer cells - ints on matrix rep cell count immune cells - ints on matrix rep potential cell kills

(edit below paragraph) Each cell is not actually represented in this model but rather the number of cells on a given site is recorded on a matrix. The number of cells on that site can change following derived probabilities dependent on the various chemical concentrations at the site. In this current incarnation the type of cells tracked include cancer cells and immune cells though there are plans for future versions to include normal cells as well.

(maybe talk about the shapes of the probability curves?)

12.4 Behavior of Cancer Cells

Cancer cells have are randomly flagged for one of three actions: divide, move or die. The probabilities are then systematically evaluated and resulting cell count changes implemented. It is important to note that the sites are flagged for an action not the cell counters themselves. This is done for simplicity and ease of implementation.

Division If a site is flagged for division a probably based on the consitration of the nutrients N, nutrients vital for cell division, are first checked. Then a death probability must be overcome based on the consitration of chemo drug at the site. This death probability is added because most chemo drugs kill the cell in the division phase. If the cell dies then a counter is removed from the site. If the cell divides then a counter is added to either 1) a neighboring cell if there are any neighboring cells that are not cancer signifying the invasion of a normal cell by a cancer cell or 2) to the present site if it is surrounded by cancer cells ie inside the tumor.

$$P_{div}(\vec{x}) = 1 - \exp\left[-\left(\frac{N}{\sigma_c\theta_{div}}\right)^2\right] \tag{12.13}$$

Move After checking to see if the site is successful in moving based on how much ethical nutrients are at the site (M). A site flagged for movement first the neighboring cells are checked to see if there are any non-cancer cells. If there are then a cancer counter is randomly added to a non-cancer neighboring cell there by signifying that the cancer has invaded a normal cell and the old site is marked as neurotic or dead.

$$P_{move}(\vec{x}) = 1 - \exp\left[-\sigma_c\left(\frac{M}{\theta_{div}}\right)^2\right] \tag{12.14}$$

Death A site flagged for death will behave with probability dependent on the essential nutrient consitration (M). If a cell dies then the counter at that site decreases by one unless the last cancer cell dies. If the last cancer cell dies then the site is marked as neurotic.

$$P_{del}(\vec{x}) = \exp\left[-\left(\frac{M}{\sigma_c\theta_{div}}\right)^2\right] \tag{12.15}$$

12.5 Behavior of Immune Cells

Emergence Immune cells emerge randomly on a normal site with a given probability dependent on how many cells there already are on the total grid. This is then modified by a chemo concentration term.

$$P_{emg} = (r - \frac{I_{pop}}{S})\exp(-(\frac{C}{\theta_{ci}})^2) \tag{12.16}$$

where r is the "normal" ratio of immune to cell sites, I_{pop} the total number of immune cells in the grid, S is the total number of cell sites and θ_{ci} controls the sensitivity of the immune cells to the chemo drug. Biologically this corresponds to the immune cells emerging from the lymph system into neighborhood of cells. Chemotherapy adversely affects this by inhibiting cell production and there for immersion.

Movement If an immune cell is not on a site infected with cancer then it moves to a neighboring site. First the immune cell looks for cancer cells next to them. If they find a cancer cell then they move to that site. Otherwise they move randomly to a neighboring normal or neurotic site.

Death Immune cells die when they have expended all of their invasion killing abilities through interactions with cancer cells.

12.6   Implimentation

12.6.1   Data Structures

The data structuresd used to store this data were the defult matrix classes in Matlab. Where appropreate we used sparse matricies to store data.

The immune information was stored as a integer count of the number of cell kills left to each immune cell on a sparse matrix. Cancer, neucrotic and normal cells were stored on one matrix where a neucrotic cell was represented by -1, normal cell by 0 and the number of cancer cells occupying a site was some iteger greater then 1. Chemical consitrations were stored on seperate matricies.

12.6.2   Algorithms

The basic outline of the code is as follows:
- Get parameters
- Initialize system
- Begin for-loop
    - Move immune cells around
    - Regenerate immune cells as needed
    - Move cancer cells

      – Recalculate chemical distributions

      – Check for end conditions

- End for-loop
- Output results

Get Parameters   First we set the various variables from the system using user input (Appendix D.1) and default values. This is basicaly one large series of if statements.

Initialize System   Next we initialize the chemical consitrations and celluar systems using the parameters (Appendix D.2). Here we start with an itial cancer cell seed of 1 cell located in the middle of the grid. The immune cells emerge with their appreate probabilities on a blank grid (Appendix D.6). Each nutrient consitration are calculated based on the itialized cancer matrix. The chemo treatement is started at 0 consintration and then turned on later in the for loop after a certain population of cancer is reached representing a detection thresh-hold.

Move Immune Cells   Here we move the immune cells by iterating through each one and evaluating the movements and cancer kills. If the cell is on a cancer occupied site then it illiminates one of the cancer cells. Decreasing the cancer count at that site by one until it reaches 0 at which point it is marked as neucrotic with a -1 also decreasing the immune kill count on that site by one. Otherwise if the immune cell is not on a cancer site it looks at neighboring sites to see if any of those are cancer sites and moves randomly to a cancer site if there are any near by and a normal or neucrotic site otherwise (Appendix D.3).

Regenerate Immune Cells   Somewhere along the line in the moviement of immune cells some immune cells die due to depletion of their kill factor. We however want to keep a controlled ratio between the normal and the immune cells thus the emersion probability (Equation 12.16) must be applied after every immune cell change. Thus every none immune occupied cell is tested from immune cell emersion.

Move Cancer Cells   Cancer cells now are given the opertunity to move, divide or die based on the scheme mentioned earlier (Section 12.4) with the appropreate probabilities (Equations 12.13, 12.14, 12.15). These changes are then saved in two seprate matrices (one

storing the positive cell changes while another saving the negative cell changes) and then reconded at the end of the function. (Appendix D.4, D.8, D.9)

Recalculate Chemical Distributions   As the cancer cell changes the consumption of nutrience and chemo drug also change. Thus it is nessacary to recalculate the chemical distribution. To do this we need to solve a PDE of the form:

$$\frac{\partial N(\vec{x},t)}{\partial t} = D\nabla^2 N(\vec{x},t) - \gamma N(\vec{x},t)\sigma_n(\vec{x},t) - \lambda_N \gamma N(\vec{x},t)\sigma_c(\vec{x},t) \tag{12.17}$$

This can be further simplified when we consider that chemcials difuse much faster then our iterative time step (consider that we reach a tumor population of 3×10^5 in 666 iterations (**cite experiment**) for a compact tumor similar to Andeocarcinoma breast which has a double time of 129 days [24] implying it would take around 6.5 years which would translate to 1 iteration every 3.6 days) thus it is logical to consider the PDE at steady state which results in the folowing problem:

$$PDE : 0 = \nabla^2 N(\vec{x},t) - \alpha^2 N\sigma_n - \lambda_n \alpha^2 N\sigma_c$$
$$BC : N(0,y,t) = 1$$
$$N(x,0,t) = N(x,L,t)$$
$$\frac{\partial N(L,y,t)}{\partial t} = 0$$

We used a standard Crank-Nicolson scheme [32] implimented in Appendix D.7.

Check For End Conditions   The simulation was ended if the tumor reached the top or either side of the grid (Appendix D.2).

Output Results   The results were then ploted using Matlabs *plot* or *surf* functions where approeate (Appendix D.10).

Part IV

Deterministic PDE Model

Chapter 13

An Immunotheraputic Extension of the Jackson Model

13.1 Overview

We propose to modify Jackson's 2002 model [72] to include immunotherapy in addition to chemotherapy and vascular tumor growth. We intend to develop two coupled sets of equations, the first of which will model the immune and drug interaction at the tumor and will consequently include both spatial and temporal dependence, and the second of which will model the system-wide populations of drugs and immune cells and will thus include only temporal dependence. The two sets of equations will be linked through conditions on the boundary of the tumor.

13.2 Assumptions

Drawing on the assumptions and analysis of de Pillis *et al.* [39] and Jackson [72], we formulate the following assumptions for our model of vascular tumor growth:

1. We follow the evolution of the following populations:
    - the tumor cell population in the tumor itself;
    - the concentrations of a chemotheraputic drug in the tumor, in the blood stream, and in the surrounding tissue;
    - the natural killer (NK) cell population in the tumor and in the surrounding tissue;
    - the CD8$^+$ T-cell population in the tumor and in the surrounding tissue;
    - the circulating lymphocytes in the body.

    We also monitor the extent of vascularization within the tumor (which we take to be constant), the pressure inside the tumor, and the boundary of the tumor, and we relate this internal pressure to a local cell velocity.

2. The tumor cells are uniformly susceptible to drug treatment and immune interactions, and there is negligible necrosis in the tumor.

3. All cells and drugs within the tumor undergo diffusion and convection.

4. Tumor cells grow exponentially in the absence of chemotherapy and immune response. This is taken from Jackson [72]; de Pillis *et al.* [39] indicate this growth rate could also be logistic.

5. The chemotheraputic drug, the NK cells, the $CD8^+$ cells, and the circulating lymphocytes all become inactive over time at rates proportional to their population sizes.

6. NK cells, $CD8^+$ cells, and the drug can all kill tumor cells. The NK and $CD8^+$ kill rates increase when the tumor cells have been ligand-transduced.

7. The interaction with tumor cells inactivates some fraction of the NK and the $CD8^+$ cells.

8. Presence of a tumor activates both NK and $CD8^+$ cells.

9. A chemical signal generated by the tumor tissue attracts NK and $CD8^+$ cells. We take this chemical signal to be monocyte chemoattract protein-1 (MCP-1), which Kelly *et al.* [78] and Byrne *et al.* [22] both use as a chemotactic signal in their model of macrophage infiltration into tumors. Owen and Sherratt [99] also use MCP-1 as a chemotactic signal in their modelling of similar macrophage-tumor interactions.

10. Circulating lymphocytes stimulate the growth of NK cells. Both NK cells and circulating lymphocytes stimulate the growth of $CD8^+$ cells in the presence of a tumor.

11. Circulating lymphocytes increase at some constant rate.

12. The NK cells regulate the size of the $CD8^+$ population, reducing it if it is too large.

13. Drug diffuses between the tumor tissue and the tumor vasculature at a rate proportional to the difference in the blood and tumor concentrations.

14. The drug kills NK, $CD8^+$, and circulating lymphocytes in addition to the tumor cells. Some of the drug becomes inactive as a result of this interaction. Jackson [72] assumes this interaction follows Michaelis-Menten kinetics in Jackson, while de Pillis *et al.* [39] assume an exponentially saturating kinetics $(1 - e^{-kD})$. Furthermore, this exponential form is validated by Gardner [59] for a number of chemotherapy drug, including doxorubicin.

13.3 Quantities and Parameters

13.3.1 Quantities

We define the following dependent variables for use in the equations of the model:

Variable	Description	Units
$T(\mathbf{r}, t)$	Density of tumor cells within the tumor.	tumor-cells/volume
$V(\mathbf{r}, t)$	Density of vasculature within the tumor. Taken to be constant.	vessels/volume
$D(\mathbf{r}, t)$	Concentration of drug within tumor tissue.	drug/volume
$N(\mathbf{r}, t)$	Density of NK cells within tumor tissue.	NK-cells/volume
$C(\mathbf{r}, t)$	Density of CD8$^+$ cells within tumor tissue.	CD8$^+$-cells/volume
$S(\mathbf{r}, t)$	Concentration of chemical signal that attracts immune cells.	moles-signal/volume
$\mathbf{u}(\mathbf{r}, t)$	Local cell velocity inside tumor	length/time
$p(\mathbf{r}, t)$	Internal pressure inside tumor.	1
$D_B(t)$	Concentration of drug in bloodstream.	drug/volume
$D_N(t)$	Concentration of drug in normal tissue surrounding the tumor.	drug/volume
$N_N(t)$	Density of NK cells in normal tissue surrounding the tumor.	NK-cells/volume
$C_N(t)$	Density of CD8$^+$ cells in normal tissue surrounding the tumor.	CD8$^+$-cells/volume
$L(t)$	Density of circulating lymphocytes in the bloodstream.	L-cells/volume

We note that we have interchanged the symbols used in the ODE model for CD8$^+$ cells and circulating lymphocytes, so that C represents the CD8$^+$ cells and L represents the lymphocytes.

13.3.2 Parameters

The following parameters are used in the model's partial differential equations below:

Parameter	Description	Units
d_i	Diffusion or cell motility constant for population i.	length^2/time
λ_i	Natural growth or death rate for population i.	1/time
u_i	Rate at which the drug is inactivated in its interaction with population i.	drug/i-cell
i_N, i_C	Rates at which NK and CD8$^+$ cells are inactivated from interaction with the tumor.	volume/(time · tumor-cell)
l_N, l_C	Rates at which the NK and CD8$^+$ cells kill tumor cells.	volume/(time · i-cell)
Γ	Permeability coefficient between the tumor vasculature and tissue.	1/time
a_N, a_C	Attraction coefficient for NK and CD8$^+$ cells in response to the tumor signal.	length^5/(moles-signal · time)
α_S	Rate of signal production by tumor cells.	moles-signal/(tumor-cells · time)
V_c	Average volume of a tumor cell.	volume/tumor-cell
V_v	Average volume of a blood vessel in the tumor.	volume/vessel

The next set of parameters is used in the ordinary differential equations. Many of these are similar to those used in the original ODE model.

Parameter	Description	Units
k_{12}, k_{21}	Rates of drug transfer from the bloodstream to tissue and *vice versa*.	1/time
k_e	Rate at which drug is cleared from the plasma.	1/time
α_L	Constant source of circulating lymphocytes.	L-cells/(time · volume)
λ_L	First-order death rate for circulating lymphocytes.	L-cells/volume
f	Rate of circulating lymphocyte-induced NK production.	NK-cells/(L-cells · time)

Parameter	Description	Units
g	Tumor-induced NK cell recruitment rate.	1/time
h	Steepness coefficient of the NK recruitment curve.	(tumor-cells)^2
j	Tumor-induced CD8$^+$ cell recruitment rate.	1/time
k	Steepness coefficient of the CD8$^+$ recruitment curve.	(tumor-cells)^2 · CD8$^+$-cells / volume
s	Stimulation rate of tumor-specific CD8$^+$ cells.	CD8$^+$-cells/(time · NK-cell · tumor-cell)
v	Regulation rate of CD8$^+$ cells by NK cells.	volume^2/(NK-cell · CD8$^+$-cell · time)

13.4 Governing Equations

13.4.1 Local Cell and Drug Conservation Equations

We use the following equations to model the spatio-temporal behavior of the tumor. The first three equations govern the concentrations of tumor cells, the chemotherapy drug, and the signal secreted by the tumor:

$$\frac{\partial T}{\partial t} + \underbrace{\nabla \cdot (\mathbf{u}T)}_{\text{convection}} = \underbrace{d_T \nabla^2 T}_{\text{diffusion}} + \underbrace{\lambda_T T}_{\text{growth}} - \underbrace{I_{DT}(D,T)}_{\text{death from drug}} - \underbrace{l_C I_{CT}(C,T)}_{\text{death from CD8}^+} - \underbrace{l_N I_{NT}(N,T)}_{\text{death from NK}}, \quad (13.1)$$

$$\frac{\partial D}{\partial t} + \underbrace{\nabla \cdot (\mathbf{u}D)}_{\text{convection}} = \underbrace{d_D \nabla^2 D}_{\text{diffusion}} - \underbrace{\lambda_D D}_{\text{decay}} + \underbrace{\Gamma(D_b(t) - D)}_{\text{from vasculature}} - \underbrace{u_T I_{DT}(D,T)}_{\text{used on tumor}} - \underbrace{u_C I_{CD}(C,D)}_{\text{used on CD8}^+}$$
$$- \underbrace{u_N I_{ND}(N,D)}_{\text{used on NK}}, \quad (13.2)$$

$$\frac{\partial S}{\partial t} + \underbrace{\nabla \cdot (\mathbf{u}S)}_{\text{convection}} = \underbrace{d_S \nabla^2 S}_{\text{diffusion}} - \underbrace{\lambda_S S}_{\text{decay}} + \underbrace{\alpha_S T \, H(-B(\mathbf{r},t))}_{\text{production by tumor}}. \quad (13.3)$$

Here, H is the standard Heaviside step function. These next two equations govern the densities of NK and CD8$^+$ cells in the tumor tissue:

$$\frac{\partial N}{\partial t} + \underbrace{\nabla \cdot (\mathbf{u}\,N)}_{\text{convection}} + \underbrace{a_N \nabla \cdot (N \nabla S)}_{\text{signal gradient}} = \underbrace{d_N \nabla^2 N}_{\text{diffusion}} - \underbrace{\lambda_N N}_{\text{nat. death}} - \underbrace{i_N I_{NT}(N,T)}_{\text{inactivation}} - \underbrace{I_{ND}(N,D)}_{\text{death from drug}},$$

(13.4)

$$\frac{\partial C}{\partial t} + \underbrace{\nabla \cdot (\mathbf{u}\,C)}_{\text{convection}} + \underbrace{a_C \nabla \cdot (C \nabla S)}_{\text{signal gradient}} = \underbrace{d_C \nabla^2 C}_{\text{diffusion}} - \underbrace{\lambda_C C}_{\text{nat. death}} - \underbrace{i_C I_{CT}(C,T)}_{\text{inactivation}} - \underbrace{I_{CD}(C,D)}_{\text{death from drug}}.$$

(13.5)

The I functions used above represent the interaction terms between the various populations within the tumor. For example, $I_{DT}(D,T)$ represents the interaction between the drug and the tumor cells, which we expect to depend only on the local concentrations D and T. For the sake of simplicity, we assume that the interaction has the same effect on each population involved, up to some scaling multiplier. Jackson *et al.* [72, 74] uses this approach in modeling the tumor-drug interactions, although de Pillis *et al.* [40] indicate that this approach may not be sufficiently accurate. We elect to leave these interaction terms unspecified for the time being.

We assume that each local species is subject both to diffusion and to convection resulting from the local cell velocity. The tumor cells have some natural growth rate, but are killed by the drug and the immune cells. The drug decays at some constant rate, diffuses into (or out of) the tumor from the bloodstream, and is deactivated at some rate in its interactions with both the tumor cells and the immune cells. Each immune cell population undergoes natural death or inactivation as well as death or inactivation resulting from its interactions with the tumor cells and the drug. In addition, we assume that the tumor secretes a chemical that attracts the body's immune cells. While the process by which tumor cells are attracted to the tumor is not well understood, this provides a reasonable explanation for use in this model. We also assume that this chemical decays at some natural rate and is produced only within the tumor boundary.

13.4.2 *Volume Fraction Equation*

We assume that the volume of the immune cells is negligible, so that the only types of tissue contributing to the volume are the tumor cells and the vasculature. Thus, we have

the relation

$$V_c T + V_v V = 1. \tag{13.6}$$

Because we are assuming that the vasculature V is constant and uniform throughout the tumor, this implies that T will also be constant.

13.4.3   Boundary and Pressure Equations

We define the tumor boundary as a level surface of some function $B(\mathbf{r}, t)$:

$$B(\mathbf{r}, t) = r - R(\theta, \phi, t) = 0. \tag{13.7}$$

The motion of a point on the boundary $B(\mathbf{r}, t) = 0$ is then determined by

$$\mathbf{n}_v \cdot \frac{d\mathbf{r}}{dt} = \mathbf{u} \cdot \mathbf{n}_v, \tag{13.8}$$

where $\mathbf{n}_v$ is an outward normal vector to the tumor boundary. Additionally, we use Darcy's law,

$$\mathbf{u} = -d_T \nabla p, \tag{13.9}$$

to relate the internal pressure p and the cell velocity u. Byrne and Chaplain [19, 20] justify the use of Darcy's Law in tumors with the tumor cell motility d_T as the constant of proportionality. For the most part, however, we elect to focus on the local cell velocity instead of this internal pressure.

13.4.4   Systemic Drug and Immune Cell Equations

We use a system of ODEs to model the concentration of drug in the bloodstream and the normal tissue and the populations of NK cells, CD8$^+$ cells, and circuating lymphocytes in the body. The first two equations determine the drug concentrations, and are in part taken from Jackson [74]. We modify the equtions slightly, however, to reflect that the blood compartment and the normal tissue compartment have different volumes V_B and V_N, respectively, and thus drug transferred between the components will be diluted according to the destination component's volume. If we do not take these volumes into consideration, we lose conservation of drug mass. We first treat Jackson's equations as though they deal with drug quantities, not concentrations, and then replace the drug

quantities with their concentrations times the component volume. Thus, we have

$$V_B \frac{dD_B}{dt} = -k_{12}V_B D_B + k_{21}V_N D_N - k_e V_B D_B + V_B D_p(t), \tag{13.10}$$

$$V_N \frac{dD_N}{dt} = k_{12}V_B D_B - k_{21}V_N D_N. \tag{13.11}$$

Simplifying, we have

$$\frac{dD_B}{dt} = -k_{12}D_B + k_{21}\frac{V_N}{V_B}D_N - k_e D_B + D_p(t), \tag{13.12}$$

$$\frac{dD_N}{dt} = k_{12}\frac{V_B}{V_N}D_B - k_{21}D_N. \tag{13.13}$$

In these equations, $D_p(t)$ represents the prescribed chemotherpy treatment. Assuming bang-bang treatments, therefore, we expect to be able to develop piecewise solutions for D_N and D_B.

We draw the remaining equations as much as possible from the ODE model. The equation governing the circulating lymphocyte concentration is

$$\frac{dL}{dt} = \alpha_L - \lambda_L L - K_L(L, D_N), \tag{13.14}$$

where $K_L(L, D_N)$ describes the effect of the chemotherapy drug on the lymphocytes. Thus, the lymphocytes grow at a constant zeroth-order rate, die at a first-order rate, and are killed by the drug. Retaining the terms in the ODE model that describe systemic interactions, the equations governing the NK cell and CD8$^+$ cell concentrations in the normal tissue are

$$\frac{dN_N}{dt} = \underbrace{fL}_{\text{nat. growth}} - \underbrace{\lambda_N N_N}_{\text{nat. death}} + \underbrace{g\frac{\tau^2}{h+\tau^2}N_N}_{\text{recruitment}} - \underbrace{K_N(N_N, D_N)}_{\text{drug effect}}, \tag{13.15}$$

$$\frac{dC_N}{dt} = - \underbrace{\lambda_C C_N}_{\text{nat. death}} + \underbrace{j\frac{(C_N\tau)^2}{k+(C_N\tau)^2}C_N}_{\text{recruitment}} + \underbrace{sN_N\tau}_{\text{recruit. from NK}} - \underbrace{vN_N C_N^2}_{\text{NK regulation}} - \underbrace{K_C(C_N, D_N)}_{\text{drug effect}}, \tag{13.16}$$

where τ is some measure of how large the body perceives the tumor to be and K_N and K_C describe the effects of the drug on the system-wide NK cell and CD8$^+$ cell concentrations.

13.5   Initial and Boundary Conditions

We introduce following parameters to be used in specifying the initial and boundary conditions of the system.

Parameter	Description	Units
T_0	Initial density of tumor cells.	tumor-cells/volume
V_0	Initial density of vasculature.	vessels/volume
D_0	Initial concentration of drug in the bloodstream.	drug/volume
N_0	Initial concentration of NK cells in the body tissue.	NK-cells/volume
C_0	Initial concentration of CD8$^+$ cells in the body tissue.	CD8$^+$-cells/volume
L_0	Initial concentration of circulating lymphocyte cells in the body tissue.	L-cells/volume

We impose the following initial conditions and boundary conditions on the system. We suppose that initially the only populations present in the tumor itself are the tumor and the tumor vasculature. Thus, for the PDE system, we have

$$T(\mathbf{r}, 0) = T_0, \quad V(\mathbf{r}, 0) = V_0, \quad D(\mathbf{r}, 0) = 0, \quad N(\mathbf{r}, 0) = 0, \quad C(\mathbf{r}, 0) = 0, \quad S(\mathbf{r}, 0) = 0.$$
$$(13.17)$$

Systemically, we suppose that initially there is no drug and that there are specified populations of NK cells, CD8$^+$ cells, and circulating lymphocytes. Thus, for the ODE system, we have

$$D_B(0) = 0, \quad D_N(0) = 0, \quad N_N(0) = N_0, \quad C_N(0) = C_0, \quad L(0) = L_0. \quad (13.18)$$

At $\mathbf{r} = 0$, we have the Neumann boundary conditions

$$\frac{\partial D}{\partial r} = 0, \qquad \frac{\partial N}{\partial r} = 0, \qquad \frac{\partial C}{\partial r} = 0, \qquad \frac{\partial S}{\partial r} = 0, \qquad u(0, t) = 0. \qquad (13.19)$$

We connect the temporal and spatio-temporal equations through continuity conditions at the boundary. Therefore, at the boundary $B(\mathbf{r}, t) = 0$, we have

$$D(\mathbf{r}, t) = D_N(t), \qquad N(\mathbf{r}, t) = N_N(t), \qquad C(\mathbf{r}, t) = C_N(t). \qquad (13.20)$$

Finally, we prescribe the initial boundary of the tumor $B(\mathbf{r}, t) = 0$.

13.6 Determination of Interaction Functions

We introduce a new set of parameters to be used in the interaction terms.

Parameter	Description	Units
κ_i	Susceptibility of population i to the drug.	1/time
σ_i	Drug saturation coefficient for population i.	volume/drug

We now give appropriate definitions for the interaction functions I_{ij} in the PDE. Based on the ODE model and the analysis presented in de Pillis *et al.* [40], we model the tumor-immune cell interactions as product terms:

$$I_{CT} = CT, \qquad\qquad I_{NT} = NT. \qquad (13.21)$$

De Pillis *et al.* [40] indicate that more complex terms may be more accurate, especially in modelling the interaction's effect on the tumor cells. For the drug's interaction with the tumor and the immune cells, in both the systemic and local equation we follow the exponential model presented by de Pillis *et al.* [40] and by Gardner [59]. We change Gardner's derivation slightly so that the kill fraction in a time interval from t to $t + \Delta t$ is

$$-\frac{P(t + \Delta t) - P(t)}{P(t)} = \kappa(1 - e^{-\sigma D})\Delta t, \qquad (13.22)$$

where P is some cell population or population density. Rearranging and taking the limit as Δt goes to 0, we have

$$\frac{dP}{dt} = \lim_{\Delta t \to 0} \frac{P(t + \Delta t) - P(t)}{\Delta t} = -\kappa(1 - e^{-\sigma D})P(t). \qquad (13.23)$$

Thus we take the local drug-cell interaction terms to be

$$I_{DT} = \kappa_T(1 - e^{-\sigma_T D})T, \quad I_{ND} = \kappa_N(1 - e^{-\sigma_N D})N, \quad I_{CD} = \kappa_C(1 - e^{-\sigma_C D})C. \quad (13.24)$$

and the systemic drug-cell interaction terms to be

$$K_N(N_N, D_N) = \kappa_N(1 - e^{-\sigma_N D_N})N_N, \qquad (13.25)$$

$$K_C(C_N, D_N) = \kappa_C(1 - e^{-\sigma_C D_N})C_N, \qquad (13.26)$$

$$K_L(L, D_N) = \kappa_L(1 - e^{-\sigma_L D_N})L. \qquad (13.27)$$

This introduces two additional groups of parameters, κ_i, which represents the suscepti-bility of population i to the drug, and σ_i, which represents the rate of saturation. We note that κ_i has units of inverse time and σ_i has units of volume/drug.

Chapter 14

Spherically Symmetric Case

14.1 Spatio-temporal Equations

We now consider this model in the case of complete spherical symmetry, so that there is no angular dependence to any of the spatially dependent variables, and now the tumor boundary is determined by $B(\mathbf{r}, t) = r - R(t) = 0$. Also, now $\mathbf{u} = u(r, t)\hat{\mathbf{r}}$, where $\hat{\mathbf{r}}$ is the radial unit vector. Taking into account that T is constant, the spatial equations reduce to

$$\frac{T}{r^2}\frac{\partial}{\partial r}\left(r^2 u\right) = \lambda_T T - \kappa_T (1 - e^{-\sigma_T D})T - l_C CT - l_N NT, \tag{14.1}$$

$$\frac{\partial D}{\partial t} + \nabla \cdot (\mathbf{u}D) = \frac{d_D}{r^2}\frac{\partial}{\partial r}\left(r^2\frac{\partial D}{\partial r}\right) - \lambda_D D + \Gamma(D_B(t) - D) - u_T\kappa_T(1 - e^{-\sigma_T D})T$$
$$- u_N\kappa_N(1 - e^{-\sigma_N D})N - u_C\kappa_C(1 - e^{-\sigma_C D})C, \tag{14.2}$$

$$\frac{\partial S}{\partial t} + \nabla \cdot (\mathbf{u}S) = \frac{d_S}{r^2}\frac{\partial}{\partial r}\left(r^2\frac{\partial S}{\partial r}\right) - \lambda_S S + \alpha_S H(R(t) - r)T, \tag{14.3}$$

and

$$\frac{\partial N}{\partial t} + \nabla \cdot (\mathbf{u}N) + a_N\left\{\frac{\partial S}{\partial r}\frac{\partial N}{\partial r} + \frac{N}{r^2}\frac{\partial}{\partial r}\left(r^2\frac{\partial S}{\partial r}\right)\right\} = \frac{d_N}{r^2}\frac{\partial}{\partial r}\left(r^2\frac{\partial N}{\partial r}\right) - \lambda_N N$$
$$- i_N NT - \kappa_N(1 - e^{-\sigma_N D})N, \tag{14.4}$$

$$\frac{\partial C}{\partial t} + \nabla \cdot (\mathbf{u}C) + a_C\left\{\frac{\partial S}{\partial r}\frac{\partial C}{\partial r} + \frac{C}{r^2}\frac{\partial}{\partial r}\left(r^2\frac{\partial S}{\partial r}\right)\right\} = \frac{d_C}{r^2}\frac{\partial}{\partial r}\left(r^2\frac{\partial C}{\partial r}\right) - \lambda_C C$$
$$- i_C CT - \kappa_C(1 - e^{-\sigma_C D})C. \tag{14.5}$$

The initial boundary of the tumor is now given by $r = R_0$, and its evolution now follows

$$\frac{dR}{dt} = u(R(t), t). \tag{14.6}$$

14.2 Temporal Equations

We now define τ, the immune system's measure of the perceived tumor size. We choose to relate this to the volume of the tumor, so that

$$\tau = \rho R(t)^3, \tag{14.7}$$

where ρ is some constant of proportionality with units tumor-cell/volume. The temporal equations then become as follows:

$$\frac{dD_B}{dt} = -k_{12}D_B + k_{21}D_N - k_e D_B + D_p(t) \tag{14.8}$$

$$\frac{dD_N}{dt} = k_{12}D_B - k_{21}D_N, \tag{14.9}$$

$$\frac{dL}{dt} = \alpha_L - \lambda_L L - \kappa_L(1 - e^{-\sigma_L D_N})L, \tag{14.10}$$

$$\frac{dN_N}{dt} = fL - \lambda_N N_N + g\frac{(\rho R^3)^2}{h + (\rho R^3)^2}N_N - \kappa_N(1 - e^{-\sigma_N D_N})N_N, \tag{14.11}$$

$$\frac{dC_N}{dt} = -\lambda_C C_N + j\frac{(C_N(\rho R^3))^2}{k + (C_N(\rho R^3))^2}C_N + sN_N(\rho R^3) - vN_N C_N^2 - \kappa_C(1 - e^{-\sigma_C D_N})C_N, \tag{14.12}$$

14.3 Nondimensionalization

We now introduce dimensionless variables and parameters, represented by overbarred versions of the original quantities and defined as follows:

$$r = R_0 \bar{r}, \qquad t = t_0 \bar{t}, \qquad \frac{\partial}{\partial r} = \frac{1}{R_0}\frac{\partial}{\partial \bar{r}}, \qquad \frac{\partial}{\partial t} = \frac{1}{t_0}\frac{\partial}{\partial \bar{t}}, \quad (14.13)$$

$$u = \frac{R_0}{t_0}\bar{u}, \qquad T = \frac{1}{V_c}\bar{T}, \qquad T_0 = \frac{1}{V_c}\bar{T}_0, \qquad V = \frac{1}{V_v}\bar{V}, \quad (14.14)$$

$$V_0 = \frac{1}{V_v}\bar{V}_0, \qquad D = D_0\bar{D}, \qquad N = f\alpha_L t_0^2 \bar{N}, \qquad C = \frac{sf\alpha_L t_0^3 R_0^3}{V_c}\bar{C}, \quad (14.15)$$

$$S = \frac{\alpha_S t_0}{V_c}\bar{S}, \qquad L = \alpha_L t_0 \bar{L}, \qquad L_0 = \alpha_L t_0 \bar{L}_0, \qquad D_B = D_0 \bar{D}_B, \quad (14.16)$$

$$D_p = \frac{D_0}{t_0}\bar{D}_p, \qquad D_N = D_0 \bar{D}_N, \qquad N_N = f\alpha_L t_0^2 \bar{N}_N, \qquad N_0 = f\alpha_L t_0^2 \bar{N}_0, \quad (14.17)$$

$$C_N = \frac{sf\alpha_L t_0^3 R_0^3}{V_c}\bar{C}_N, \quad C_0 = \frac{sf\alpha_L t_0^3 R_0^3}{V_c}\bar{C}_0 \qquad \lambda_D = \frac{1}{t_0}\bar{\lambda}_D, \qquad \lambda_N = \frac{1}{t_0}\bar{\lambda}_N, \quad (14.18)$$

$$\lambda_C = \frac{1}{t_0}\bar{\lambda}_C, \qquad \lambda_S = \frac{1}{t_0}\bar{\lambda}_S, \qquad d_D = \frac{R_0^2}{t_0}\bar{d}_D, \qquad d_N = \frac{R_0^2}{t_0}\bar{d}_N, \quad (14.19)$$

$$d_C = \frac{R_0^2}{t_0}\bar{d}_C, \qquad d_S = \frac{R_0^2}{t_0}\bar{d}_S, \qquad u_T = D_0 V_c \bar{u}_i, \qquad u_N = \frac{D_0}{f\alpha_L t_0^2}\bar{u}_i, \quad (14.20)$$

$$u_C = \frac{D_0 V_c}{sf\alpha_L t_0^3 R_0^3}\bar{u}_i, \qquad i_i = \frac{V_c}{t_0}\bar{i}_i, \qquad l_N = \frac{1}{f\alpha_L t_0^3}\bar{l}_N, \qquad l_C = \frac{V_c}{sf\alpha_L t_0^4 R_0^3}\bar{l}_C, \quad (14.21)$$

$$\Gamma = \frac{1}{t_0}\bar{\Gamma}, \qquad a_i = \frac{V_c R_0^2}{\alpha_S t_0^2}\bar{a}_i, \qquad k_{12} = \frac{1}{t_0}\bar{k}_{12}, \qquad k_{21} = \frac{1}{t_0}\bar{k}_{21}, \quad (14.22)$$

$$k_e = \frac{1}{t_0}\bar{k}_e, \qquad \lambda_L = \frac{1}{t_0}\bar{\lambda}_L, \qquad g = \frac{1}{t_0}\bar{g}, \qquad h = \frac{R_0^6}{V_c^2}\bar{h}, \quad (14.23)$$

$$j = \frac{1}{t_0}\bar{j}, \qquad k = \left(\frac{sf\alpha_L t_0^3 R_0^6}{V_c^2}\right)^2 \bar{k}, \qquad v = \frac{V_c}{sf^2\alpha_L^2 t_0^6 R_0^3}\bar{v}, \qquad \kappa_i = \frac{1}{t_0}\bar{\kappa}_i, \quad (14.24)$$

$$\sigma_i = \frac{1}{D_0}\bar{\sigma}_i, \qquad \rho = \frac{1}{V_c}\bar{\rho}, \qquad R(t) = R_0 \bar{R}(t). \quad (14.25)$$

We also make $t_0 = 1/\lambda_T$, so that the principal time scale is that of the tumor growth. Substituting these into the radial spatio-temporal equations yields, after simplification and after dropping the bars for notational convenience,

$$\frac{1}{r^2}\frac{\partial}{\partial r}\left(r^2 u\right) = 1 - \kappa_T(1 - e^{-\sigma_T D})T - l_C C - l_N N, \tag{14.26}$$

$$\frac{\partial D}{\partial t} + \nabla \cdot (\mathbf{u}D) = \frac{d_D}{r^2}\frac{\partial}{\partial r}\left(r^2 \frac{\partial D}{\partial r}\right) - \lambda_D D + \Gamma(D_B - D)$$
$$- \left\{u_T \kappa_T(1 - e^{-\sigma_T D})T + u_N \kappa_N(1 - e^{-\sigma_N D})N + u_C \kappa_C(1 - e^{-\sigma_C D})C\right\}, \tag{14.27}$$

$$\frac{\partial S}{\partial t} + \nabla \cdot (\mathbf{u}S) = \frac{d_S}{r^2}\frac{\partial}{\partial r}\left(r^2 \frac{\partial S}{\partial r}\right) - \lambda_S S + TH(R(t) - r). \tag{14.28}$$

and

$$\frac{\partial N}{\partial t} + \left\{u\frac{\partial N}{\partial r} + \frac{N}{r^2}\frac{\partial}{\partial r}\left(r^2 u\right)\right\} + a_N \left\{\frac{\partial S}{\partial r}\frac{\partial N}{\partial r} + \frac{N}{r^2}\frac{\partial}{\partial r}\left(r^2 \frac{\partial S}{\partial r}\right)\right\}$$
$$= \frac{d_N}{r^2}\frac{\partial}{\partial r}\left(r^2 \frac{\partial N}{\partial r}\right) - \lambda_N N - i_N NT - \kappa_N(1 - e^{-\sigma_N D})N, \tag{14.29}$$

$$\frac{\partial C}{\partial t} + \left\{u\frac{\partial C}{\partial r} + \frac{C}{r^2}\frac{\partial}{\partial r}\left(r^2 u\right)\right\} + a_C \left\{\frac{\partial S}{\partial r}\frac{\partial C}{\partial r} + \frac{C}{r^2}\frac{\partial}{\partial r}\left(r^2 \frac{\partial S}{\partial r}\right)\right\}$$
$$= \frac{d_C}{r^2}\frac{\partial}{\partial r}\left(r^2 \frac{\partial C}{\partial r}\right) - \lambda_C C - i_C CT - \kappa_C(1 - e^{-\sigma_C D})C. \tag{14.30}$$

The evolution of the tumor boundary is now specified by

$$\frac{dR}{dt} = u(R(t), t). \tag{14.31}$$

The temporal equations simplify to

$$\frac{dD_B}{dt} = -k_{12}D_B + k_{21}D_N - k_e D_B + D_p(t), \tag{14.32}$$

$$\frac{dD_N}{dt} = k_{12}D_B - k_{21}D_N, \tag{14.33}$$

$$\frac{dL}{dt} = 1 - \lambda_L L - \kappa_L(1 - e^{-\sigma_L D_N})L, \tag{14.34}$$

$$\frac{dN_N}{dt} = L - \lambda_N N_N + g\frac{\rho^2 R^6}{h + \rho^2 R^6}N_N - \kappa_N(1 - e^{-\sigma_N D_N})N_N, \tag{14.35}$$

$$\frac{dC_N}{dt} = -\lambda_C C_N + j\frac{(C_N(\rho R^3))^2}{k + (C_N(\rho R^3))^2}C_N + N_N(\rho R^3) - vN_N C_N^2 - \kappa_C(1 - e^{-\sigma_C D_N})C_N. \tag{14.36}$$

We now consider the initial boundary conditions under this nondimensionalization scheme. The spatial initial conditions and boundary conditions at $r = 0$ and the tumor boundary remain as in Equations (13.17), (13.19), and (13.20), although Equation (13.6) is now

$$T_0 + V_0 = 1, \tag{14.37}$$

making $V_0 = 1 - T_0$. The ODE initial conditions simplify to

$$D_B(0) = 0, \quad D_N(0) = 0, \quad N_N(0) = N_0, \quad C_N(0) = C_0, \quad L(0) = L_0. \tag{14.38}$$

14.4 Front-Fixing Transformation

This spherical case formulation of the equations applies on the spatial domain $[0, R(t)]$. Because $R(t)$ varies with time, this system is difficult to solve numerically. In order to make this system computationally tractable, we follow Jackson [74] in applying a front-fixing method from Crank [32] to the spatial equations in the model, which scales the spatial coordinate by the domain length $R(t)$ according to the transformation

$$\tilde{r} = \frac{r}{R(t)}. \tag{14.39}$$

The chain rule then leads to the derivatives

$$\frac{\partial}{\partial r} = \frac{1}{R(t)}\frac{\partial}{\partial \tilde{r}}, \qquad \frac{\partial^2}{\partial r^2} = \frac{1}{(R(t))^2}\frac{\partial^2}{\partial \tilde{r}^2}, \qquad \left.\frac{\partial}{\partial t}\right|_r = -\frac{\tilde{r}}{R(t)}\frac{dR}{dt}\frac{\partial}{\partial \tilde{r}} + \left.\frac{\partial}{\partial t}\right|_{\tilde{r}}. \tag{14.40}$$

This transforms Equations (14.26)–(14.30) as follows:

$$\frac{1}{\tilde{r}^2 R}\frac{\partial}{\partial \tilde{r}}(\tilde{r}^2 u) = 1 - \kappa_T(1 - e^{-\sigma_T D})T - l_C C - l_N N, \tag{14.41}$$

$$\frac{\partial D}{\partial t} = \frac{d_D}{R^2}\frac{\partial^2 D}{\partial \tilde{r}^2} + \left(\frac{\tilde{r}}{R}\frac{dR}{dt} - \frac{u}{R} + \frac{2d_D}{\tilde{r}R}\right)\frac{\partial D}{\partial \tilde{r}} - \left[\frac{1}{\tilde{r}^2 R}\frac{\partial}{\partial \tilde{r}}(\tilde{r}^2 u) + \lambda_D + \Gamma\right]D$$
$$+ u_T\kappa_T(1 - e^{-\sigma_T D})T + u_N\kappa_N(1 - e^{-\sigma_N D})N + u_C\kappa_C(1 - e^{-\sigma_C D})C + \Gamma D_B, \tag{14.42}$$

$$\frac{\partial S}{\partial t} = \frac{d_S}{R^2}\frac{\partial^2 S}{\partial \tilde{r}^2} + \left(\frac{\tilde{r}}{R}\frac{dR}{dt} - \frac{u}{R} + \frac{2d_S}{\tilde{r}R}\right)\frac{\partial S}{\partial \tilde{r}} - \left(\frac{1}{\tilde{r}^2 R}\frac{\partial}{\partial \tilde{r}}(\tilde{r}^2 u) + \lambda_S\right)S + TH(1 - \tilde{r}), \tag{14.43}$$

$$\frac{\partial N}{\partial t} = \frac{d_N}{R^2}\frac{\partial^2 N}{\partial \tilde{r}^2} + \left(\frac{\tilde{r}}{R}\frac{dR}{dt} - \frac{u}{R} - \frac{a_N}{R^2}\frac{\partial S}{\partial \tilde{r}} + \frac{2d_N}{\tilde{r}R}\right)\frac{\partial N}{\partial \tilde{r}}$$
$$- \left(\frac{1}{\tilde{r}^2 R}\frac{\partial}{\partial \tilde{r}}(\tilde{r}^2 u) + \frac{a_N}{R^2}\left(\frac{\partial^2 S}{\partial \tilde{r}^2} + \frac{2R}{\tilde{r}}\frac{\partial S}{\partial \tilde{r}}\right) + \lambda_N + i_N T + \kappa_N(1 - e^{-\sigma_N D})\right)N, \tag{14.44}$$

$$\frac{\partial C}{\partial t} = \frac{d_C}{R^2}\frac{\partial^2 C}{\partial \tilde{r}^2} + \left(\frac{\tilde{r}}{R}\frac{dR}{dt} - \frac{u}{R} - \frac{a_C}{R^2}\frac{\partial S}{\partial \tilde{r}} + \frac{2d_C}{\tilde{r}R}\right)\frac{\partial C}{\partial \tilde{r}}$$
$$- \left(\frac{1}{\tilde{r}^2 R}\frac{\partial}{\partial \tilde{r}}(\tilde{r}^2 u) + \frac{a_C}{R^2}\left(\frac{\partial^2 S}{\partial \tilde{r}^2} + \frac{2R}{\tilde{r}}\frac{\partial S}{\partial \tilde{r}}\right) + \lambda_C + i_C T + \kappa_C(1 - e^{-\sigma_C D})\right)C. \tag{14.45}$$

These are the equations for which our PDE solver computes numerical solutions on the spatial domain $[0, 1]$.

Chapter 15

Parameter Estimation

We have insufficient experimental data to provide well-supported estimates for all the parameters in our model. Nevertheless, we can derive some parameter values from those used in the ODE model, Jackson's models, and other sources, and we can provide reasonable value ranges for other unknown parameters.

15.1 ODE Model Parameters

We can derive a number of the parameters for the spatio-temporal model directly from the ODE model. Some of these parameters must also be scaled an appropriate volume factor to account for our use of cell population densities rather than absolute cell populations. We introduce three volume parameters, a blood-volume factor, V_B, a normal-tissue-volume factor, V_N, and a characteristic tumor volume, V_T. The parameters that require no such adjustment are listed below:

Parameter	Value	Source
λ_N	0.0412/day	ODE f
λ_C	0.2044/day	ODE patient 9 m
λ_L	0.012/day	ODE human β
g	0.01245/day	ODE g
h	2.019×10^7 tumor-cells^2	ODE h
j	0.0249/day	ODE human j
s	1.1×10^{-7} CD8$^+$-cells/NK-cell $\cdot$ tumor-cell $\cdot$ day	ODE r_1

We take $V_B = 6.0$ L and $V_N = 17.0$ L [64]. To determine V_T, we note that an accepted tumor-volume-to-cell-count factor is 10^9 cells per mL of tumor tissue [26, 39]. From this, we estimate V_c, the characteristic tumor cell volume, as 10^{-12} L/tumor-cell. Assuming a characteristic tumor size of 10^7 cells, we then have $V_T = 10^{-5}$ L. In order to scale the ODE parameters correctly, we assume that the ODE model total-population variables correspond to the PDE model density variables times the appropriate characteristic volume.

We then factor out the PDE density variables to determine the correspondence between the ODE and PDE parameters. For example, from the ODE model, we have $\frac{dL}{dt} = -uNL^2$. In the PDE model variables, then, $V_N \frac{dC}{dt} = -u(V_N N)(V_N C)^2$, so $\frac{dC}{dt} = -u V_N^2 NC^2$ and thus $v = u V_N^2$. The scaled parameters are listed below. For the sake of consistency, we use the centimeter (cm) as the natural length scale, so that the natural volume scale becomes $cm^3 = 1$ mL.

Parameter	Value	Source
V_c	10^{-9} mL/tumor-cell	[26, 39]
l_N	1.47×10^{-6} mL/NK-cell $\cdot$ day	ODE human $c \times V_N$
l_C	1.47×10^{-6} mL/NK-cell $\cdot$ day	ODE human $c \times V_N$
i_N	2.6×10^{-8} mL/tumor-cell $\cdot$ day	ODE human $p \times V_T$
i_C	2.6×10^{-8} mL/tumor-cell $\cdot$ day	ODE human $q \times V_T$
α_L	2.1×10^4 L-cells/mL $\cdot$ day	ODE human α/V_B
f	4.37×10^{-7} NK-cells/L-cell $\cdot$ day	ODE $e \times V_B/V_N$
v	5.78 mL^2/NK-cell $\cdot$ CD8$^+$-cell $\cdot$ day	ODE human $u \times V_N^2$

We also estimate $l_C \approx l_N$. For the time being, we take $l_C = l_N$.

Since ρ is a proportionality constant between $R(t)^3$ and the number of cells in the tumor nd since we assume a spherical tumor geometry, we expect that the size of the tumor is $\frac{4}{3}\pi R(t)^3$ and thus that the number of tumor cells it contains is $\frac{4}{3}\pi R(t)^3/V_c$. We therefore have the following estimate for ρ:

Parameter	Value	Source
ρ	$\frac{4}{3}\pi/V_c$	

In nondimensionalized units, $\rho = \frac{4}{3}\pi \approx 4.1888$ exactly. [FIXME: Add adjustment for k | Fix me! | parameter, which will require dealing with the ODE D term.]

15.2 Jackson Model Parameters

We also derive some of our model's parameters from Jackson [72, 74, 73]. Among these are parameters specifying the local behavior of the drug and the tumor and the systemic pharmacokinetics of the drug. We take the following parameters directly from Jackson [72, 74]:

Parameter	Value	Source
R_0	0.4 cm	R_0 [72]
$\lambda_T = 1/t_0$	1/7 day^{-1}	α [72]
Γ	16/day	Γ [72]
d_D	1.7 cm^2/day	D [72]
ξ_1	60/day	ξ_1 [72]
ξ_2	6/day	ξ_2 [72]

We convert all dosages to moles of doxorubicin, using the molecular weight $M_{\text{DOX}} = 544.8$ g/mol [24]. Thus, a $D_0 = 6$ mg/kg dose [79] corresponds to a dose of 11 μmol/kg. Assuming that the patient has a mass of 60 kg and that the drug disperses through the bloodstream immediately upon intravenous injection, we can estimate D_0. Jackson et $al.$ [74] give formulas for computing k_e, k_{12}, and k_{21} from ξ_1 and ξ_2 as well as A and B, two parameters associated with the pharmacokinetics of a single bolus dose of doxorubicin:

$$k_e = \frac{A+B}{A/\xi_1 + B/\xi_2}, \qquad k_{21} = \frac{A\xi_2 + B\xi_1}{A+B}, \qquad k_{12} = \frac{AB}{(A+B)^2}\frac{(\xi_1 - \xi_2)^2}{k_{21}}. \qquad (15.1)$$

While Jackson does not give explicit values for A and B, we need only the ratio $A/(A+B)$ to compute the k_i values. From Greenblatt et $al.$ [64] and from Jackson [73], we take $A/(A+B) = 0.75$. Then we have the following estimates for D_0, k_{12}, k_{21}, and k_e:

Parameter	Value	Source
D_0	110 nmol/mL	D_0 [72] $\times M_{\text{DOX}} \times 60$ kg$/V_B$
k_{12}	28.0/day	
k_{21}	19.5/day	
k_e	18.5/day	

Jackson [73] also provides an estimate for the tumor cell motility ($\sim 10^{-5}$ cm^2/day). We expect that the body's immune cells will be significantly more motile than the tumor cells, so we take d_N and d_C to be at least one order of magnitude higher than this value. Owen and Sherratt [99] provide an estimate for d_S of 0.17 cm^2/day using Stokes-Einstein theory; we also note that the molecular weight of MCP-1 is approximately 10,000 g/mol [99, 109], 20 times that of doxorubicin, so we expect d_S to be approximately an order of magnitude less than d_D. Thus, we have the following estimates for the diffusion parameters:

Parameter	Value	Source
d_N, d_C	10^{-2}–10^{-4} cm^2/day	D_p [73] $\times 10^1$–10^3
d_S	0.17 cm^2/day	D_f [99]

Jackson [73] gives some information about the natural decay rate of doxorubicin, although her decay parameter λ encompasses both the natural decay of the drug and its depletion from killing tumor cells. We take her parameter as our λ_D, but note that it probably accounts for our u_i parameters as well. Thus, we take these parameters to be effectively 0.

Parameter	Value	Source
λ_D	1.9/day	λ [73]
u_T, u_N, u_C	0	

15.3 Dose-Response Parameter Estimation

If a tumor-cell population is exposed to a constant doxorubicin level of D over a time T, the exponential form of the drug response predicts that its size will be $S(T, D)$ that of a comparable, untreated tumor, where

$$S(T, D) = \exp\left(-\kappa_T(1 - e^{-\sigma_T D})T\right). \tag{15.2}$$

We curve-fit this expression to drug-response data for doxorubicin on wild-type A2780 human ovarian cancer cells [86] to obtain estimates for κ_T and σ_T. To account for the lower susceptibility of immune cells to the drug, we take $\sigma_N = \sigma_C = \sigma_L = \sigma_T/3$.

Parameter	Value	Source
κ_i	42.8/day	Parameter Fitting
σ_T	1.179 mL/nmol	Parameter Fitting
$\sigma_N, \sigma_C, \sigma_L$	0.393 mL/nmol	$\sigma_T/3$

The σ_T value also close matches the corresponding parameter a in Gardner [59], which is given as $a = 1.063$ L/μmol.

15.4 Chemotactic Signal Parameters

We unfortunately have little data on the process of immune cell chemotaxis, including the decay rate λ_S, the coefficients of chemotactic attraction, a_N and a_C, and the production rate

per tumor cell, α_S. Owen and Sherratt [99] recognize the limited data on this subject and provide reasonable ranges for the corresponding parameters. We recover dimensioned parameters from their analysis.

Parameter	Value	Source
λ_S	0.2–1.7/day	δ_l [99]
a_N, a_C	1.7×10^9–5.3×10^9 cm^5/tumor-cell $\cdot$ day	χ_l [99]
α_S	10^{-22}–10^{-21} moles/tumor-cell $\cdot$ day	β [99]

We note that we inflate the α_S value slightly in order to achieve equilibrium concentrations of the MCP-1 signal close to the 10^{-10} M levels of Owen and Sherratt [99]. We also remark that our model's NK-cells and CD8$^+$-cells may have different rates of chemoattraction than Owen and Sherratt's macrophages, so the ranges we specify for a_N and a_C may not be biologically accurate.

15.5 Initial Conditions

Based on the initial conditions used in the human ODE model simulations, we establish reasonable ranges for the PDE model initial conditions. The ODE model asserts that a healthy immune system has approximately 10^5 NK cells, 100 CD8$^+$ cells, and 6×10^9 circulating lymphocytes, while a depleted system has 10^3 NK cells, 10 CD8$^+$ cells, and 6×10^9 circulating lymphocytes. We thus take these as reasonable bounds for our initial conditions N_0, C_0, and L_0. We also recognize that these parameters must be scaled by V_B or V_N as is appropriate.

Parameter	Value	Source
N_0	10^{-2}–10 NK-cells/mL	ODE human N_0/V_N
C_0	10^{-4}–10^{-2} CD8$^+$-cells/mL	ODE human C_0/V_N
L_0	10^6–10^7 L-cells/mL	ODE human L_0/V_B

Chapter 16

Analytic Solutions to the Spherically Symmetric Case

We now consider analytic solutions to the spherically symmetric case of our model. We do not expect to find analytic solutions to the full model, even in the spherically symmetric case. Instead, we seek solutions to particular equations using additional sets of assumptions. In general, we present these solutions without the front-fixing transformation, which is cumbersome to deal with in the differential equations but easily applied after the solution is obtained, should it be necessary.

16.1 Uninhibited Tumor Growth

In the absence of both the drug and the immune system ($D = L = N = C = 0$), we can solve for the growth of the tumor. In this situation, Equation (14.26) becomes

$$\frac{1}{r^2}\frac{\partial}{\partial r}(r^2 u) = 1, \tag{16.1}$$

so then

$$u(r) = u(0) + \frac{1}{r^2}\int_0^r (r')^2\, dr' = \frac{r}{3}. \tag{16.2}$$

Therefore, Equation (14.6) becomes

$$\frac{dR}{dt} = u(R(t), t) = \frac{R(t)}{3}, \tag{16.3}$$

so $R(t) = R_0 e^{t/3}$. Therefore, since the volume $V(t)$ of the tumor is proportional to the cube of $R(t)$, $V(t) = V_0 e^t$, where V_0 is the initial tumor volume. This is to be expected, as the natural growth rate of the tumor in non-dimensionalized units is 1.

16.2 Drug-Inhibited Tumor Growth

We now suppose that the intratumor drug concentration D is constant, so that Equation (14.26) is now

$$\frac{1}{r^2}\frac{\partial}{\partial r}(r^2 u) = 1 - \kappa_T(1 - e^{-\sigma_T D}). \tag{16.4}$$

Integrating as above, this is

$$u(r) = u(0) + \frac{1 - \kappa_T(1 - e^{-\sigma_T D})}{r^2}\int_0^r (r')^2\, dr' = \frac{1 - \kappa_T(1 - e^{-\sigma_T D})}{3}r, \tag{16.5}$$

so Equation (14.6) becomes

$$\frac{dR}{dt} = u(R(t), t) = \frac{1 - \kappa_T(1 - e^{-\sigma_T D})}{3}R(t), \tag{16.6}$$

implying that the tumor radius evolves as

$$R(t) = R_0 e^{(1 - \kappa_T(1 - e^{-\sigma_T D}))/3}. \tag{16.7}$$

Thus, the ratio of the volumes of the drug-inhibited and uninhibited tumors is

$$\exp\left(-\kappa_T(1 - e^{-\sigma_T D})\right), \tag{16.8}$$

which we compare to the data in Levasseur *et al.* [86] to estimate κ_T and σ_T. This result also matches the growth ratio we predicted in Equation (15.2).

16.3 Analytic Solution of Signal Equation

Following the approach used by Jackson *et al.* [72, 74], we make the assumption that the chemical signal S secreted by the tumor diffuses much more quickly than the tumor grows. Thus, we take the factor $R_0^2/d_S t_0$ as nearly 0, so that the signal reaches steady state nearly instantly and thus the left hand side of Equation (14.28) is taken to be 0. The λ_S term and the Heaviside step function we leave in the equation because we take λ_S to be relatively large, so λ_S/d_S is on the order of 1. Then the normalized form of Equation (14.28) is

$$\frac{1}{r^2}\frac{\partial}{\partial r}\left(r^2\frac{\partial S}{\partial r}\right) - \frac{\lambda_S}{d_S}S + \frac{T}{d_S}H(R(t) - r) = 0. \tag{16.9}$$

To eliminate the Heaviside step function, we split the above equation into two equations, the first involving the inner signal concentration S^i and the second involving the outer signal concentration S^o. On the domain $0 \leq r \leq R(t)$, S^i satisfies

$$\frac{\partial^2 S^i}{\partial r^2} + \frac{2}{r}\frac{\partial S^i}{\partial r} - \frac{\lambda_S}{d_S}S^i + \frac{T}{d_S} = 0, \tag{16.10}$$

and on $R(t) < r < \infty$, S^o satisfies

$$\frac{\partial^2 S^o}{\partial r^2} + \frac{2}{r}\frac{\partial S^o}{\partial r} - \frac{\lambda_S}{d_S}S^o = 0. \tag{16.11}$$

Furthermore, S^i and S^o are subject to the boundary and continuity conditions

$$\left.\frac{\partial S^i}{\partial r}\right|_{r=0} = 0, \quad S^o(\infty) = 0, \quad S^i(R(t)) = S^o(R(t)), \quad \left.\frac{\partial S^i}{\partial r}\right|_{r=R(t)} = \left.\frac{\partial S^o}{\partial r}\right|_{r=R(t)}. \tag{16.12}$$

Since $T = T_0$ is constant under our assumptions, a particular solution to Equation (16.10) is

$$S_p^i = \frac{T}{\lambda_S}, \tag{16.13}$$

so we now need find only the general solution to Equation (16.11), which is the homogeneous form of Equation (16.10). We first assume a solution of the form

$$S^o = \frac{1}{r}F(r, t), \tag{16.14}$$

which yields

$$\frac{\partial^2 F}{\partial r^2} - \frac{\lambda_S}{d_S}F = 0, \tag{16.15}$$

and which consequently produces the general solution

$$S^o = \frac{c_1^o(t)e^{\zeta r} + c_2^o(t)e^{-\zeta r}}{r}, \tag{16.16}$$

where we define $\zeta = \sqrt{\lambda_S/d_S}$. Similarly, Equation (16.10) has the homogeneous solution

$$S_h^i = \frac{c_1^i(t)\sinh \zeta r + c_2^i(t)\cosh \zeta r}{r}. \tag{16.17}$$

Applying the $S^o(\infty) = 0$ condition forces $c_1^o(t) = 0$. We differentiate S^i to obtain

$$\frac{\partial S^i}{\partial r} = c_1^i(t)\frac{\zeta r \cosh \zeta r - \sinh \zeta r}{r^2} + c_2^i(t)\frac{\zeta r \sinh \zeta r - \cosh \zeta r}{r^2}. \qquad (16.18)$$

In order that S_r^i go to 0 as r goes to 0, we require that $c_2^i(t) = 0$. We therefore must satisfy the continuity conditions

$$c_1^i(t)\frac{\sinh \zeta R}{R} + \frac{T}{\lambda_S} = c_2^o(t)\frac{e^{-\zeta R}}{R}, \quad c_1^i(t)\frac{\zeta R \cosh \zeta R - \sinh \zeta R}{R^2} = -c_2^o(t)e^{-\zeta R}\frac{\zeta R + 1}{R}. \qquad (16.19)$$

Solving this linear system for c_1^i and c_2^o yields

$$S^i(r,t) = \frac{T}{\lambda_S}\left(1 - e^{-\zeta R(t)}\sinh \zeta r\frac{\zeta R(t) + 1}{\zeta r}\right), \qquad (16.20)$$

$$S^o(r,t) = \frac{T}{\lambda_S}e^{-\zeta r}\frac{\zeta R(t)\cosh \zeta R(t) - \zeta R(t)}{\zeta r}. \qquad (16.21)$$

We note that the quasi-steady-state assumption forces the solution to S to violate the initial condition $S(r,0) = 0$. This is to be expected, as this assumption essentially causes the time evolution of the signal to occur instantaneously. These solutions are nevertheless more consistent with the assumption that the tumor produces the signal prior to time $t = 0$ than is the initial condition. Figure 16.1 shows a sample radial plot of these functions for particular parameter values at a particular time, and Figure 16.2 shows a plot of S as the tumor radius evolves with time.

16.4 Analytic Solution of Local Drug Equation

We can make similar assumptions regarding the chemotherapy drug to obtain analytic solutions to the distribution of D in some cases. We first assume that the drug diffuses much faster than the tumor grows,just as the signal does in Section 16.3, so that $R_0^2/d_D t_0 \approx 0$ and the left-hand side of Equation (14.27) is taken to be 0. Again, we retain the right-hand side terms because we take them to be of order 1. Second, we consider the case in which there is no local immune presence, so that $N = C = 0$. This yields the normalized
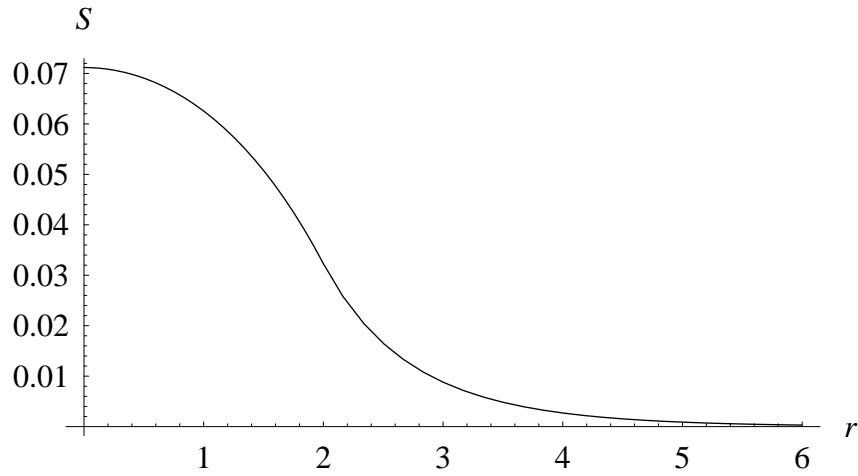
Figure 16.1: Sample plot of $S(r,t)$ for the nondimensional parameter values $T = 0.8$, $R = 2$, $\lambda_S = 6$, $d_S = 7.5$. The maximum S value corresponds to an MCP-1 concentration of approximately 10^{-10} M.
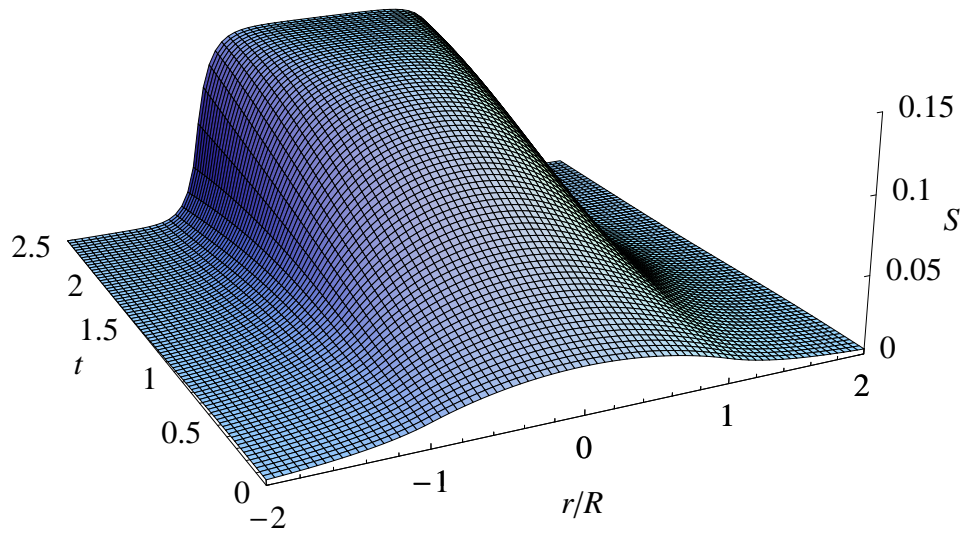
Figure 16.2: Sample plot of $S(r,t)$ for the nondimensional parameter values from Figure 16.1 as the tumor radius grows as $R = 2e^t$. The radial coordinate in this plot is front-fixed, so that the tumor boundary is always at $r/R = \pm 1$.

equation

$$\frac{1}{r^2}\frac{\partial}{\partial r}\left(r^2\frac{\partial D}{\partial r}\right) - \frac{1}{d_D}\left(\lambda_D D - \Gamma(D_B - D) + u_T\kappa_T(1 - e^{-\sigma_T D})T\right) = 0, \tag{16.22}$$

subject to the initial boundary conitions $D_r(0) = 0$ and $D(R(t)) = D_N(t)$. If we assume low drug concentrations, then $1 - e^{-\sigma_T D} \approx \sigma_T D$ and we have the linearized equation

$$\frac{1}{r^2}\frac{\partial}{\partial r}\left(r^2\frac{\partial D}{\partial r}\right) - \frac{1}{d_D}\left(\lambda_D D - \Gamma(D_B - D) + u_T\kappa_T\sigma_T DT\right) = 0. \tag{16.23}$$

We define the quantity

$$\xi_D^2 = \frac{\lambda_D + \Gamma + u_T\kappa_T\sigma_T T}{d_D}, \tag{16.24}$$

so that we now have the nonhomogeneous ODE

$$\frac{1}{r^2}\frac{\partial}{\partial r}\left(r^2\frac{\partial D}{\partial r}\right) - \xi_D^2 D = -\frac{\Gamma}{d_D}D_B(t). \tag{16.25}$$

A particular solution to this equation is $D = \frac{\Gamma}{d_D\xi_D^2}D_B(t)$. As above, we write $D = F(r,t)/r$, so that the homogeneous equation is $F'' - \xi_D^2 F = 0$. Thus, D has the general solution

$$D(r,t) = \frac{a(t)\sinh\xi_D r + b(t)\cosh\xi_D r}{r} + \frac{\Gamma}{d_D\xi_D^2}D_B(t). \tag{16.26}$$

As above, in order to satisfy the boundary condition $D_r(0) = 0$, we require that $b(t) = 0$. At $r = R(t)$, then, we have

$$D(R(t),t) = a(t)\frac{\sinh\xi_D R}{R} + \frac{\Gamma}{d_D\xi_D^2}D_B(t) = D_N(t), \tag{16.27}$$

so we can solve for $a(t)$ to yield

$$D(r,t) = \left(D_N(t) - \frac{\Gamma}{d_D\xi_D^2}D_B(t)\right)\frac{R(t)\sinh\zeta r}{r\sinh\zeta R(t)} + \frac{\Gamma}{d_D\xi_D^2}D_B(t). \tag{16.28}$$

As with the signal density S, the quasi-steady-state assumption that $R_0^2/d_D t_0 = 0$ forces the solution to violate the initial condition $D(r,0) = 0$.

16.5 Analytic Solution of Systemic Drug Equations

We now develop general solutions to Equations (14.32) and (14.33), assuming "bang-bang" chemotheraputic treatments. Suppose that we have the initial conditions $D_B(0) = D_{B,0}$ and $D_N(0) = D_{N,0}$. We first consider the homogeneous case, which yields the system of DEs

$$
\begin{pmatrix} D_B \\ D_N \end{pmatrix}' = \begin{pmatrix} -(k_{12} + k_e) & \frac{V_N}{V_B} k_{21} \\ \frac{V_B}{V_N} k_{12} & -k_{21} \end{pmatrix} \begin{pmatrix} D_B \\ D_N \end{pmatrix}. \tag{16.29}
$$

The general solutions of D_B and D_N for this system are biexponentials of the form $Ae^{-\xi_1 t} + Be^{-\xi_2 t}$, where we define

$$
\xi_1 = \frac{k_{12} + k_{21} + k_e + \sqrt{(k_{12} + k_{21} + k_e)^2 - 4k_{21}k_e}}{2}, \tag{16.30}
$$

$$
\xi_2 = \frac{k_{12} + k_{21} + k_e - \sqrt{(k_{12} + k_{21} + k_e)^2 - 4k_{21}k_e}}{2}. \tag{16.31}
$$

Then the solutions to D_B and D_N satisfying the above initial conditions are

$$
\begin{aligned}
D_B(t) = \frac{1}{k_e(\xi_1 - \xi_2)} &\left\{ e^{-\xi_1 t} \left[D_{B,0} \frac{V_N}{V_B} \xi_1 (k_e - \xi_2) - D_{N,0} \xi_1 \xi_2 \right] \right. \\
&\left. + e^{-\xi_2 t} \left[D_{B,0} \frac{V_N}{V_B} \xi_2 (\xi_1 - k_e) + D_{N,0} \xi_1 \xi_2 \right] \right\},
\end{aligned} \tag{16.32}
$$

$$
\begin{aligned}
D_N(t) = \frac{1}{k_e(\xi_1 - \xi_2)} &\left\{ e^{-\xi_1 t} \left[D_{B,0} \frac{V_B}{V_N} (\xi_1 - k_e)(\xi_2 - k_e) + D_{N,0} \xi_2 (\xi_1 - k_e) \right] \right. \\
&\left. + e^{-\xi_2 t} \left[D_{B,0} \frac{V_B}{V_N} (\xi_1 - k_e)(k_e - \xi_2) + D_{N,0} \xi_1 (k_e - \xi_1) \right] \right\}
\end{aligned} \tag{16.33}
$$

Assuming a constant administered dose rate of D_p, the corresponding nonhomogeneous system is

$$
\begin{pmatrix} D_B \\ D_N \end{pmatrix}' = \begin{pmatrix} -(k_{12} + k_e) & \frac{V_N}{V_B} k_{21} \\ \frac{V_B}{V_N} k_{12} & -k_{21} \end{pmatrix} \begin{pmatrix} D_B \\ D_N \end{pmatrix} + \begin{pmatrix} D_p \\ 0 \end{pmatrix}, \tag{16.34}
$$

and consequently the solutions to D_B and D_N are

$$
\begin{aligned}
D_B(t) = \frac{D_p}{k_e} &+ \frac{1}{k_e(\xi_1 - \xi_2)} \left\{ e^{-\xi_1 t} \left[D_{B,0}\frac{V_N}{V_B}\xi_1(k_e - \xi_2) - D_{N,0}\xi_1\xi_2 + D_p(\xi_2 - k_e) \right] \right. \\
&+ \left. e^{-\xi_2 t} \left[D_{B,0}\frac{V_N}{V_B}\xi_2(\xi_1 - k_e) + D_{N,0}\xi_1\xi_2 + D_p(k_e - \xi_1) \right] \right\},
\end{aligned}
$$

$$(16.35)$$

$$
\begin{aligned}
D_N(t) = \frac{D_p(\xi_1 - k_e)(k_e - \xi_2)}{k_e\xi_1\xi_2} &\frac{V_B}{V_N} \\
+ \frac{1}{k_e(\xi_1 - \xi_2)} \left\{ e^{-\xi_1 t} \right. &\left[-D_{B,0}\frac{V_B}{V_N}(\xi_1 - k_e)(k_e - \xi_2) + D_{N,0}\xi_2(\xi_1 - k_e) \right. \\
&\left. + D_p\frac{V_B}{V_N}\frac{(\xi_1 - k_e)(k_e - \xi_2)}{\xi_1} \right] + e^{-\xi_2 t} \left[D_{B,0}\frac{V_B}{V_N}(\xi_1 - k_e)(k_e - \xi_2) \right. \\
&\left. \left. + D_{N,0}\xi_1(k_e - \xi_2) - D_p\frac{V_B}{V_N}\frac{(\xi_1 - k_e)(k_e - \xi_2)}{\xi_2} \right] \right\}.
\end{aligned}
$$

$$(16.36)$$

Figure 16.3 illustrates a sample plot of the D_B and D_N concentrations for a particular drug regimen.
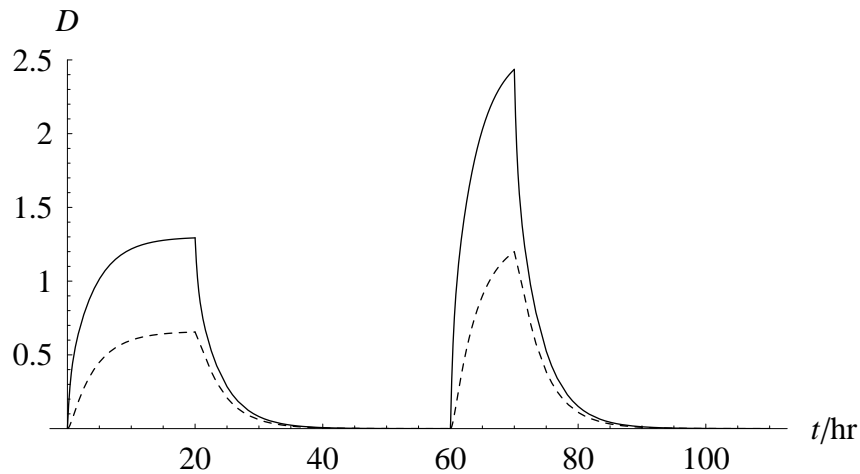
Figure 16.3: Sample plots of $D_B(t)$ and $D_N(t)$ for the parameter values $\xi_1 = 60/\text{day}$, $\xi_2 = 6/\text{day}$, $k_e = 18.5/\text{day}$ for the drug doxorubicin. Here, a unit dose of chemotherapy is applied for 20 hours, then 40 hours later double the dose is applied for 10 hours. The solid line represents D_B and the dotted line D_N.

16.6   Systemic Immune Populations in the Absence of Drug

We now consider situations in which there is no drug, so that $D = D_B = D_N = 0$, and in which the tumor is relatively large, so that $(\rho R^3)^2 \gg h$ and the quotient term $\rho^2 R^6/(h + \rho^2 R^6)$ is close to 1. Then Equations ((14.34)) and (14.35) become

$$\frac{dL}{dt} = 1 - \lambda_L L, \qquad\qquad \frac{dN_N}{dt} = L + (g - \lambda_N)N_N.$$

Solving these equations with integrating factor techniques, the general solutions to L and N_N are then

$$L(t) = \frac{1}{\lambda_L} + C_1 e^{-\lambda_L t}, \tag{16.37}$$

and

$$N_N = -\frac{1}{(g - \lambda_N)\lambda_L} - \frac{C_1}{g - \lambda_N + \lambda_L} e^{-\lambda_L t} + C_2 e^{(g - \lambda_N)t}. \tag{16.38}$$

Thus, L approaches a limiting value of $1/\lambda_L$, and if $g < \lambda_N$, N_N approaches a limiting value of $1/\lambda_L(\lambda_N - g)$. If instead $g > \lambda_N$, N_N will increase without bound. We expect that this case will eventually violate the assumptions of this analysis, as the flood of NK-cells would infiltrate the tumor and reduce its size to the point where the assumption $(\rho R^3)^2 \gg h$ no longer applies.

Chapter 17

Cylindrically Symmetric Case

17.1 Spatio-temporal Equations

We now consider the model under the case of cylindrical symmetry when there is no significant axial dependence to the tumor. Such a case might arise when considering a tumor cord surrounding a blood vessel, for example, as in Bertuzzi *et al.* [12, 13]. Thus, as in the case of spherical symmetry, all spatial dependence is reduced to dependence on r, the distance from the axis in the cylindrical coordinate system. Therefore, the boundary of the tumor is described by $B(r,t) = r - R(t) = 0$, and $\mathbf{u} = u(r,t)\hat{\mathbf{r}}$, where $\hat{\mathbf{r}}$ is the radial unit vector in cylindrical coordinates. Thus, Equations (13.1)–(13.5) become as follows:

$$\frac{T}{r}\frac{\partial}{\partial r}(ru) = \lambda_T T - \kappa_T(1 - e^{-\sigma_T D})T - l_C CT - l_N NT, \tag{17.1}$$

$$\frac{\partial D}{\partial t} + \nabla \cdot (\mathbf{u}D) = \frac{d_D}{r}\frac{\partial}{\partial r}\left(r\frac{\partial D}{\partial r}\right) - \lambda_D D + \Gamma(D_B(t) - D) - u_T\kappa_T(1 - e^{-\sigma_T D})T \tag{17.2}$$
$$- u_N\kappa_N(1 - e^{-\sigma_N D})N - u_C\kappa_C(1 - e^{-\sigma_C D})C,$$

$$\frac{\partial S}{\partial t} + \nabla \cdot (\mathbf{u}S) = \frac{d_S}{r}\frac{\partial}{\partial r}\left(r\frac{\partial S}{\partial r}\right) - \lambda_S S + \alpha_S H(R(t) - r)T, \tag{17.3}$$

and

$$\frac{\partial N}{\partial t} + \nabla \cdot (\mathbf{u}N) + a_N\left\{\frac{\partial S}{\partial r}\frac{\partial N}{\partial r} + \frac{N}{r}\frac{\partial}{\partial r}\left(r\frac{\partial S}{\partial r}\right)\right\}$$
$$= \frac{d_N}{r}\frac{\partial}{\partial r}\left(r\frac{\partial N}{\partial r}\right) - \lambda_N N - i_N NT - \kappa_N(1 - e^{-\sigma_N D})N, \tag{17.4}$$

$$\frac{\partial C}{\partial t} + \nabla \cdot (\mathbf{u}C) + a_C\left\{\frac{\partial S}{\partial r}\frac{\partial C}{\partial r} + \frac{C}{r}\frac{\partial}{\partial r}\left(r\frac{\partial S}{\partial r}\right)\right\}$$
$$= \frac{d_C}{r}\frac{\partial}{\partial r}\left(r\frac{\partial C}{\partial r}\right) - \lambda_C C - i_C CT - \kappa_C(1 - e^{-\sigma_C D})C. \tag{17.5}$$

The initial boundary of the tumor is now given by $r = R_0$, and its evolution now follows

$$\frac{dR}{dt} = u(R(t), t). \tag{17.6}$$

17.2 Temporal Equations

We define τ, the immune system's measure of the perceived tumor size. We choose to relate this to the volume of the tumor, so that

$$\tau = \rho R(t)^2 \ell, \tag{17.7}$$

where ρ is some constant of proportionality with units tumor-cells/volume and ℓ is the axial length of the tumor. The temporal equations then become as follows:

$$\frac{dD_B}{dt} = -k_{12}D_B + k_{21}D_N - k_e D_B + D_p(t) \tag{17.8}$$

$$\frac{dD_N}{dt} = k_{12}D_B - k_{21}D_N, \tag{17.9}$$

$$\frac{dL}{dt} = \alpha_L - \lambda_L L - \kappa_L(1 - e^{-\sigma_L D_N})L, \tag{17.10}$$

$$\frac{dN_N}{dt} = fL - \lambda_N N_N + g\frac{(\rho R^2 \ell)^2}{h + (\rho R^2 \ell)^2}N_N - \kappa_N(1 - e^{-\sigma_N D_N})N_N, \tag{17.11}$$

$$\frac{dC_N}{dt} = -\lambda_C C_N + j\frac{(C_N(\rho R^2 \ell))^2}{k + (C_N(\rho R^2 \ell))^2}C_N + sN_N(\rho R^2 \ell) - vN_N C_N^2 - \kappa_C(1 - e^{-\sigma_C D_N})C_N, \tag{17.12}$$

17.3 Nondimensionalization

Using the nondimensionalization presented in Section 14.3, and adding the relation $\ell = R_0\bar{\ell}$, our spatio-temporal equations transform to

$$\frac{1}{r}\frac{\partial}{\partial r}(ru) = 1 - \kappa_T(1 - e^{-\sigma_T D})T - l_C C - l_N N, \tag{17.13}$$

$$\frac{\partial D}{\partial t} + \nabla \cdot (\mathbf{u}D) = \frac{d_D}{r}\frac{\partial}{\partial r}\left(r\frac{\partial D}{\partial r}\right) - \lambda_D D + \Gamma(D_B - D)$$
$$- \left\{u_T\kappa_T(1 - e^{-\sigma_T D})T + u_N\kappa_N(1 - e^{-\sigma_N D})N + u_C\kappa_C(1 - e^{-\sigma_C D})C\right\}, \tag{17.14}$$

$$\frac{\partial S}{\partial t} + \nabla \cdot (\mathbf{u}S) = \frac{d_S}{r}\frac{\partial}{\partial r}\left(r\frac{\partial S}{\partial r}\right) - \lambda_S S + TH(R(t) - r). \tag{17.15}$$

and

$$\frac{\partial N}{\partial t} + \left\{u\frac{\partial N}{\partial r} + \frac{N}{r}\frac{\partial}{\partial r}(ru)\right\} + a_N\left\{\frac{\partial S}{\partial r}\frac{\partial N}{\partial r} + \frac{N}{r}\frac{\partial}{\partial r}\left(r\frac{\partial S}{\partial r}\right)\right\}$$
$$= \frac{d_N}{r}\frac{\partial}{\partial r}\left(r\frac{\partial N}{\partial r}\right) - \lambda_N N - i_N NT - \kappa_N(1 - e^{-\sigma_N D})N, \tag{17.16}$$

$$\frac{\partial C}{\partial t} + \left\{u\frac{\partial C}{\partial r} + \frac{C}{r}\frac{\partial}{\partial r}(ru)\right\} + a_C\left\{\frac{\partial S}{\partial r}\frac{\partial C}{\partial r} + \frac{C}{r}\frac{\partial}{\partial r}\left(r\frac{\partial S}{\partial r}\right)\right\}$$
$$= \frac{d_C}{r}\frac{\partial}{\partial r}\left(r\frac{\partial C}{\partial r}\right) - \lambda_C C - i_C CT - \kappa_C(1 - e^{-\sigma_C D})C. \tag{17.17}$$

The evolution of the tumor boundary is now specified by

$$\frac{dR}{dt} = u(R(t), t). \tag{17.18}$$

The temporal equations simplify to

$$\frac{dD_B}{dt} = -k_{12}D_B + k_{21}D_N - k_e D_B + D_p(t), \tag{17.19}$$

$$\frac{dD_N}{dt} = k_{12}D_B - k_{21}D_N, \tag{17.20}$$

$$\frac{dL}{dt} = 1 - \lambda_L L - \kappa_L(1 - e^{-\sigma_L D_N})L, \tag{17.21}$$

$$\frac{dN_N}{dt} = L - \lambda_N N_N + g\frac{\rho^2 R^4 \ell^2}{h + \rho^2 R^4 \ell^2}N_N - \kappa_N(1 - e^{-\sigma_N D_N})N_N, \tag{17.22}$$

$$\frac{dC_N}{dt} = -\lambda_C C_N + j\frac{(C_N(\rho R^2 \ell))^2}{k + (C_N(\rho R^2 \ell))^2}C_N + N_N(\rho R^2 \ell) - v N_N C_N^2 - \kappa_C(1 - e^{-\sigma_C D_N})C_N. \tag{17.23}$$

We now consider the initial boundary conditions under this nondimensionalization scheme. The spatial initial conditions and boundary conditions at $r = 0$ and the tumor boundary remain as in Equations (13.17), (13.19), and (13.20), although Equation (13.6) is now

$$T_0 + V_0 = 1, \tag{17.24}$$

making $V_0 = 1 - T_0$. The ODE initial conditions simplify to

$$D_B(0) = 0, \quad D_N(0) = 0, \quad N_N(0) = N_0, \quad C_N(0) = C_0, \quad L(0) = L_0. \tag{17.25}$$

17.4 Front-Fixing Transformation

As in the spherical case, we apply a front-fixing transformation [32] to the spatial equations to change their spatial domain from $[0, R(t)]$ to $[0, 1]$ for the sake of computational tractability. Thus, applying Equations (14.39) and (14.40), Equations (17.13)–(17.17) be-

come

$$\frac{1}{\tilde{r}^2 R}\frac{\partial}{\partial \tilde{r}}(\tilde{r}^2 u) = 1 - \kappa_T(1 - e^{-\sigma_T D})T - l_C C - l_N N, \tag{17.26}$$

$$\frac{\partial D}{\partial t} = \frac{d_D}{R^2}\frac{\partial^2 D}{\partial \tilde{r}^2} + \left(\frac{\tilde{r}}{R}\frac{dR}{dt} - \frac{u}{R} + \frac{d_D}{\tilde{r}R}\right)\frac{\partial D}{\partial \tilde{r}} - \left[\frac{1}{\tilde{r}R}\frac{\partial}{\partial \tilde{r}}(\tilde{r}u) + \lambda_D + \Gamma\right]D$$
$$+ u_T\kappa_T(1 - e^{-\sigma_T D})T + u_N\kappa_N(1 - e^{-\sigma_N D})N + u_C\kappa_C(1 - e^{-\sigma_C D})C + \Gamma D_B, \tag{17.27}$$

$$\frac{\partial S}{\partial t} = \frac{d_S}{R^2}\frac{\partial^2 S}{\partial \tilde{r}^2} + \left(\frac{\tilde{r}}{R}\frac{dR}{dt} - \frac{u}{R} + \frac{d_S}{\tilde{r}R}\right)\frac{\partial S}{\partial \tilde{r}} - \left(\frac{1}{\tilde{r}R}\frac{\partial}{\partial \tilde{r}}(\tilde{r}u) + \lambda_S\right)S + TH(1 - \tilde{r}), \tag{17.28}$$

$$\frac{\partial N}{\partial t} = \frac{d_N}{R^2}\frac{\partial^2 N}{\partial \tilde{r}^2} + \left(\frac{\tilde{r}}{R}\frac{dR}{dt} - \frac{u}{R} - \frac{a_N}{R^2}\frac{\partial S}{\partial \tilde{r}} + \frac{d_N}{\tilde{r}R}\right)\frac{\partial N}{\partial \tilde{r}}$$
$$- \left(\frac{1}{\tilde{r}R}\frac{\partial}{\partial \tilde{r}}(\tilde{r}u) + \frac{a_N}{R^2}\left(\frac{\partial^2 S}{\partial \tilde{r}^2} + \frac{R}{\tilde{r}}\frac{\partial S}{\partial \tilde{r}}\right) + \lambda_N + i_N T + \kappa_N(1 - e^{-\sigma_N D})\right)N, \tag{17.29}$$

$$\frac{\partial C}{\partial t} = \frac{d_C}{R^2}\frac{\partial^2 C}{\partial \tilde{r}^2} + \left(\frac{\tilde{r}}{R}\frac{dR}{dt} - \frac{u}{R} - \frac{a_C}{R^2}\frac{\partial S}{\partial \tilde{r}} + \frac{d_C}{\tilde{r}R}\right)\frac{\partial C}{\partial \tilde{r}}$$
$$- \left(\frac{1}{\tilde{r}R}\frac{\partial}{\partial \tilde{r}}(\tilde{r}u) + \frac{a_C}{R^2}\left(\frac{\partial^2 S}{\partial \tilde{r}^2} + \frac{R}{\tilde{r}}\frac{\partial S}{\partial \tilde{r}}\right) + \lambda_C + i_C T + \kappa_C(1 - e^{-\sigma_C D})\right)C. \tag{17.30}$$

17.5 Additional Parameter Estimation

The only additional parameter that the cylindrical case introduces is the tumor axial length, ℓ. We estimate this parameter to range from 0.05 cm to 1 cm. We also reformulate ρ as π/V_c to account for the cylindrical shape of the tumor; with this value, $\rho R^2 \ell$ gives the number of tumor cells in a cylinder of radius R and length ℓ.

Chapter 18

Analytic Solutions to the Cylindrically Symmetric Case

We present solutions to particular cases of the cylindrical case. The solutions developed in Sections 16.5 and 16.6 still apply in the cylidrical case, as they treat only the systemic behavior of the equations. As in the spherical case, we find it convenient not to apply the front-fixing transformation, which is advantageous primarily in a computational setting.

18.1 Uninhibited Growth

In the absence of both the drug and the immune system ($D = L = N = C = 0$), we can solve for the growth of the tumor. In this situation, Equation (17.13) becomes

$$\frac{1}{r}\frac{\partial}{\partial r}(ru) = 1, \tag{18.1}$$

so then

$$u(r) = u(0) + \frac{1}{r}\int_0^r r'\, dr' = \frac{r}{2}. \tag{18.2}$$

Therefore, Equation (17.6) becomes

$$\frac{dR}{dt} = u(R(t), t) = \frac{R(t)}{2}, \tag{18.3}$$

so $R(t) = R_0 e^{t/2}$. Therefore, since the volume $V(t)$ of the tumor is proportional to the square of $R(t)$, $V(t) = V_0 e^t$, where V_0 is the initial tumor volume. This is to be expected, as the natural growth rate of the tumor in non-dimensionalized units is 1.

18.2   Drug-Inhibited Tumor Growth

We now suppose that the intratumor drug concentration D is constant, so that Equation (17.13) is now

$$\frac{1}{r}\frac{\partial}{\partial r}(ru) = 1 - \kappa_T(1 - e^{-\sigma_T D}). \tag{18.4}$$

Integrating as above, this is

$$u(r) = u(0) + \frac{1 - \kappa_T(1 - e^{-\sigma_T D})}{r}\int_0^r r'\,dr' = \frac{1 - \kappa_T(1 - e^{-\sigma_T D})}{2}r, \tag{18.5}$$

so Equation (17.6) becomes

$$\frac{dR}{dt} = u(R(t), t) = \frac{1 - \kappa_T(1 - e^{-\sigma_T D})}{2}R(t), \tag{18.6}$$

implying that the tumor radius evolves as

$$R(t) = R_0 e^{(1 - \kappa_T(1 - e^{-\sigma_T D}))/2}. \tag{18.7}$$

Thus, the ratio of the volumes of the drug-inhibited and uninhibited tumors is

$$e^{-\kappa_T(1 - e^{-\sigma_T D})}. \tag{18.8}$$

The cylindrical and spherical cases produce the same solution for the volume elvolution of the tumor in these uninhibited and drug-inhibited cases, indicating that the shape of the tumor in these circumstances does not have a significant effect on the growth rate of the tumor.

18.3   Analytic Solution of Signal Equation

Under the same assumptions used in Section 16.3, the local signal equation, (17.15), reduces to

$$\frac{1}{r}\frac{\partial}{\partial r}\left(r\frac{\partial S}{\partial r}\right) - \frac{\lambda_S}{d_S}S + \frac{T}{d_S}H(R(t) - r) = 0. \tag{18.9}$$

As in the spherical case, we eliminate the Heaviside step function H by splitting the equation into two cases, the first involving the intra-tumor signal concentration S^i and the

second involving the extra-tumor concentration S^o. For convenience, we also make the spatial transform $x = \zeta r$, $\tilde{R}(t) = \zeta R(t)$, where ζ is as defined in Section 16.3. Thus, S^i now satisfies

$$\frac{d^2 S^i}{dx^2} + \frac{1}{x}\frac{dS^i}{dx} - S^i = -\frac{T}{\lambda_S} \tag{18.10}$$

on the domain $[0, \tilde{R}(t)]$, and S^o satisfies

$$\frac{d^2 S^o}{dx^2} + \frac{1}{x}\frac{dS^o}{dx} - S^o = 0 \tag{18.11}$$

on the domain $[\tilde{R}(t), \infty]$, subject to the initial and boundary conditions

$$\left.\frac{\partial S^i}{\partial x}\right|_{x=0} = 0, \quad S^o(\infty) = 0, \quad S^i(\tilde{R}(t)) = S^o(\tilde{R}(t)), \quad \left.\frac{\partial S^i}{\partial x}\right|_{x=R(t)} = \left.\frac{\partial S^o}{\partial x}\right|_{x=\tilde{R}(t)}. \tag{18.12}$$

We recognize Equation 18.11 as the modified Bessel equation of order 0 [8], so S^o has the general solution

$$S^o(x) = c_1^o(t) I_0(x) + c_2^o(t) K_0(x), \tag{18.13}$$

where $I_0(x)$ and $K_0(x)$ are the modified Bessel functions of the first and second kind of order 0, respectively. Noting that $T = T_0$ is constant, we recognize that $S_p^i = T_0/\lambda_S$ is a particular solution to Equation (18.10), so the general solution is

$$S^i(x) = c_1^i(t) I_0(x) + c_2^i(t) K_0(x) + \frac{T_0}{\lambda_S}. \tag{18.14}$$

We now satisfy the initial boundary conditions. Noting that the derivatives of $I_0(x)$ and $K_0(x)$ are $I_1(x)$ and $-K_1(x)$, respectively, our first boundary condition becomes

$$c_1^i(t) I_1(0) - c_2^i(t) K_1(0) = 0. \tag{18.15}$$

Since $I_1(0) = 0$ and $K_1(x) \to \infty$ as $x \to 0$, we require that $c_2^i(t) = 0$ but can impose no additional constraints on $c_1^i(t)$. Since $I_0(x) \to \infty$ and $K_0(x) \to 0$ as $x \to \infty$, we also require $c_1^o(t) = 0$ in order that $S^o(\infty) = 0$. With these simplifications, the continutity conditions above become

$$c_1^i(t) I_0(\tilde{R}(t)) + \frac{T_0}{\lambda_S} = c_2^o(t) K_0(\tilde{R}(t)), \qquad c_1^i(t) I_1(\tilde{R}(t)) = -c_2^o(t) K_1(\tilde{R}(t)). \tag{18.16}$$

Solving this linear system for c_1^i and c_2^o yields

$$c_1^i(t) = -\frac{T_0}{\lambda_S}\left(\frac{K_1(\tilde{R})}{I_1(\tilde{R})K_0(\tilde{R}) + I_1(\tilde{R})K_0(\tilde{R})}\right), \quad c_2^o(t) = \frac{T_0}{\lambda_S}\left(\frac{I_1(\tilde{R})}{I_1(\tilde{R})K_0(\tilde{R}) + I_1(\tilde{R})K_0(\tilde{R})}\right),$$

(18.17)

so the solutions to S^i and S^o under these conditions and assumptions are

$$S^i(r,t) = \frac{T_0}{\lambda_S}\left(1 - \frac{K_1(\zeta R)I_0(\zeta r)}{I_1(\zeta R)K_0(\zeta R) + I_1(\zeta R)K_0(\zeta R)}\right),$$

(18.18)

$$S^o(r,t) = \frac{T_0}{\lambda_S}\left(\frac{I_1(\zeta R)}{I_1(\zeta R)K_0(\zeta R) + I_1(\zeta R)K_0(\zeta R)}\right),$$

(18.19)

converting x and $\tilde{R}$ back into r and R.

18.4 Analytic Solution of Local Drug Equation

Applying the same assumptions as are stated in Section 16.4, Equation 17.14 reduces to

$$\frac{1}{r}\frac{\partial}{\partial r}\left(r\frac{\partial D}{\partial r}\right) - \frac{1}{d_D}\left(\lambda_D D - \Gamma(D_B - D) + u_T\kappa_T(1 - e^{-\sigma_T D})T\right) = 0,$$

(18.20)

with the boundary conditions $\frac{dD}{dr} = 0$ and $D(R(t),t) = D_N(t)$. Assuming that $\sigma_T D$ is small, we can aproximate $1 - e^{-\sigma_T D}$ with $\sigma_T D$ to obtain a linearized version of this equation,

$$\frac{1}{r}\frac{\partial}{\partial r}\left(r\frac{\partial D}{\partial r}\right) - \frac{1}{d_D}\left(\lambda_D D - \Gamma(D_B - D) + u_T\kappa_T\sigma_T DT\right) = 0.$$

(18.21)

Defining ξ_D as above, we now have

$$\frac{1}{r}\frac{\partial}{\partial r}\left(r\frac{\partial D}{\partial r}\right) - \xi_D^2 D = -\frac{\Gamma}{d_D}D_B(t),$$

(18.22)

which we recognize as a nonhomogeneous version of the modified Bessel equation in the variable $\xi_D r$. A particular solution to this equation is $D_p = \frac{\Gamma}{d_D\xi_D^2}D_B(t)$, so the general solution is

$$D(r,t) = c_1(t)I_0(\xi_D r) + c_2(t)K_0(\xi_D r) + \frac{\Gamma}{d_D\xi_D^2}D_B(t).$$

(18.23)

We immediately set $c_2(t) = 0$ to cancel the K_0 term, the derivative of which diverges as r goes to 0. Then, to satisfy the boundary condition at $r = R(t)$, we have

$$D(R(t), t) = c_1(t) I_0(\xi_D R(t)) + \frac{\Gamma}{d_D \xi_D^2} D_B(t) = D_N(t), \tag{18.24}$$

so solving for c_1 and substituting back into D,

$$D(r, t) = \left(D_N(t) - \frac{\Gamma}{d_D \xi_D^2} D_B(t) \right) \frac{I_0(\xi_D r)}{I_0(\xi_D R(t))} + \frac{\Gamma}{d_D \xi_D^2} D_B(t), \tag{18.25}$$

which is our complete analytic solution for the local drug density under the above quasi-steady-state assumptions.

Part V

Conclusion

Chapter 19

Discussion

intro Here we present our final results as well as possibilities for further work.

19.1 Results and Conclusions

19.1.1 ODE Model

The ordinary differential equations model shows that combination therapy is more effective than either chemotherapy or immunotherapy alone. This is consistent with experimental results. In mouse experiments involving vaccine therapy, combination therapy was more effective for a number of different chemotherapeutic drugs citemachiels:. Dienfechbach. Rosenberg. Kuznetsov comparison of model.

Evaluate results of Optimal Control if possible?

Tumor Dormancy: Our ordinary differential equations model lacks tumor dormancy. The low tumor equilibrium is always unstable until it merges with the high tumor equilibrium. Tumor dormancy is apparant in Kuzentsov's model which is similar to ours, but we have an additional immune cell population and a modified Michaelis-Menton term. With various parameter adjustments, we can obtain a state of tumor dormancy. However this case is not realistic because this causes the region below tumor dormancy to have trajectories going off to infinity in the NK cell direction.

19.1.2 Probability Model

19.1.3 PDE Model

19.2 Directions for Further Work

19.2.1 ODE Model

For the ordinary differential equation model, it would be beneficial to alter the system of equations by changing the $-uNL^2$ term. This exact mechanism remains elusive. One

might also include an additional immune cell population, possibly one that activates the $CD8^+$ T cells by producing cytokines in the body, such as CD4 or CD3 cell.

Extension on optimal control with experiments involving different constraints and combinations of constraints. It is necessary to include analytic solutions to these objective functions in order to determin wherther DIRCOL is producing optimal solutions, as well as investigating the possiblity of bang-bang solutions.

In order to justify the model's form and to obtain more realistic parameters so that quantitative experiments can be simulated, it is necessary to fit various sets of experimental data to our equations. Experimental data from human clinical trials involving various forms of immunotherapy should prove more beneficial than mouse expereiments.

19.2.2 Probability Model

19.2.3 PDE Model

sectionWrap Up

Appendix A

ODE Parameter Tables

Parameter	Description	Units
a	Logistic tumor growth rate.	day^{-1}
b	b^{-1} is the tumor carrying capacity.	$cell^{-1}$
c	Fractional tumor cell kill by NK cells.	$cell^{-1} \cdot day^{-1}$
d	Saturation level of fractional tumor cell kill by CD8$^+$ T-cells.	day^{-1}
e	Fractional rate of NK cell production by stem cells. (Stem cell levels measured by number of circ. lymph. generated)	day^{-1}
eL	Exponent of fractional tumor cell kill by CD8$^+$ T-cells.	dimensionless
f	Fracional death rate of NK cells.	day^{-1}
g	Maximum KN cell recruitment rate by tumor cells.	day^{-1}
h	Steepness coefficient of NK cell recruitment	$cell^2$
j	Maximum CD8$^+$ recruitment rate.	day^{-1}
k	Steepness coefficient of the CD8$^+$ T-cell recruitment curve.	$cell^2$
m	Death rate of CD8$^+$ T-cells.	day^{-1}
p	NK cell inactivation rate by tumor cells.	$cell^{-1} \cdot day^{-1}$
q	CD8$^+$ T-cell inactivation rate by tumor cells.	$cell^{-1} \cdot day^{-1}$
r_1	Rate CD8$^+$ T-cells are stimulated to be produced by tumor cells killed by NK cells.	$cell^{-1} \cdot day^{-1}$
r_2	Rate CD8$^+$ T-cells are stimulated to be produced by tumor cells killed by circulating lymphocytes.	$cell^{-1} \cdot day^{-1}$

Parameter	Description	Units
s	Steepness coefficient of the tumor-CD8$^+$ competition term.	dimensionless
u	Regulatory function by NK cells on CD8$^+$ T-cells.	cell$^{-2} \cdot$ day^{-1}
K_T	Fractional tumor cell kill by chemotherapy.	day^{-1}
K_N	Fractional NK cell kill by chemotherapy.	day^{-1}
K_L	Fractional CD8$^+$ T-cell kill by chemotherapy.	day^{-1}
K_C	Fractional circulating lymphocyte cell kill by chemotherapy.	day^{-1}
α	Constant source of circulating lymphocytes.	cell $\cdot$ day^{-1}
β	Natural death and differentiation of circulating lymphocytes.	day^{-1}
γ	Rate of chemotherapy drug decay.	day^{-1}

Table A.1: Units and Descriptions of ODE Model Parameters

Parameter	Description	Units
p_i	Maximum CD8$^+$ T-cell recruitment rate.	day^{-1}
g_i	Steepness coefficient of CD8$^+$ T-cell recruitment curve by IL2.	cells^2
μ_i	Rate of IL-2 drug decay.	day^{-1}

Table A.2: Units and Descriptions of ODE Model Parameters

Appendix B

Routh Test

The Routh test [14] is a technique used to determine whether all the roots of a polynomial (in our case all eigenvalues in the characteristic equation) have negative real parts.

Given the Jacobian below,

$$J = \begin{bmatrix} -1 - \chi N - \delta\frac{dD}{dT} & -\chi & -\delta\frac{dD}{dL} \\ N(2\tau\eta - \pi) & -\epsilon + \tau - \pi & 0 \\ \frac{2\theta\kappa LD\frac{dD}{dT}}{(\kappa+D^2)^2} - \xi L + \rho_1 N + \frac{\rho_2\alpha}{\beta} & \rho_1 - \zeta L^2 & \frac{-\mu+\theta D^2}{\kappa+D^2} + \frac{\theta\kappa LD\frac{dD}{dL}}{(\kappa+D^2)^2 - \xi T - 2\zeta NL} \end{bmatrix}$$

we must determine its eigenvalues. For simplicity, let us denote the elements of J as

$$J = \begin{bmatrix} a & d & g \\ b & e & 0 \\ c & f & h \end{bmatrix}.$$

Now let λ be an eigenvalue such that

$$\det(J - I\lambda) = (a - \lambda)(e - \lambda)(h - \lambda) - d(b(h - \lambda)) + g(bf - (e - \lambda)c).$$

Therefore, the characteristic equation for this system is

$$\lambda^3 + \lambda^2(-a - e - h) + \lambda(ae + eh - bd - gc) + (dbh + egc - aeh - gbf) = 0$$

The Routh test states that, given a characteristic equation of the form

$$\lambda^3 + a_2\lambda^2 + a_1\lambda + a_0 = 0,$$

if all coefficients are positive and if $a_2 a_1 > a_0$, then all the eigenvalues, i.e. roots of the characteristic equation, are negative. Expanding a_2 with the values from our Jacobian

matrix J,

$$a_2 = \left(1 + \chi N + \delta \frac{dD}{dT}\right) + (\epsilon - \tau + \pi) + \frac{-\mu + \theta D^2}{\kappa + D^2} + \frac{\theta \kappa L D \frac{dD}{dL}}{(\kappa + D^2)^2 - \xi T - 2\zeta NL}.$$

If we can force a_2 to be negative, the point loses its stability. We choose this quantity to vary since it is the simplest of the coefficients in our characteristic equation. We now expand a_0 and a_1:

$$
\begin{aligned}
a_1 = {} & \left(1 + \chi N + \delta \frac{dD}{dT}\right)(\epsilon - \tau + \pi) \\
& - \left(1 + \chi N + \delta \frac{dD}{dT}\right)\left(\frac{-\mu + \theta D^2}{\kappa + D^2} + \frac{\theta \kappa L D \frac{dD}{dL}}{(\kappa + D^2)^2 - \xi T - 2\zeta NL}\right) \\
& + (-\epsilon + \tau - \pi)\left(\frac{-\mu + \theta D^2}{\kappa + D^2} + \frac{\theta \kappa L D \frac{dD}{dL}}{(\kappa + D^2)^2 - \xi T - 2\zeta NL}\right) \\
& + (N(2\tau\eta - \pi)\chi + \delta \frac{dD}{dL}\left(\frac{2\theta \kappa L D \frac{dD}{dT}}{(\kappa + D^2)^2} - \xi L + \rho_1 N + \frac{\rho_2 \alpha}{\beta}\right)
\end{aligned}
$$

$$
\begin{aligned}
a_0 = {} & -\delta \frac{dD}{dL}(N(2\tau\eta - \pi))\left(\frac{-\mu + \theta D^2}{\kappa + D^2} + \frac{\theta \kappa L D \frac{dD}{dL}}{(\kappa + D^2)^2 - \xi T - 2\zeta NL}\right) \\
& + (-\epsilon + \tau - \pi)\left(-\delta \frac{dD}{dL}\right)\left(\frac{2\theta \kappa L D \frac{dD}{dT}}{(\kappa + D^2)^2} - \xi L + \rho_1 N + \frac{\rho_2 \alpha}{\beta}\right) \\
& + \left(1 + \chi N + \delta \frac{dD}{dT}\right)(-\epsilon + \tau - \pi)\left(\frac{2\theta \kappa L D \frac{dD}{dT}}{(\kappa + D^2)^2} - \xi L + \rho_1 N + \frac{\rho_2 \alpha}{\beta}\right) \\
& + \delta \frac{dD}{dL}(N(2\tau\eta - \pi))(\rho_1 - \zeta L^2)
\end{aligned}
$$

Neither of these expressions simplifies appreciably, so we have chosen to alter parameters numerically and leave this analytic solution to the appendix. The important thing to note is that the three parameters, π, ξ, and ζ are two degrees of magnitude larger than the other parameters. This assumption allows us to see that each term in the Jacobian is dominated by only one or two parameters. For instance, if we were to make the Jacobian entries of the diagonal postive, each of the equations a would have one more positive term to add

in.

Appendix C

Optimal Control Details

C.1 Optimal Control Code

user.c

```c
/* User-provided functions for DIRCOL.
 *
 * Optimal control of cancer treatment
 *   Research project with Professor de Pillis, Summer 2003.
 *
 * The system of equations included here is the non-dimensionalized system of
 * equations.
 *
 * C code written to interface with Fortran.  f2c used to help converting the
 * function prototypes properly.
 */

#include <stdio.h>
#include <stdlib.h>
#include <unistd.h>
#include <math.h>

/* The time after which no more chemotherapy may be administered (so that tumor
 * will evolve only under influence of immune system). */
static double first_chemo_time = 0.0;
static double last_chemo_time = 8.0;

/* Default parameters used in the equations. */
struct params {
    double delta, epsilon, zeta, eta, theta, kappa, lambda, mu, xi;
    double pi, rho1, rho2, tau, chi, gamma, eL, s, kT, kN, kL, kC;
    double pI, gI, muI;
};

/* Mouse data (nn). */
static struct params p = {
    .delta = 1.8494,
    .epsilon = 0.09564,
    .zeta = 1.0e4, /* 675914.2909, */
    .eta = 9.495e-09,
    .theta = 0.28901,
    .kappa = 1.4959e-08,
    .lambda = 0.027856,
    .mu = 0.046427,
    .xi = 0.036631,
    .pi = 10.7045,
    .rho1 = 0.080618,
    .rho2 = 1.5917e-05,
    .tau = 0.28901,
    .chi = 4.6978e-05,
    .gamma = 2.0892,
```

```
        .eL = 0.8673,
        .s = 1.1042,
        .kT = 2.0892,
        .kN = 1.3928,
        .kL = 1.3928,
        .kC = 1.3928,
        .pI = 2321.4,
        .gI = 2.0,
        .muI = 23.214
};

static const int parameter_count = sizeof(p)/sizeof(double);

/* Typedefs for Fortran types, taken from f2c header file. */
typedef long int integer;
typedef float real;
typedef double doublereal;
typedef long int ftnlen;

/* Square a real number.  This is a handy helper function since there is no
 * built-in exponention operator. */
static double
square(double x)
{
    return x * x;
}

/* Return the value given if the number is positive, or zero if the number is
 * not positive. */
static double
pos(double x)
{
    return (x > 0) ? x : 0;
}

/* Modified logarithm function, that has a lower cut-off below which the value
 * stops changing. */
static double
modlog(double x)
{
    const double cutoff = 1e-5;

    if ( x < cutoff ) {
        return log(cutoff);
    } else {
        return log(x);
    }
}

/* DIRCOM: Initialization function. */
int
dircom_(void)
{
    return 0;
}

/* USRDEQ: Differential equation to solve (x' = f(x, u, p, t)). */
int
usrdeq_(integer *iphase, integer *nx, integer *lu,
        integer *lp, doublereal *x, doublereal *u, doublereal *params,
        doublereal *t, doublereal *f, integer *ifail)
{
    /* Population sizes are first four state variables, followed by
```

```
     * chemotherapy and IL-2 concentrations. */
    double T = pos(x[0]);
    double N = pos(x[1]);
    double L = pos(x[2]);
    double C = pos(x[3]);
    double M = pos(x[4]);
    double I = pos(x[5]);

    /* Chemotherapy administration function is the first control variable.
     * IL-2 administration is the second. */
    double v = u[0];
    double vI = u[1];

    /* Compute D, but be careful in doing so to avoid potential division by
     * zero errors.  We have defined D to be zero if L is zero. */
    double D;
    if ( L == 0 ) {
        D = 0;
    } else {
        D = pow(L, p.eL) / (p.s * pow(T, p.eL) + pow(L, p.eL)) * T;
    }

    f[0] = T*(1.0-T) - p.chi*N*T - p.delta*D - p.kT*(1.0-exp(-M))*T;
    f[1] = p.epsilon*(C - N) + p.tau*square(T)/(p.eta+square(T))*N - p.pi*N*T
            - p.kN*(1.0-exp(-M))*N;
    f[2] = -p.mu*L + p.theta*square(D)/(p.kappa+square(D))*L - p.xi*L*T
            + (p.rho1*N+p.rho2*C)*T - p.zeta*N*square(L)
            + p.pI*I/(p.gI + I)*L - p.kL*(1.0-exp(-M))*L;
    f[3] = p.lambda*(1.0 - C) - p.kC*(1.0-exp(-M))*C;
    f[4] = v - p.gamma*M;
    f[5] = vI - p.muI*I;

    /* Auxiliary state variables used to compute objective function. */
    f[6] = T;
    f[7] = C;
    f[8] = -v;
    f[9] = -vI;

    return 0;
}

/* USROBJ: Objective function (to be minimized). */
int
usrobj_(integer *nr, integer *nx, integer *lu, integer *lp,
        doublereal *xl, doublereal *ul, doublereal *p, doublereal *enr,
        doublereal *fobj, doublereal *xr, doublereal *ur, doublereal *tf,
        integer *ifail)
{
    /* For single-phase problem, should only ever care about *nr == 1 case. */
    if ( *nr == 1 ) {
        /* Objective: Minimize the sum of the final tumor burden and the
         * average tumor burden. */
        *fobj = xr[0] + xr[6] / *tf;

    } else {
        *fobj = 0.0;
    }

    return 0;
}

/* USRNBC: Nonlinear boundary and swiching conditions. */
int
```

```
usrnbc_(integer *ikind, integer *nrnln, integer *nx,
        integer *lu, integer *lp, doublereal *xl, doublereal *ul,
        doublereal *p, doublereal *el, doublereal *rb, doublereal *xr,
        doublereal *ur, doublereal *er, integer *ifail)
{
    /* The case *ikind == -1 corresponds to explicit end conditions. */
    if ( *ikind == -1 ) {
        xr[8] = 0.0;                /* Should use all available drugs. */
        xr[9] = 0.0;
    }

    return 0;
}


/* USRNIC: Nonlinear inequality constraints. */
int
usrnic_(integer *iphase, integer *ngnln, integer *needg,
        integer *nx, integer *lu, integer *lp, doublereal *x, doublereal *u,
        doublereal *p, doublereal *t, doublereal *g, integer *ifail)
{
    return 0;
}


/* USRNEC: Nonlinear equality constraints. */
int
usrnec_(integer *iphase, integer *nhnln, integer *needh,
        integer *nx, integer *lu, integer *lp, doublereal *x, doublereal *u,
        doublereal *p, doublereal *t, doublereal *h, integer *ifail)
{
    /* If enabled, do not allow any chemotherapy or immunotherapy to be
     * administered after some fixed time. */
    if ( *nhnln > 0 ) {
        if ( *t < first_chemo_time || *t >= last_chemo_time ) {
            h[0] = u[0] + u[1];
        } else {
            h[0] = 0.0;
        }
    }

    return 0;
}


/* USRSTV: Initial estimates for x, u, p, and E. */
int
usrstv_(integer *iphase, integer *nx, integer *lu,
        doublereal *tau, doublereal *x, doublereal *u, integer *ifail)
{
    if ( *iphase > 0 ) {
        /* Initial estimates of x(tau) and u(tau).  For simplicity, all data
         * starts off zero. */
        x[0] = 0.0;
        x[1] = 0.0;
        x[2] = 0.0;
        x[3] = 0.0;
        x[4] = 0.0;
        x[5] = 0.0;
        x[6] = 0.0;
        x[7] = 0.0;

        u[0] = 0.0;
        u[1] = 0.0;

    } else if ( *iphase == 0 ) {
```

```c
        /* Initial estimates of events, E. */
        u[0] = 0.0;
        u[1] = 1.0;

    } else if ( *iphase < 0 ) {
        /* Initial estimates of parameters, p. */
    }

    return 0;
}


/* VISUALIZATION HELPER FUNCTIONS */

/* USRREV: Actual expected values for control and state variables, for
 * comparison in visualization. */
int
usrrev_(integer *nsmax, integer *iphase, integer *i,
        integer *ns, real *xs, real *ys, char *ktyp, ftnlen ktyp_len)
{
    return 0;
}

/* USRREA: Actual expected values for adjoint variables, for visualization. */
int
usrrea_(integer *indx, integer *iord, integer *iphase,
        integer *nsmax, integer *ns, real *xs, real *ys, char *ktyp,
        ftnlen ktyp_len)
{
    return 0;
}

/* USRREM: Reference values for multiplier functions of active constraints, for
 * visualization. */
int
usrrem_(integer *iwhat, integer *indx, integer *iord,
        integer *iphase, integer *nsmax, integer *ns, real *xs, real *ys,
        char *ktyp, ftnlen ktyp_len)
{
    return 0;
}

/* USRFCN: Arbitrary user-defined functions for visualization. */
int
usrfcn_(integer *iphase, integer *needfcn, integer *nx,
        integer *lu, integer *lp, doublereal *x, doublereal *u, doublereal *p,
        doublereal *t, doublereal *lam, doublereal *munic, doublereal *munec,
        doublereal *mub, doublereal *fcn)
{
    /* Call to determine number of user-defined functions.  We do not implement
     * any. */
    if ( *iphase <= 0 ) {
        *iphase = 0;
    }

    return 0;
}
```

Appendix D

Code for Probability Model

D.1   runtumor.m

```
function x =  runtumor()
%Programer: KEO Todd-Brown
%Date: June 4, 2003
%Preconditions:
%Postconditions:
%Purpose:

%%%Default%%%
q=false;
ls = 10000;              %for loop size
mysize=500;              %size of cell grid you are working with
num_plots=4;             %how many plots do you want...
                         %be sure to put a square number
                         %...if you use subplots
flag=3;                  %1=subplots; 2=figures

%%modeling parameters
thata_mov=1000;          %%%atm move is turned off to simulate Farreira

                         %Controls the probability curve for cancer cell
                         %...movement
thata_div=0.3;           %Controls the probability curve for cancer cell
                         %...division
thata_del=0.01;          %Controls the probability curve for cancer cell
                         %...death
thata_c=0.1;             %Controls the chemo kill curve for cancer cells
thata_ci=0.1;            %Controls the chemo kill curve for immuno cells

alpha=1/mysize;          %
lamda_n=25;              %N nutrient consumption
lamda_m=10;              %M nutrient consumption
lamda_c=25;              %relitive Chemo cc

ip=1e-3;                  %ratio of immuno:normal cells

cancer_tol=1e4;          %number of cancer cells nessacary to activate chemo

while(q==false)
    x=input(['r=run;q=quit; n=number of iterations;', ...
            ' s=grid size; v=print variables; m=more options\n'],'s');
    if x=='m'
        x=input(['tm=thata_mov; td=thata_div; tk=thata_del;',...
                'tc=thata_c; ti=thata_ci; a=alpha;', ...
                'ln=lamda_n; lm=lamda_m; lc=lamda_c; m=more\n'],'s');
    end
    if x=='m'
            x=input('ip=immuno cell proportion; ct=cancer_tol\n');
    end
```

```
if x=='r'
    !rm data/*.mat
    save('data/parameters', 'ls', 'mysize', 'thata_mov', 'thata_div', ...
        'thata_del', 'thata_c', 'thata_ci', 'alpha',...
        'lamda_n', 'lamda_m', 'lamda_c', 'ip', 'cancer_tol');
    timeflag=cputime;
    tumor(ls, mysize, thata_mov, thata_div, thata_del, thata_c, ...
        thata_ci, alpha, lamda_n, lamda_m, lamda_c, ip, cancer_tol);
    timeflag=cputime-timeflag
    beep; beep; beep;
elseif x=='v'
    (['$grid size=', num2str(mysize), ...
            ';$ $\theta_{move}=',num2str(thata_mov),...
            ';$ $\theta_{del}=', num2str(thata_del),...
            ';$ $\theta_div=', num2str(thata_div),...
            ';$ $\theta_c=', num2str(thata_c),...
            ';$ $\theta_{ci}=', num2str(thata_ci),...
            ';$ $a=', num2str(alpha*mysize),...
            ';$ $\lambda_n=', num2str(lamda_n), ...
            ';$ $\lambda_m=',num2str(lamda_m),...
            ';$ $\lambda_c=', num2str(lamda_c), ...
            ';$ $ip=', num2str(ip),...
            ';$ $cancer_tol=', num2str(cancer_tol),'$'])

elseif x=='n'
    ls
    ls=input('number of iterations?\n');
elseif x=='s'
    mysize
    mysize=input('grid size?\n');
elseif x=='a'
    a=alpha*mysize
    a=input('alpha=a/(grid size), enter a\n');
    alpha=a/mysize;
elseif x=='q'
    q=true;
elseif x=='tm'
    thata_mov
    thata_move=input('thata_move(turned off atm)?\n');
elseif x=='td'
    thata_div
    thata_div=input('thata_div?\n');
elseif x=='tc'
    thata_c
    thata_c=input('thata_c?\n');
elseif x=='ln'
    lamda_n
    lamda_n=input('landa_n?\n');
elseif x=='lm'
    lamda_m
    lamda_m=input('landa_n?\n');
elseif x=='lc'
    lamda_c
    lamda_c=input('landa_c?\n');
elseif x=='tk'
    thata_del
    thata_del=input('thata_del?\n');
elseif x=='ti'
    thata_ci
    thata_ci=input('thata_ci?\n');
elseif x=='ip'
    ip
    ip=input('proportion of cells that are immuno?\n');
```

```
    elseif x=='ct'
        cancer_tol
        cancer_tol=input('cancer cell tolerence?\n');
    else
        'Bad choice, pick again.\n'
    end
end
```

D.2 tumor.m

```
function mycells = tumor(ls, mysize, thata_mov, thata_div, thata_del, thata_c, ...
                        thata_ci, alpha, lamda_n, lamda_m, lamda_c, immunoprob, ...
                        cancer_tol)
%Programer: KEO Todd-Brown
%Date: June 4, 2003
%Purpose:  This is the main function for a tumor simulation
%Preconditions: ls - an integer which is the size of the run loop
%               mysize - an integer which indicates what size the cell grid
%                        is
%               thata_move - controlls the probability curve for move
%               thata_div - controlls the probablitiy curve for divition
%               thata_del - controls the probability curve for natural death
%               thata_c - controls the probability curve for chemo death of
%                         a cancer cell
%               thata_ci - controls the probability curve for chemo death
%                          of a immuno cell
%               alpha - celluar nutrient consumption
%               lamda_n - ratio of cancer to normal cell consumption of N
%               lamda_m - ratio of cancer to normal cell consumption of M
%               lamda_c - ratio of cancer to normal cell consumption of C
%               immunoprob - ratio of immune cells to cell sites ie normal
%                            number of cells
%               cancer_tol - number of cancer cells nessacary to activate
%                            chemo
%
%Postconditions: tumor returns the last cell site information

%%Initialize stuff
mycells = sparse(mysize, mysize);   %stores the cell type
                                    %...(normal/nucrotic/cancer) on a give
                                    %...cite (0=normal; -1=nucrotic; >0
                                    %...x number of cancer)
mycells(floor(mysize/2),floor(mysize/2))=1;
                                    %seeds site with one cancer cell

cancer_pop=[];                      %stores cancer population at each iteration
immuno_pop=[];                      %stores immune population at each iteration

I= sparse(mysize, mysize);          %stores immune cells
N=sparse(mysize, mysize)            %stores N nutrient consintration
M=sparse(mysize, mysize)            %stores the M nutrient consintration
C=sparse(mysize, mysize);           %stores the chemo consitrations

chemo=false;                        %start off with no chemo theropy
mr=1;                               %ratio that immuno cells move vs cell cycle

[lhs, rhs]=standard_rhs(mysize);
                                    %creates the general right hand side of the
                                    %... linear system for the PDE's method
                                    %... (0=grad^2(N) note that rhs is sparse
```

```
%%***Nutrience Consintrations**
                               %Calculates the itital chemical consitrations
[N, guessN]=CN_PDEsolver(lhs, rhs, mysize, mycells, lamda_n, alpha, 1, 'N');

[M, guessM]=CN_PDEsolver(lhs, rhs, mysize, mycells, lamda_m, alpha, 1, 'M');%, L, U);

if chemo==true                    %but don't bother calculating C if chemo isn't on
    [C, guessC]=CN_PDEsolver(lhs, rhs, mysize, mycells, lamda_c, alpha, 1, 'C');
end

%%***Seed immune system
I = gen_immuno(mysize, mycells, I, C, thata_ci, immunoprob);

%***Count the immuno population
count=sum(sum(I>0));
immuno_pop=[immuno_pop, count];

%***Count the cancer population
count=sum(sum((mycells>0).*mycells));
cancer_pop=[cancer_pop, count];

%***Save the data
save('data/mycells1','mycells');
save('data/N1', 'N');
save('data/M1', 'M');
save('data/C1', 'C');
save('data/I1', 'I');
save('data/old_mycells','mycells');
save('data/old_N', 'N');
save('data/old_M', 'M');
save('data/old_C', 'C');
save('data/old_I', 'I');

for i=2:ls,

    %***Move Stuff***
    for n=1:mr
        [I, mycells]=Ijiggle(mysize, I, mycells);
                               %move immune cells
        I = gen_immuno(mysize, mycells, I, C, thata_ci, immunoprob);
                               %generate new immune cells

        %***Count and save the immuno population
        count=sum(sum(I>0));
        immuno_pop=[immuno_pop, count];
        save('data/immuno_pop', 'immuno_pop');
    end

    mycells=Jiggle(mysize, N, M, C, mycells, thata_mov, thata_div,...
        thata_del, thata_c, chemo);
                               %do divide, move, die to cancer cells

    %***Re-calculate Nutrient consintrations
    [N, guessN] =CN_PDEsolver(lhs, rhs, mysize, mycells, lamda_n, alpha, 0, 'N', guessN);
    [M, guessM] =CN_PDEsolver(lhs, rhs, mysize, mycells, lamda_m, alpha, 0, 'M', guessM);

    if chemo==true                %again don't bother with Chemo unless it's on
        if bang==(i-1)            %calculate the first Chemo
            [C, guessC] = CN_PDEsolver(lhs, rhs, mysize, mycells, lamda_c, alpha, 1, 'C');
        else
            [C, guessC] = CN_PDEsolver(lhs, rhs, mysize, mycells, lamda_c, alpha, 0, 'C', guessC);
        end
```

```
        end

    %***Save stuff again***
    if ls>100                %save every 100 frames
        if mod(i,100)==0
            save(['data/mycells', int2str(i)],'mycells');
            save(['data/N', int2str(i)], 'N');
            save(['data/M', int2str(i)], 'M');
            save(['data/C', int2str(i)], 'C');
            save(['data/I', int2str(i)], 'I');
        end
    else
        save(['data/mycells', int2str(i)],'mycells');
        save(['data/N', int2str(i)], 'N');
        save(['data/M', int2str(i)], 'M');
        save(['data/C', int2str(i)], 'C');
        save(['data/I', int2str(i)], 'I');
    end

    %always save to old stuff so we can track it as it runs
    save('data/old_mycells','mycells');
    save('data/old_N', 'N');
    save('data/old_M', 'M');
    save('data/old_C', 'C');
    save('data/old_I', 'I');

    %***Count tumor cells and save***
    count=sum(sum((mycells>0).*mycells));
    cancer_pop=[cancer_pop, count];
    save('data/cancer_pop', 'cancer_pop');

    %***Check for the end***
    if sum(mycells(1,:)>0) | count == 0 | sum(mycells(:,1)>0) | sum(mycells(:,mysize)>0)
                                    %if the cancer 1) gets to the first
                                    %...row (ie to the blood vessel)
                                    %...or 2) the total number of
                                    %...cancer cells drop below 0 or 3) runs
        ls=i;                       %...off the grid then set ls to i
        break                       %...for cellplot and end the iterations
    end

    %***Turn chemo on***
    if count > cancer_tol & chemo==false
        chemo=true;
        bang=i
    end

end

%***Save the last frame***
save(['data/mycells', int2str(i)],'mycells');
save(['data/N', int2str(i)], 'N');
save(['data/M', int2str(i)], 'M');
save(['data/C', int2str(i)], 'C');
save(['data/I', int2str(i)], 'I');
save('data/cancer_pop', 'cancer_pop');

%***Plot***
ls
cellplot(ls);
```

D.3 Ijiggle.m

```
function [I, mycells]=Ijiggle(mysize, I, mycells)

%Wonder randomly around and eat cancer until you die or chemo kills you

%newmycells=mycells;
%newI=I;

immuncells=find(I~=0);
mylen=size(immuncells);
mylen=mylen(1);
for k=1:mylen
   i=immuncells(k);
     if mycells(i) >0       %check for cancer on present site
         I(i)=I(i)-1;              %spend a cell_kill
         mycells(i)=mycells(i)-1;

         if mycells(i)==0
             mycells(i)=-1;    %skip the normal cell
         end


     else                 %check for cancer on neighboring site and move there

         %%Look for where the cell is
         %a | d | f
         %b | x | g
         %c | e | h

         a = i-1-mysize;     %1
         b = i-mysize;       %2
         c = i+1-mysize;     %3
         d = i-1;            %4
         e = i+1;            %5
         f = i-1+mysize;     %6
         g = i+mysize;       %7
         h = i+1+mysize;     %8

         %%something to do later might be to put in wrapping

         if mod(i, mysize)==1    %top
             if 1==i                                %left side
                 neigh_cells=[e g h];
             elseif (1+mysize*(mysize-1))==i        %right side
                 neigh_cells=[b c e];
             else
                 neigh_cells=[b c e g h];
             end

         elseif mod(i, mysize)==0%bottom
             if i==mysize                        %left side
                 neigh_cells=[d f g];
             elseif i==(mysize*mysize)           %right side
                 neigh_cells=[a b d];
             else
                 neigh_cells=[a b d f g];
             end
         elseif (1<=i) & (i<=mysize)             %left side
             %top and bottom already taken care of
             neigh_cells=[d e f g h];
         elseif ((1+mysize*(mysize-1))<=i) & (i<=(mysize*mysize))    %right side
```

```
            %top and bottom already taken care of
            neigh_cells=[a b c d e];
        else                                    %move somewhere random
            neigh_cells=[a b c d e f g h];
        end

        %neigh_cells
        %%find free cells around it

        free_n_cells=[];    %array of sites not occupied by immune cells
        free_cn_cells=[];   %array of sites occumpied by cancer cells

        for j=neigh_cells
            if I(j)==0              %no immune cells
                free_n_cells=[free_n_cells, j];
                if mycells(j)>0     %cancer present
                    free_cn_cells=[free_cn_cells, j];
                end
            end
        end

        %%figure out which free cell to move to
        if size(free_cn_cells)~=0
            move_i=ceil(rand*(sum(free_cn_cells>0)));
            move_to=free_cn_cells(move_i);
        else
            move_i=ceil(rand*(sum(free_n_cells>0)));
            move_to=free_n_cells(move_i);
        end

        %%move there
        I(move_to)=I(i);
        I(i)=0;
    end

end
```

D.4   Jiggle.m

```
function [mycells] = Jiggle(mysize, N, M, C, mycells, thata_mov, thata_div, thata_del, thata_c, chemo)
%Programer: KEO Todd-Brown
%Date: June 4, 2003
%Preconditions: Jiggle(mysize, N, M, mycells, thata_mov, thata_div, thata_del)
%               where mysize is the size of N, M, and mycells which are
%               square matrices, and thata_mov, thata_div and thata_del
%               are all numbers.  lamda_n, lamda_m, alpha and omega are
%               used to calculate the nutrient consintrations
%Postconditions: Jiggle returns a mysize matrix
%Purpose: The purpose of this function is to find the cells at the next
%         time step
%         This is done by calculating the related
%         probablities for movement, cellular division and death of tumor
%         cells and then carry out these probablities on each cell by
%         generating a uniformly distributed random number between 0 and
%         1.  Each cell site is also assigned 0,1 or 2 randomly with
%         equal probability to determine if the site tries to divid, move
%         or die

%%***declarations***
old_cells = mycells;            %stores the old cell data
```

```
%***Action Flag**
%***figure out what cells we want to Jiggle
action=floor(rand(mysize)*3);    %rand has a uniform distribution

[S, T]=find(old_cells>0);        %returns the indexes of non-zeros entries
                                 %...of old_cells
loopend=size(S);                 %returns a vector of the size of the loop

plus_changes=sparse(mysize, mysize);
                                 %storage for positive change
minus_changes=sparse(mysize, mysize);
                                 %storage for negative change
%***Jiggle stuff around
for k=1:loopend

        i=S(k);
        j=T(k);

        %%Take action!
        if (action(i,j)==0) & (rand <= (1-exp(- (N(i,j)/ ((old_cells(i,j)~=-1)...
                *old_cells(i,j)*thata_div) ) ^2 )) )
                                 %check for dividing flag and probability
            if chemo & (rand <= (1-exp(-(C(i,j)/((old_cells(i, j)~=-1)...
                    *old_cells(i,j)*thata_c) )^2)))
                                 %check for chemo death
                minus_changes(i,j)=-1;
            else
                plus_changes=plus_changes+divide(mysize,old_cells, i, j);
            end

        elseif (action(i,j)==1) & false %rand <= (1-exp(- (old_cells(i,j)~=-1))...
                %* old_cells(i,j) * (M(i,j)/thata_mov) ^2 )
                                 %check for movement flag and probability
            plus_changes=plus_changes+move(mysize, old_cells, i, j);
            minus_changes(i,j)=-1;

        elseif (action(i,j)==2) & ( rand <= exp(-( M(i,j) / ( ((old_cells(i,j)~=-1))...
                * old_cells(i,j) * thata_del ) )^2) )
                                 %check for natural death
            minus_changes(i,j)=-1;
        end
end

mycells=mycells+plus_changes;
for a=find(plus_changes>0 & mycells<0)
    mycells(a)=mycells(a)+1;     %skip normal cell ie 0
end


mycells=mycells+minus_changes;
for a=find(minus_changes<0 & mycells==0)
        mycells(a)=-1;           %skip normal cell ie 0
end
```

D.5 standard_rhs.m

```
function [lhs, rhs] = standard_rhs(mysize)
%standard_rhs(mysize)
%Programer: KEO Todd-Brown
%Date: June 10, 2003
%Precondition: mysize is the size of the difusion grid
%Postconditions: lhs is the left hand side for a linear system of equations
%                that solve a 2-d PDE system with a source term on top and
%                Neuman condition on bottom.  rhs is the corrisponding right
%                hand side.  Both are sparse.
%Purpose: Generate the info for a linear system to solve dN/dt=grad^2N with
%           boundry conditions


%|----------------------|     |-------------------------|
%|        | i,j-1 |      |     |        |n-mysize|       |
%|----------------------|     |-------------------------|
%| i-1,j  |  i,j  | i+1,j |    |  n-1   |   n    | n+1    |
%|----------------------|     |-------------------------|
%|        | i,j+1 |      |     |        |n+mysize|       |
%|----------------------|     |-------------------------|

%The centered difference approach states that
%...grad^2N(i,j) = 1/h^2*(N(i,j-1)+N(i,j+1)+N(i-1,j)+N(i+1,j)-4*N(i,j))
%...we are solving the following system
%...dN/dt=grad^2N-N*c
%...as it goes to steady state -> 0=dN/dt=grad^2N-N*c
%...The top is held constant at 1 and dN/dy=0 at the bottom ie
%...0=N(i-1,j)-N(i,j)

%flag=cputime;
rhs=sparse(mysize*mysize,mysize*mysize);
lhs=sparse(mysize*mysize,1);
counter=1:mysize*mysize;

lhs=sparse([ones(1,mysize), sparse(1,mysize*(mysize-1))])';
                            %top is constant, grad in middle is 0, slope at
                            %...bottom is 0

temp=[ones(1,mysize), -4*ones(1,mysize*(mysize-2)), -1*ones(1, mysize)];
                            %changes entry to 1 if on top and -1 if on
                            %...bottom

rhs=rhs+diag(sparse(temp),0);
                            %puts all the entries in temp on the main
                            % diagonal of rhs

temp=[sparse(1, mysize), ones(1, mysize*(mysize-2))];
                            %changes entry to 0 on top/bottom or 1 else
                            %add to rhs at appropreate spots
                            %...note1: you don't have to worry about wrapping
                            %...here

rhs=rhs+diag(sparse(temp),mysize);      %deal with ones below

temp=ones(1,mysize*(mysize-1));
rhs=rhs+diag(sparse(temp),-mysize);     %deals with ones on top

counter=1:mysize*(mysize-2);
```

```
temp=[sparse(1, mysize), (mod(counter(:),mysize)~=0)'.*...
        ones(1, mysize*(mysize-2)), sparse(1, mysize-1)]; %right left
rhs=rhs+diag(sparse(temp),1);  %deals with one on right
rhs=rhs+diag(sparse(temp),-1); %deals with one on left


temp=[sparse(1, mysize), (mod(counter(:),mysize)==1)'.*...
        ones(1, mysize*(mysize-2)), sparse(1, mysize-(mysize-1))];
rhs=rhs+diag(sparse(temp),(mysize-1));  %deals with wrap on left
rhs=rhs+diag(sparse(temp),-(mysize-1)); %deals with wrap on right


return
```

D.6 gen_immuno.m

```
function newI = gen_immuno(mysize, mycells, I, C, thata_ci, prob)

%if sum(sum(mycells>1))==0
%    newI=I;
%    return
%end

cell_kill=4;                            %number of cancer cells each immune
                                        %...cell can kill before it dies

count=sum(sum(I(2:mysize,:)>0));        %total number of immuno cells

newI=sparse(mysize, mysize);            %new place for immuno cells

P=full(rand(mysize-1, mysize) < ((prob-count/(mysize*(mysize-1)))*...
                    (exp(-(C(2:mysize,:)/thata_ci).^2))));
%Cell Birth
newI(2:mysize,:)=(P).*(mycells(2:mysize,:) <= 0 ).*(I(2:mysize,:)==0)...
                    *cell_kill+I(2:mysize,:);
                                        %cell site not occupied by a tumor*
                                        %...nor is it occupied by another
                                        %...immune cell*cell successeds in
                                        %...materializing next to the
                                        %...bloodvessel (possibly make this
                                        %...a function of the immuno and
                                        %...cancer cell counts
```

D.7 CN_PDEsolver.m

```
%function myans = CN_PDEsolver(lhs, rhs, mysize, cancer, lamda, alpha, flag, M1, M2)
function [myans, new_guess] = CN_PDEsolver(lhs, rhs, mysize, cancer, lamda, alpha, flag, type, guess)
%[myans, new_guess] = CN_PDEsolver(lhs, rhs, mysize, cancer, lamda, alpha, flag, type, guess)
%Programer: KEO Todd-Brown
%Date: June 4, 2003
%Purpose: The purpose of this function is to solve the nutrient
%           distribution for a given cell grid
%Preconditions: mysize is the size of the square matrix cancer,
%               lamda and alpha - are constants for the distribution PDE
%               lhs - is the left hand side of the linear system to solve the
%               PDE
%               rhs - is the right hand side of the linear system to solve
%               the PDE
%               cancer - stores the information about the cells on the grid
```

```
%              flag - tells what solver to use 1 is matlab's default solver
%                  anything else trys bicgstab first and if it doesn't
%                  converg then use the default solver
%              type - is what type of chemical we are solving for
%              guess - is used in bicgstab
%Postconditions: myans - (mysize x mysize) matrix with
%              the appropreate nutrient consintrations
%              new_guess - the same info as myans but it's in the
%              (mysize*mysize x 1) format

temp_nxn=zeros(mysize, mysize);
                         %an nxn matrix that
                         %allows for easy assignment of consumption
                         %...constants
temp_nnx1=zeros(mysize*mysize,1);
                         %an n^2x1 matrix that temarily holds the
                         %...nutrient consitrations
myans=zeros(mysize);

temp_nxn((2:mysize-1), :)=0-alpha^2*(cancer((2:mysize-1), :)==0)...
                         -lamda*alpha^2*cancer((2:mysize-1),:).*(cancer((2:mysize-1),:)>0);
                         %assign consumption constants, temp_nxn is nxn
                         %...note: cancer(:)==0 is a normal cell count
                         %...   cancer(:)+(cancer(:)<0) is a purely
                         %...   cancer count (ie we take out the dead
                         %...   cells which we represent as a -1 by adding
                         %...   1 to the cell sites which are under 0)
temp_nxn=temp_nxn';       %take the transpose because we are counting accross rows not
                         %... columns (matlab default)
temp_nnx1(:)=temp_nxn(:);
rhs=rhs+(diag(sparse(temp_nnx1)));
                         %takes the info in tempnxn and adds it into
                         %...rhs reading by rows


if flag==1
    new_guess=rhs\lhs;     %solver starts to be unweldly around mysize=100
                         %... takes 365.4800 secs at grid = 500
else
    [new_guess x relres iter]=bicgstab(rhs, lhs, 1e-4, [], [], [], guess);

    if x ~= 0              %if the solver does not converge then use the long
                         %... method
        new_guess=rhs\lhs;
    end
end

myans(:)=new_guess(:);
myans=myans';
```

D.8   divide.m

```
function plus_changes = divide(mysize, mycells, n, m)
%Programer: KEO Todd-Brown
%Date: May 29, 2003
%Preconditions: mysize - size of the square matricies mycells
%              and num_sites, (n, m) is a valid index for mycells
%Postconditions: plus_changes - sparce matrix of size mysize which is
%              1 if a cell is added to the site
%
```

```
%Purpose: Create a celluar divide function with the following rules:
%          If the cancer cell is inside the tumor then add a daughter
%            cell to the cell site
%          Else pick a random neighbor and add the cell to that cite
%        This function returns the changes that are made to the cell
%        grid ie a grid with zeros everywhere except where the daughter
%        cell is added.
i=mysize*(m-1)+n;

if mycells(i) <= 0
    error('Error in divide: trying to divide a normal or neucortic');
end
        %%Look for where the cell is
        %1 | 4 | 6
        %2 | x | 7
        %3 | 5 | 8

        a = i-1-mysize;     %1
        b = i-mysize;       %2
        c = i+1-mysize;     %3
        d = i-1;            %4
        e = i+1;            %5
        f = i-1+mysize;     %6
        g = i+mysize;       %7
        h = i+1+mysize;     %8

        %%something to do later might be to put in wrapping

        if mod(i, mysize)==1    %top
            if 1==i                             %left side
                neigh_cells=[e g h];
            elseif (1+mysize*(mysize-1))==i        %right side
                neigh_cells=[b c e];
            else
                neigh_cells=[b c e g h];
            end

        elseif mod(i, mysize)==0%bottom
            if i==mysize                        %left side
                neigh_cells=[d f g];
            elseif i==(mysize*mysize)             %right side
                neigh_cells=[a b d];
            else
                neigh_cells=[a b d f g];
            end
        elseif (1<=i) & (i<=mysize)             %left side
            %top and bottom already taken care of
            neigh_cells=[d e f g h];
        elseif ((1+mysize*(mysize-1))<=i) & (i<=(mysize*mysize))    %right side
            %top and bottom already taken care of
            neigh_cells=[a b c d e];
        else                                    %move somewhere random
            neigh_cells=[a b c d e f g h];
        end

        %neigh_cells
        %%find free cells around it

        free_n_cells=[];    %array of sites not occupied by cancer cells

        for j=neigh_cells
            if mycells(j)<1             %no cancer cells
                free_n_cells=[free_n_cells, j];
```

```
            end
        end

        %%figure out which free cell to move to
        if size(free_n_cells)~=0
            move_index=ceil(rand*(sum(free_n_cells>0)));
            move_to=free_n_cells(move_index);
        else
            move_index=i;
        end

        %%move there
        plus_changes=sparse(mysize, mysize);
        plus_changes(move_to)=1;
```

D.9   *move.m*

```
function plus_changes = move(mysize, mycells, n, m)
%Programer: KEO Todd-Brown
%Date: May 29, 2003
%Preconditions: mysize is the size of the square matricies mycells
%               and num_sites, (i, j) is a valid index for mycells
%Postconditions: changes is a sparce matrix of size mysize
%
%Purpose: Create a celluar move function with the following rules:
%           If the cancer cell is inside the tumor move the cell to a
%             random neighbor site
%           Else pick a random neighbor that is not a cancer site and move
%             the cell
%           Also if either of these actions result in a empty cell site
%             mark the site as neucrotic/dead by setting the site to -1
%         This function returns the changes that are made to the cell
%         grid ie a grid with zeros everywhere except -1 where the cell was
%         1 where the cell is now and -2 if any neucrotic/dead cell site
%         was created.

i=mysize*(m-1)+n;

        %%Look for where the cell is
        %1 | 4 | 6
        %2 | x | 7
        %3 | 5 | 8

        a = i-1-mysize;     %1
        b = i-mysize;       %2
        c = i+1-mysize;     %3
        d = i-1;            %4
        e = i+1;            %5
        f = i-1+mysize;     %6
        g = i+mysize;       %7
        h = i+1+mysize;     %8

        %%something to do later might be to put in wrapping

        if mod(i, mysize)==1    %top
            if 1==i                             %left side
                neigh_cells=[e g h];
            elseif (1+mysize*(mysize-1))==i        %right side
                neigh_cells=[b c e];
            else
```

```
            neigh_cells=[b c e g h];
        end

    elseif mod(i, mysize)==0%bottom
        if i==mysize                        %left side
            neigh_cells=[d f g];
        elseif i==(mysize*mysize)           %right side
            neigh_cells=[a b d];
        else
            neigh_cells=[a b d f g];
        end
    elseif (1<=i) & (i<=mysize)            %left side
        %top and bottom already taken care of
        neigh_cells=[d e f g h];
    elseif ((1+mysize*(mysize-1))<=i) & (i<=(mysize*mysize))    %right side
        %top and bottom already taken care of
        neigh_cells=[a b c d e];
    else                                    %move somewhere random
        neigh_cells=[a b c d e f g h];
    end

    %neigh_cells
    %%find free cells around it

    free_n_cells=[];    %array of sites not occupied by cancer cells

    for j=neigh_cells
        if mycells(j)<1            %no cancer cells
            free_n_cells=[free_n_cells, j];
        end
    end

    %%figure out which free cell to move to
    if size(free_n_cells)~=0
        move_index=ceil(rand*(sum(free_n_cells>0)));
        move_to=free_n_cells(move_index);
    else
        move_index=ceil(rand*(sum(neigh_cells>0)));
        move_to=free_n_cells(move_index);
    end

    %%move there
    plus_changes=sparse(mysize, mysize);
    plus_changes(move_to)=1;
```

D.10   cellplot.m

```
function x = cellplot(ls)
%function x = cellplot(ls)
%Programer: KEO Todd-Brown
%Date: June 4, 2003
%Purpose: The purpose of this is to print num number of cancer plots to either
%          subplots or figures
%Preconditions: ls is a int who does not excede the number of mycells
%               stored in data/.  This is suppose to be the last cell shot;
%               cancer_pop stores the cancer populations as they grow over
%               the iterations
%Postconditions: outputs a dummy variable x
```

```
figure(1)                          %first figure is the tumor
load (['data/old_mycells'])        %get the last frame
surf(mycells);                     %plot using surf
shading interp
lighting phong;
colorbar('vert');                  %insert a color bar
title([int2str(ls), 'th cell shot'])


figure(2)                          %second figure is the cancer cell
load('data/cancer_pop')             %...population over time
plot(cancer_pop);
title('cancer population')
xlabel('iteration')
ylabel('total cancer cells')

figure(3)
load('data/immuno_pop')
plot(immuno_pop);
title('Immune population')
xlabel('Iteration')
ylabel('Total cell count')
```

Bibliography

[1] *Mouse normative data.* Available at `http://www.molbio.princeton.edu/facility/restricted/viv_restricted/mou%se.html`.

[2] J. ADAM AND S. MAGGELAKIS, *Mathematical models of tumor growth. IV. effects of a necrotic core*, Mathematical Biosciences, 97 (1989), pp. 121–136.

[3] J. A. ADAM, *A simplified mathematical model of tumor growth*, Mathematical Biosciences, 81 (1986), pp. 229–244.

[4] ——, *A mathematical model of tumor growth. II. effects of geometry and spatial nonuniformity on stability*, Mathematical Biosciences, 86 (1987), pp. 183–211.

[5] ——, *A mathematical model of tumor growth. III. comparison with experiment*, Mathematical Biosciences, 86 (1987), pp. 213–227.

[6] J. A. ADAM AND N. BELLOMO, eds., *A Survey of Models for Tumor-Immune System Dynamics*, Birkhäuser, Boston, 1997.

[7] E. D. ANGELIS AND L. MESIN, *Modelling of the immune response: Conceptual frameworks and applications*, Mathematical Models and Methods in Applied Science, 11 (2001), pp. 1609–1630.

[8] G. ARFKEN, *Mathematical Methods for Physicists*, Academic Press, New York, second ed., 1970.

[9] J. W. BAISH, Y. GAZIT, D. A. BERK, M. NOZUE, L. T. BAXTER, AND R. K. JAIN, *Role of tumor vasculature architecture in nutrient and drug delivery: An invasion percolation-based network model*, Microvascular Research, 51 (1996), pp. 327–346.

[10] L. BANNOCK, *Nutrition.* Found at `http://www.doctorbannock.com/nutrition.html`.

[11] N. BELLOMO AND L. PREZIOSI, *Modelling and mathematical problems related to tumor evolution and its interaction with the immune system*, Mathematical and Computer Modelling, 32 (2000), pp. 413–452.

[12] A. BERTUZZI, A. FASANO, A. GANDOLFI, AND D. MARANGI, *Cell kinetic in tumour cords studied by a model with variable cell cycle length*, Mathematical Biosciences, 177&178 (2002), pp. 103–125.

[13] A. BERTUZZI AND A. GANDOLFI, *Cell kinetics in a tumour cord*, Journal of Theoretical Biology, 204 (2000), pp. 587–599.

[14] R. BORRELLI AND C. COLEMAN, *Differential Equations: A Modeling Perspective*, John Wiley and Sons, Inc., New York, 1998.

[15] M. BRAIN, *How your immune system works*. Found at `http://science.howstuffworks.com/immune-system4.htm`.

[16] C. BREWARD, H. BYRNE, AND C. LEWIS, *The role of cell-cell interactions in a two-phase model for avascular tumour growth*, Journal of Mathematical Biology, 45 (2002), pp. 125–152.

[17] H. BYRNE AND M. CHAPLAIN, *Growth of nonnecrotic tumors in the presence and absence of inhibitors*, Mathematical Biosciences, 130 (1995), pp. 151–181.

[18] ——, *Growth of necrotic tumors in the presence and absence of inhibitors*, Mathematical Biosciences, 135 (1996), pp. 187–216.

[19] ——, *Modelling the role of cell-cell adhesion in the growth and development of carcinomas*, Mathematical and Computational Modelling, 24 (1996), pp. 1–17.

[20] ——, *Free boundary value problems associated with the growth and development of multicellular spheroids*, European Journal of Applied Mathematics, 8 (1997), pp. 639–658.

[21] H. M. BYRNE, *A weakly nonlinear analysis of a model of avascular solid tumour growth*, Journal of Mathematical Biology, 39 (1999), pp. 59–89.

[22] H. M. Byrne, S. M. Cox, and C. E. Kelly, *Macrophage-tumor interactions: in vivo dynamics*. Accepted for publication in *Discrete and Continuous Physical Systems*, April 2003.

[23] L. Cabrera, J. Galvez, F. Lajarin, G. Rubio, P. Aparicio, and P. Garcia-Peñarrubia, *Conjugation between cloned human NK cells (H7.8) and K562/MOLT4 tumor cell systems: Saturability, binding parameters, and population distribution of conjugates*, Cellular Immunology, 169 (1996), pp. 133–141.

[24] P. Calabresi and P. S. Schein, eds., *Medical Oncology: Basic Principles and Clinical Management of Cancer*, McGraw-Hill, New York, second ed., 1993.

[25] L. H. Carvalho, J. C. Hafalla, and F. Zavala, *ELISPOT assay to measure antigen-specific murine $CD8^+$ T cell responses*, Journal of Immunological Methods, 252 (2001), pp. 207–218.

[26] D. A. Casciato, ed., *Manual of Clinical Oncology*, Lippincott Williams & Wilkins, fourth ed., 2000.

[27] M. Chaplain, M. Ganesh, and I. Graham, *Spatio-temporal pattern formation on spherical surfaces: numerical simulation and application to solid tumor growth*, Journal of Mathematical Biology, 42 (2001), pp. 387–423.

[28] C. Chen, H. Byrne, and J. King, *The influence of growth-induced stress from the surrounding medium on the development of spheroids*, Journal of Mathematical Biology, 43 (2001), pp. 191–220.

[29] W.-Y. Chen, P. E. Annamreddy, and L. Fan, *Modeling growth of a heterogeneous tumor*, Journal of Theoretical Biology, 221 (2003), pp. 205–227.

[30] J. O. E. Clark, ed., *A Visual Guide to the Human Body: A Comprehensive Atlas of the Structures of the Human Body*, Barnes and Noble, 1999.

[31] S. Cox and P. Matthews, *Exponential time differencing for stiff systems*, Journal of Computational Physics, 176 (2002), pp. 430–455.

[32] J. CRANK, *Free and Moving Boundary Problems*, Oxford University Press, Oxford, 1984.

[33] V. CRISTINI, J. LOWENGRUB, AND Q. NIE, *Nonlinear simulation of tumor growth*, Journal of Mathematical Biology, 46 (2003), pp. 191–224.

[34] S. CUI AND A. FRIEDMAN, *Analysis of a mathematical model of the effect of inhibitors on the growth of tumors*, Mathematical Biosciences, 164 (2000), pp. 103–137.

[35] ——, *Analysis of a mathematical model of the growth of necrotic tumors*, Journal of Mathematical Analysis and Applications, 255 (2001), pp. 636–677.

[36] B. CURTI, A. OCHOA, W. URBA, G. ALVORD, W. KOPP, G. POWERS, C. HAWK, S. CREEKMORE, B. GAUSE, J. JANIK, J. HOLMLUND, P. KREMERS, R. FENTON, L. MILLER, M. SZNOL, J. S. II, W. SHARFMAN, AND D. LONGO, *Influence of interleukin-2 regimens on circulating populations of lymphocytes after adoptive transfer of anti-cd3-stimulated t cells: Results from a phase i trial in cancer patients.*, Bulletin of Mathematical Biology, 19 (1996), pp. 296–308.

[37] R. DE BOER AND P. HOGEWEG, *Interactions between macrophages and T-lymphocytes: tumor sneaking through intrinsic to helper T cell dynamics*, Journal of Theoretical Biology, 120 (1986), pp. 331–51.

[38] L. DE PILLIS AND A. RADUNSKAYA, *A mathematical tumor model with immune resistance and drug therapy: an optimal control approach*, Journal of Theoretical Medicine, 3 (2001), pp. 79–100.

[39] ——, *The dynamics of an optimally controlled tumor model: A case study*, Mathematical and Computer Modeling, (2003).

[40] ——, *A mathematical model of immune response to tumor invasion*. Preprint draft; to appear in the proceedings of the Second MIT Conference on Computational and Fluid Dynamics, 2003.

[41] ——, *A mathematical model of patient-specific response to immunotherapy*, Development of Therapeutic Cancer Vaccines (online), (2003).

[42] L. DE PILLIS, A. RADUNSKAYA, AND C. WISEMAN, *A validated mathematical model of cell-mediated immune responses to tumor invasion and vaccine therapy in mice and humans.* Presentation poster., 2003.

[43] M. DELITALA, *Critical analysis and perspectives on kinetic (cellular) theory of immune competition*, Mathematical and Computer Modelling, 35 (2002), pp. 63–75.

[44] P. J. DELVES AND I. M. ROITT, *The immune system - first of two parts*, The New England Journal of Medicine, 343 (2000), pp. 37–49.

[45] ――――, *The immune system - second of two parts*, The New England Journal of Medicine, 343 (2000), pp. 108–117.

[46] A. DIEFENBACH, E. R. JENSEN, A. M. JAMLESON, AND D. H. RAULET, *Rae1 and H60 ligands of the NKG2D receptor simulate tumour immunity*, Nature, 413 (2001), pp. 165–171.

[47] M. S. DORDAL, J. N. WINTER, AND A. J. ATKINSON, JR., *Kinetic analysis of P-glycoprotein-mediated doxorubicin efflux*, The Journal of Pharmacology and Experimental Theraputics, 263 (1992), pp. 762–766.

[48] J. R. DRISCOLL AND D. M. HEALY, JR., *Computing fourier transforms and convolutions on the 2-sphere*, Advances in Applied Mathematics, 15 (1994), pp. 202–250.

[49] M. E. DUDLEY, J. R. WUNDERLICH, P. F. ROBBINS, J. C. YANG, P. HWU, D. J. SCHWARTZENTRUBER, S. L. TOPALIAN, R. SHERRY, N. P. RESTIFO, A. M. HUBICKI, M. R. ROBINSON, M. RAFFELD, P. DURAY, C. A. SEIPP, L. ROGERS-FREEZER, K. E. MORTON, S. A. MAVROUKAKIS, D. E. WHITE, AND S. A. ROSENBERG, *Cancer regression and autoimmunity in patients after clonal repopulation with antitumor lymphocytes*, Science, 298 (2002), pp. 850–854.

[50] M. L. DUSTIN AND D. R. COLMAN, *Neural and immunological synaptic relations*, Science, 298 (2002), pp. 785–789.

[51] M. EISEN, *Mathematical Methods & Models in the Biological Sciences: Nonlinear and Multidimensional Theory*, Prentice Hall, 1988.

[52] J. FARRAR, K. KATZ, J. WINDSOR, G. THRUSH, R. SCHEUERMANN, J. UHR, AND N. STREET, *Cancer dormancy. VII. a regulatory role for CD8+ T cells and IFN-gamma in establishing and maintaining the tumor-dormant state*, Journal of Immunology, 162 (1999), pp. 2842–9.

[53] S. FERREIRA, JR., M. MARTINS, AND M. VILELA, *Reaction-diffusion model for the growth of avascular tumor*, Physical Review E, 65 (2002), pp. 1–8.

[54] S. FRANKS, H. BYRNE, J. KING, J. UNDERWOOD, AND C. LEWIS, *Modelling the early growth of ductal carcinoma in situ of the breast*, Journal of Mathematical Biology, (2003).

[55] E. FURMAN-HARAN, D. GROBGELD, AND H. DEGANI, *Dynamic contrast-enhanced imaging and analysis at high spatial resolution of MCF7 human breast tumors*, Journal of Magnetic Resonance, 128 (1997), pp. 161–171.

[56] J. GALVEZ, L. CABRERA, F. LAJARIN, AND P. GARCIA-PEÑARRUBIA, *Computer simulation and data analysis of effector-target interactions: The extraction of binding parameters from effector and target conjugate frequencies data by using linear and nonlinear data-fitting transformations*, Computers and Biomedical Research, 29 (1996), pp. 93–118.

[57] P. GARCIA-PEÑARRUBIA, L. CABRERA, R. ALVAREZ, AND J. GALVEZ, *Effector-target interactions: saturability, affinity and binding isotherms*, Journal of Immunological Methods, 155 (1992), pp. 133–147.

[58] P. GARCIA-PEÑARRUBIA, N. LORENZO, J. GALVEZ, A. CAMPOS, X. FEREZ, AND G. RUBIO, *Study of the physical meaning of the binding parameters involved in effector-target conjugation using monoclonal antibodies against adhesion molecules and cholera toxin*, Cellular Immunology, 215 (2002), pp. 141–150.

[59] S. N. GARDNER, *A mechanistic, predictive model of dose-response curves for cell cycle phase-specific and -nonspecific drugs*, Cancer Research, 60 (2000), pp. 1417–1425.

[60] A. V. GETT AND P. D. HODGKIN, *A cellular calculus for signal integration by T cells*, Nature Immunology, 1 (2000), pp. 239–244.

[61] A. V. GETT, F. SALLUSTO, A. LANZAVECCHIA, AND J. GEGINAT, *T cell fitness determined by signal strength*, Nature Immunology, 4 (2003), pp. 355–360.

[62] W. W. GIBBS, *Untangling the roots of cancer*, Scientific American, (2003).

[63] A. GRAKOUI, S. K. BROMLEY, C. SUMEN, M. M. DAVIS, A. S. SHAW, P. M. ALLEN, AND M. L. DUSTIN, *The immunological synapse: A molecular machine controlling T cell activation*, Science, 285 (1999), pp. 221–227.

[64] D. J. GREENBLATT, M.D. AND J. KOCH-WESER, M.D., *Drug therapy: Clinical pharmacokinetics*, New England Journal of Medicine, 293 (1975), pp. 702–705.

[65] H. GREENSPAN, *Models for the growth of a solid tumor by diffusion*, Studies in Applied Mathematics, 51 (1972), pp. 317–340.

[66] ——, *On the growth and stability of cell cultures and solid tumors*, Journal of Theoretical Biology, 56 (1976), pp. 229–242.

[67] I. HARA, H. HOTTA, N. SATO, H. ETO, S. ARAKAWA, AND S. KAMIDONO, *Rejection of mouse renal cell carcinoma elicited by local secretion of interleukin-2.*, Japanese Journal of Cancer Research, 87 (1996), pp. 724–729.

[68] B. HAUSER, *Blood tests*, tech. rep., International Waldenstrom's Macroglobulinemia Foundation, Jan. 2001.

[69] K. HIROISHI, T. TÜTING, AND M. T. LOTZE, *IFN-α-expressing tumor cells enhance generation and promote survival of tumor-specific CTLs*, Journal of Immunology, (2000), pp. 567–572.

[70] J. F. HOLLAND AND I. EMIL FREI, eds., *Cancer Medicine*, Lea and Febiger, Philadelphia, 1973.

[71] T. HORN, *Mechanisms of T-cell depletion and regeneration in HIV disease*, The PRN Notebook, (2002), pp. 4–9.

[72] T. L. JACKSON, *Vascular tumor growth and treatment: Consequenes of polyclonality, competition and dynamic vascular support*, Journal of Mathematical Biology, 44 (2002), pp. 201–226.

[73] ——, *Intracelluar accumulation and mechanism of action of doxorubicin in a spatio-temporal tumor model*, Journal of Theoretical Biology, 220 (2003), pp. 201–213.

[74] T. L. JACKSON AND H. M. BYRNE, *A mathematical model to study the effects of drug resistance and vasculature on the response of solid tumors to chemotherapy*, Mathematical Biosciences, 164 (1999), pp. 17–38.

[75] M. I. KAMIEN AND N. L. SCHWARTZ, *Dynamic Optimization: The Calculus of Variations and Optimal Control in Economics and Management*, North Holland, New York, 1981.

[76] A.-K. KASSAM AND L. N. TREFETHEN, *Fourth-order time stepping for stiff PDEs*. Submitted to the *SIAM Journal of Scientific Computing*, 2003.

[77] D. KEEFE, R. L. CAPIZZI, AND S. A. RUDNICK, *Methotrexate cytotoxicity for L5178Y/Asn⁻ lymphoblasts: Relationship of dose and duration of exposure to tumor cell viability*, Cancer Research, 42 (1982), pp. 1641–1645.

[78] C. KELLY, R. LEEK, H. BYRNE, S. COX, A. HARRIS, AND C. LEWIS, *Modelling macrophage infiltration into avascular tumors*, Journal of Theoretical Medicine, 4 (2002), pp. 21–38.

[79] D. E. KERR, G. J. SCHREIBER, V. M. VRUDHULA, H. P. SVENSON, I. HELLSTRÖM, K. E. HELLSTRÖM, AND P. D. SENTER, *Regressions and cures of melanoma xenografts following treatment with monoclonal antibody β-lactamase conjugates in combination with anticancer prodrugs*, Cancer Research, 55 (1995), pp. 3558–3565.

[80] D. KIRSCHNER AND J. C. PANETTA, *Modeling immunotherapy of the tumor-immune interaction*, Journal of Mathematical Biology, 37 (1998), pp. 232–252.

[81] H. KNOLLE, *Cell kinetic modelling and the chemotherapy of cancer*, Springer-Verlag, Berlin, 1988.

[82] V. KUZNETSOV AND I. MAKALKIN, *Bifurcation-analysis of mathematical-model of interactions between cytotoxic lymphocytes and tumor-cells – effect of immunological amplification of tumor-growth and its connection with other phenomena of oncoimmunology*, Biofizika, 37 (1992), pp. 1063–70.

[83] V. KUZNETSOV, I. MAKALKIN, M. TAYLOR, AND A. PERELSON, *Nonlinear dynamics of immunogenic tumors: Parameter estimation and global bifurcation analysis*, Bull. of Math. Bio., 56 (1994), pp. 295–321.

[84] K.-H. LEE, A. D. HOLDORF, M. L. DUSTIN, A. C. CHAN, P. M. ALLEN, AND A. S. SHAW, *T cell receptor signaling precedes immunological synapse formation*, Science, 295 (2002), pp. 1539–1542.

[85] R. LEFEVER, J. HIERNAUX, J. URBAIN, AND P. MEYERS, *On the kinetics and optimal specificity of cytotoxic reactions mediated by T-cell clones*, Bulletin of Mathematical Biology, 54 (1992), pp. 839–873.

[86] L. M. LEVASSEUR, H. K. SLOCUM, Y. M. RUSTUM, AND W. R. GRECO, *Modeling of the time-dependency of* in vitro *drug cytotoxicity and resistance*, Cancer Research, 58 (1998), pp. 5749–5761.

[87] R. LEVEQUE, *Amath 585–6 notes*. Chapter 13 from a set of notes on finite difference methods for differential equations., 1998.

[88] A. LUMSDEN, J. CODDE, P. V. D. MEIDE, AND B. GRAY, *Immunohistochemical characterisation of immunological changes at the tumour site after chemo-immunotherapy with doxorubicin, interleukin-2 and interferon-γ.*, Anticancer Research, 167 (1996), pp. 1145–1154.

[89] J.-P. H. MACHIELS, R. T. REILLY, L. A. EMENS, A. M. ERCOLINI, R. Y. LEI, D. WEINTRAUB, F. I. OKOYE, AND E. M. JAFFEE, *Cyclophosphamide, doxorubicin, and paclitaxel enhance the antitumor immune response of granulocyte/macrophage-colony stimulating factor-secreting whole-cell vaccines in HER-2/neu tolerized mice*, Cancer Research, 61 (2001), pp. 3689–3697.

[90] R. MARTIN, *Optimal control drug scheduling of cancer chemotherapy*, Automatica. The Journal of IFAC, the International Federation of Automatic Control, 28 (1992), pp. 1113–1123.

[91] R. MARTIN, M. FISHER, R. MINCHIN, AND K. TEO, *A mathematical model of cancer chemotherapy with an optimal selection of parameters*, Mathematical Biosciences. An International Journal, 99 (1990), pp. 205–230.

[92] A. MAYER AND H. EARL, *Whither high-dose chemotherapy in breast cancer?*, Breast Cancer Research, 3 (2001), pp. 8–10.

[93] S. J. MERRILL, *Computational models in immunological methods: an historical overview*, Journal of Immunological Methods, 216 (1998), pp. 69–92.

[94] S. MORECKI, T. PUGATSCH, S. LEVI, Y. MOSHEL, AND S. SLAVIN, *Tumor-cell vaccination induces tumor dormancy in a murine model of B-cell leukemia/lymphoma (BCL1)*, International Journal of Cancer, 65 (1996), pp. 204–8.

[95] K. MORTON AND D. MAYERS, *Numerical Solution of Partial Differential Equations*, Cambridge University Press, Cambridge, 1994.

[96] M. MULLER, F. GOUNARI, S. PRIFTI, H. HACKER, V. SCHIRRMACHER, AND K. KHAZAIE, *EblacZ tumor dormancy in bone marrow and lymph nodes: active control of proliferating tumor cells by CD8+ immune T cells*, Cancer Research, 58 (1998), pp. 5439–46.

[97] J. MURRAY, *Optimal control for a cancer chemotherapy problem with general growth and loss functions*, Mathematical Biosciences. An International Journal, 98 (1990), pp. 273–287.

[98] M. OWEN AND J. SHERRATT, *Mathematical modelling macrophage dynamics in tumors*, Mathematical Models and Methods in Applied Sciences, 9 (1999), pp. 513–539.

[99] M. R. OWEN AND J. A. SHERRATT, *Pattern formation and spatiotemporal irregularity in a model for macrophage-tumour interactions*, Journal of Theoretical Biology, 189 (1997), pp. 63–80.

[100] R. PAGE, *Cancer Management: a Multidisciplinary Approach*, PRR inc., fifth ed., 2001, ch. Principles of Chemotherapy.

[101] R. PAZDUR, W. HOSKINS, L. WAGMAN, AND L. COIA, eds., *Cancer Management: A Mulitdisciplinary Approach*, Publisher Research and Representation, fifth ed., 2001, ch. Principles of Chemotherapy.

[102] M. C. PERRY, ed., *The Chemotherapy Source Book*, Lippincott Williams & Wilkins, third ed., 2001.

[103] L. PREZIOSI, *From population dynamics to modelling the competition betwen tumors and immune system*, Mathematical and Computer Modelling, 23 (1996), pp. 135–152.

[104] A. RIBAS, L. H. BUTTERFIELD, S. N. AMARNANI, V. B. DISSETTE, D. KIM, W. S. MENG, G. A. MIRANDA, H.-J. WANG, W. H. MCBRIDE, J. A. GLASPY, AND J. S. ECONOMOU, *CD40 cross-linking bypasses the absolute requirement for CD4 T cells during immunization with melanoma antigen gene-modified dendritic cells*, Cancer Research, 61 (2001), pp. 8787–8793.

[105] S. ROSENBERG AND M. LOTZE, *Cancer immunotherapy using interleukin-2 and interleukin-2-activated lymphoytes.*, Annual Review of Immunology, 4 (1986), pp. 681–709.

[106] S. J. RUUTH, *Implicit-explicit methods for reaction-diffusion problems in pattern formation*, Journal of Mathematical Biology, 34 (1995), pp. 148–176.

[107] L. SCHINDLER, D. K. M.S., AND J. KELLY, *Understanding the immune system.* website.

[108] J. A. SHERRATT AND M. A. CHAPLAIN, *A new mathematical model for avascular tumour growth*, Journal of Mathematical Biology, 43 (2001), pp. 291–312.

[109] Y.-J. SHYY, Y.-S. LI, AND P. KALATTUKUDY, *Structure of human monocyte chemotactic protein gene and its regulation by TPA*, Biochemical and Biophysical Research Communications, 169 (1990), pp. 346–351.

[110] T. STEWART, *Immune mechanisms and tumor dormancy*, Medicina (Buenos Aires), 56 (1996), pp. 74–82.

[111] H. P. SVENSSON, V. M. VRUDHULA, J. E. EMSWILER, J. F. MACMASTER, W. L. COSAND, P. D. SENTER, AND P. M. WALLACE, In Vitro *and* in vivo *activities of a doxorubicin prodrug in combination with monoclonal antibody β-lactamase conjugates*, Cancer Research, 55 (1995), pp. 2357–2365.

[112] G. W. SWAN, *Optimal control applications in the chemotherapy of multiple myeloma*, IMA Journal of Mathematics Applied in Medicine and Biology, 2 (1985), pp. 139–160.

[113] ——, *Optimal control analysis of a cancer chemotherapy problem*, IMA (Institute of Mathematics and its Applications). Journal of Mathematics Applied in Medicine and Biology, 4 (1987), pp. 171–184.

[114] A. SWIERNIAK, *Some control problems for simplest differential models of proliferation cycle*, Applied Mathematics and Computer Science, 4 (1994), pp. 223–232.

[115] A. SWIERNIAK, U. LEDZEWICZ, AND H. SCHÄTTLER, *Optimal control for a class of compartmental models in cander chemotherapy.* Accpeted subject to revision. Available at `http://www.siue.edu/~uledzew/Cancerrev.ps.`, 2002.

[116] A. SWIERNIAK AND A. POLANSKI, *Irregularity in scheduling of cancer chemotherapy*, Applied Mathematics and Computer Science, 4 (19942), pp. 263–271.

[117] A. SWIERNIAK, A. POLANSKI, AND M. KIMMEL, *Optimal control problems arising in cell-cycle-specific cancer chemotherapy*, Journal of Cell Proliferation, 29 (1996), pp. 117–139.

[118] T. TAKAYANAGI AND A. OHUCHI, *A mathematical analysis of the interactions between immunogenic tumor cells and cytotoxic T lymphocytes*, Microbiology and Immunology, 45 (2001), pp. 709–715.

[119] THE BIOLOGY PROJECT, *Introduction to immunology tutorial.* Found at `http://www.biology.arizona.edu/immunology/tutorials/immunology/page1.h%tml`.

[120] P. A. VAN DER MERWE AND S. J. DAVIS, *The immunological synapse—a multitasking system*, Science, 295 (2002), pp. 1479–1480.

[121] U. H. VON ANDRIAN AND C. R. MACKAY, *T-cell function and migration*, New England Journal of Medicine, (2000), pp. 1020–1034.

[122] O. VON STRYK, *User's guide for DIRCOL: A direct collocation method for the numerical solution of optimal control problems*, tech. rep., Technische Universität Darmstadt, Nov. 1999. Version 2.1.can be found at `http://www.sim.informatik.tu-darmstadt.de/sw/dircol/dircol.html`.

[123] S. WEBB AND J. SHERRATT, *A perturbation problem arising from the modelling of soluble Fas ligand in tumor immunology*, Mathematical and Computer Modelling, 37 (2003), pp. 323–331.

[124] S. D. WEBB, J. A. SHERRATT, AND R. G. FISH, *Cells behaving badly: a theoretical model for the Fas/FasL system in tumour immunology*, Mathematical Biosciences, 179 (2002), pp. 113–129.

[125] L. M. WEIN, J. T. WU, AND D. H. KIRN, *Validation and analysis of a mathematical model of a replication-competent oncolytic virus for cancer treatment: Implications for virus design and delivery*, Cancer Research, 63 (2003), pp. 1317–1324.

[126] D. WODARZ, *Viruses as antitumor weapons: Defining conditions for tumor remission*, Cancer Research, 61 (2001), pp. 3501–3507.